EPM–RT–2012-01

INFLUENCE OF INTERNAL LAYERS ON WATER FLOW INSIDE A LARGE WASTE ROCK PILE

Ihssan Dawood and Michel Aubertin
Département des génies civil, géologique et des mines
École Polytechnique de Montréal

March 2012

EPM-RT-2012-01

Influence of internal layers on water flow inside a large waste rock pile

Ihssan Dawood and Michel Aubertin

Département des génies civil, géologique et des mines

École Polytechnique de Montréal

March 2012

Dépôt légal :
Bibliothèque nationale du Québec, 2012
Bibliothèqueque nationale du Canada, 2012

EPM-RT-2012-2012-01
Influence of internal layers on water flow inside a large waste rock pile
Par : Ihssan Dawood, Michel Aubertin
Département des génies civil, géologique et des mines
École Polytechnique de Montréal

ABSTRACT

The method used to construct a waste rock pile on a mine site affects its internal structure. Commonly used construction methods often lead to the creation of compacted material layers inside the pile, within the loose, coarse-grained waste rock. These dense layers, which typically show a finer grain size, influence the movement and distribution of water in the pile. Long term numerical simulations of unsaturated flow in a large size pile have been conducted to investigate the effect of such structural features. The simulations, conducted with the finite element code HYDRUS-2D, lead to various observations that provide a better understanding of the hydrogeological behavior of the investigated pile (which is based on an actual field case). The results show how the water distribution and flux within the pile are influenced by the presence of fine grained material layers, and also by the magnitude of precipitation (or recharge). The effect of the pile size is also investigated by comparing the response of the large pile (more than 100 m in height) with that of a smaller pile (about 25 m in height). The report (with Appendices) presents the main results of the calculations, with some comments on their practical implications for pile design and environmental behavior.

Key words: waste rock pile, internal layers, capillary barrier, hydrogeological behavior, unsaturated flow, numerical modeling.

RÉSUMÉ

La méthode utilisée pour la construction d'une halde à stériles sur un site minier affecte sa structure interne. Les méthodes couramment utilisées conduisent souvent à la présence de couches de matériau compacté à l'intérieur des haldes, qui sont surtout constituées de matériaux grossiers et lâches. Ces couches, usuellement formées de matériaux plus fins et plus denses, influencent le mouvement et la distribution de l'eau à l'intérieur de la halde. Des simulations numériques à long terme de l'écoulement non saturé de l'eau dans une grande halde à stériles ont été menées pour étudier l'effet des caractéristiques structurales et du régime des précipitations. Ces simulations, réalisées avec le code d'éléments finis HYDRUS-2D, conduisent à diverses observations qui aident à comprendre le comportement hydrogéologique de la halde modélisée (sur la base d'un cas réel). Les résultats montrent comment la distribution d'eau et le flux dans la halde sont influencés par la présence de couches de matériaux fins et par l'ampleur des précipitations (ou de la recharge). L'effet de la dimension de la halde est également étudié en comparant la réponse de la grande halde (hauteur de plus de 100 m) avec celle d'une halde plus petite (environ 25 m). Ce rapport (avec les annexes) présente les principaux résultats des simulations, avec des commentaires sur leurs implications pratiques pour la conception des haldes et leur comportement environnemental.

Mots clés: haldes à stériles, couches internes, barrière capillaire, comportement hydrogéologique, écoulement non saturé, modélisation numérique.

TABLE OF CONTENTS

LIST OF FIGURES

LIST OF TABLES

LIST OF APPENDICES

LIST OF SYMBOLS

Symbol	Definition	Units
ψ	Water pressure (head)	L
θ	Volumetric water content	----
θ_e	Effective volumetric water content	----
θ_r	Residual volumetric water content	----
θ_s	Saturated volumetric water content	----
t	Time	T
k_x	Pressure dependent hydraulic conductivity in the horizontal direction	L/T
k_z	Pressure dependent hydraulic conductivity in the horizontal direction	L/T
$k(\theta_e)$	Unsaturated hydraulic conductivity dependent on water content	L/T
k_s	Saturated hydraulic conductivity	L/T
v	Water vertical velocity	L/T
α_v	van Genuchten model parameter	1/L
n_v and m_v	van Genuchten model parameters	----
ℓ	Pore conductivity factor	----

1. INTRODUCTION

Waste rock is a by-product of mining activities that is often produced in large volume on mine sites. Waste rocks typically represent about 50% to 75% (and more) of the extracted rock for open pit operations, while such wastes typically constitute less than 20% of the extracted rock in underground mines (Aubertin et al. 2002a). These are typically placed in waste rock piles (or dumps) on the surface. The environmental response of a pile depends on many factors, including the mineralogical composition of the waste rock and their hydro-geotechnical characteristics, including the grain size distribution, porosity, and hydrogeological properties. Acid mine drainage (AMD) or contaminated neutral drainage (CND) can be generated by waste rocks when these contain reactive minerals (e.g. Lefebvre et al. 2001; Ritchie 2003; Sracek et al. 2004; Stantec 2004; Molson et. al. 2005; Bussière et al. 2005, 2011, Fala et al. 2012). Such contaminated seepage waters may have harmful impacts on the surrounding ecosystems. There is thus a need to apply efficient measures to prevent or control such undesirable effects. The first line of defence begins with the pile design, which should aim at limiting water infiltration and flow within the waste rocks (e.g. Aubertin et al. 2002b, 2005, 2008; Wels et al. 2003; Williams and Rohde 2007; Williams et al. 2008; Dawood and Aubertin 2009). This can be accomplished by adopting suitable construction methods to raise the pile.

Typical construction methods with heavy equipments often lead to the creation of sub-horizontal layers of compacted material, especially in piles disposed on relatively flat surfaces. These layers can significantly affect the hydrogeological response of a pile (e.g. Aubertin et al. 2002a, b; Fala et. al. 2003, 2005, 2006, 2012; Martin et al. 2005).

The distribution and movement of water through a waste rock pile are however difficult to measure, interpret, and predict. The large spatial and temporal variations observed for the grain size, porosity, and in situ degree of saturation (or volumetric water content) of the waste rock make this a complex problem to analyse. Nonetheless, recent developments with laboratory and field tests, in situ

monitoring, and numerical modeling have led to a better understanding of the main phenomena that affect the hydrogeological and geochemical behaviour of waste rock piles, including the effect of localized flow and capillary barrier effects due, respectively, to the presence of macropores and horizontal or inclined layers, (e.g. Smith et al. 1995; Aubertin et al. 2002b, 2005, 2008; Bussière et al. 2011; Dawood et al. 2011). In this regard, capillary barriers, induced when compacted material layers are created above the loose coarse-grained waste rock material, constitute an important process that affects water flow in a pile. It has lately been proposed to use such effects to control the movement of water and air through piles (e.g. Lefebvre et al. 2001; Fala et al. 2003, 2005, 2006; Molson et al. 2005). Capillary barrier effects can also be used to design cover systems that limit water infiltration from the surface to the inside of piles (e.g. Zhan et al. 2001; Martin et al. 2005; Aubertin et al. 2006, 2009).

The finite element code Hydrus-2D (Simunek et al., 1999) has been used to assess the potential effects of material properties and internal features (mainly fine grained material layers) on the long term hydrological response of a large waste rock pile. Several scenarios are simulated to illustrate the potential impact of these features. The various scenarios considered here are summarized in Table 1. Two scenarios (S1 and S2) constitute the base cases with a pile made of a single material (gravely waste rock, GRV, for S1, and sandy waste rock, SBL, for S2); one simulation (S3) is used to illustrate the effect of the precipitation regime (i.e. recharge); four simulations (S4 to S7) are used to illustrate the effect of horizontal layers; two simulations (S8 and S9) show the effect of the inclination angle for the fine-grained material layers; two simulations (S10 and S11) illustrate the effect of different material properties; the last simulations (S12 to S17) investigate the effect of pile size on the water distribution and movement. The main objective of this work is to assess the potential effects of the internal structure and of some other key parameters on water movement inside the modeled pile.

Table 1: Simulated scenarios

Description	Simulation	Figure	Pile size	Main material	Fine-grained material	Number of layers	Layer inclination	Precipitation regime*
Base cases	S1	5	Large	GRV	-	-	-	P1-E
	S2	6	Large	SBL	-	-	-	P1-E
Effect of precipitation	S3	8	Large	GRV	-	-	-	P2-E
Effect of number of layers	S4	9	Large	GRV	SBL	1	Horizontal	P1-E
	S5	10	Large	GRV	SBL	2	Horizontal	P1-E
	S6	11	Large	GRV	SBL	3	Horizontal	P1-E
	S7	12	Large	GRV	SBL	4	Horizontal	P1-E
Effect of inclination angle	S8	13	Large	GRV	SBL	2	5%	P1-E
	S9	14	Large	GRV	SBL	2	10%	P1-E
Effect of material properties	S10	15	Large	GRV	SLT	2	5%	P1-E
	S11	16	Large	GRV	SLT	2	10%	P1-E
Effect of pile size	S12	17	Small	SBL	-	-	-	P1-E
	S13	18	Small	GRV	SBL	2	Horizontal	P1-E
	S14	19	Small	GRV	SBL	2	5%	P1-E
	S15	20	Small	GRV	SBL	2	10%	P1-E
	S16	21	Small	GRV	SLT	2	5%	P1-E
	S17	22	Small	GRV	SLT	2	10%	P1-E

* E: evaporation, P1: first cycle of precipitation, P2: second cycle of precipitation (E, P1 and P2 are shown in Figure 4), GRV: gravely, SBL: sandy, and SLT: silty materials

2. CHARACTERISTICS OF THE CONCEPTUAL MODEL

Analysing the hydrogeological behaviour of a waste rock pile is not a simple task. In this regard, numerical simulations can be quite useful to gain a better understanding of the influence factors that affect the pile response. Various codes can be used for modeling the flow within piles. The authors are using here the finite element code HYDRUS-2D (Simunek et al. 1999), which has also been used for

the flow analysis in smaller piles (Fala et al. 2003, 2005, 2006, 2008). This code uses Richards' (1931) unsaturated flow equation, which can be expressed as follows (for two-dimensional Cartesian coordinates, x, z):

$$\frac{\partial}{\partial x}\left[k_x(\psi)\frac{\partial \psi}{\partial x}\right]+\frac{\partial}{\partial z}\left[k_z(\psi)\frac{\partial \psi}{\partial z}\right]-\frac{\partial k_z(\psi)}{\partial z}=-\frac{\partial \theta}{\partial z} \quad [1]$$

In this equation, ψ is the water pressure (expressed as a head - L), θ is the volumetric water content (-), t is time (T), and k_x and k_z (L/T) are the pressure depend hydraulic conductivity in the horizontal and vertical directions respectively.

The two dimensional waste rock pile model, which is loosely based on an actual field case, has a base width of 260 m and a height of 109 m (Fig. 1a). The surface of the pile is open to atmospheric conditions. The base of the pile consists of two zones: the first zone (on the right hand side of Fig. 1a) is made of an impervious rock, and the second zone (on the left) represents the water table (i.e. part of the pile rests under water). The impervious vertical boundary condition imposed on the right hand side of the model corresponds to a line of separation for the flow net inside the pile. Line A-A shown in Figure 1a indicates the location where the profiles of the simulated results are created. The residual water content θ_r is applied as the initial condition in each simulation. Figure 1b shows the smaller pile, which is also analyzed in the latter part of the report. The same initial and boundary conditions are used for this small pile (with a base width of 65 m and a height of 27.25 m). The mesh, made of triangular elements, was generated using Hydrus-2D mesh generator tools. Figure 1c shows an example of the finite elements mesh used in this study. The number of elements varies from one simulation to another, depending on the number of compacted layers, their inclination angle and on the size of the pile. In general, the number of elements ranged between 32 000 and 130 000; the size of the elements

varies between 50 and 200 cm (elements sizes in the fine material layers are smaller than in the rest of the pile). Table 2 shows an example of the numerical parameters used for controlling solution convergence for some of the simulations conducted for this study (for more details about the definition of the numerical parameters, see Simunek et al. 1999). Typical calculation times for the simulations shown here varied between 2 and 14 days.

Table 2. Example of numerical parameters used for controlling the convergence of solution

Initial time	0
Final time	87600 hours
Initial time step	$1x10^{-10}$ hours
Minimum time step	$1x10^{-10}$ hours
Maximum time step	24 hours
Maximum number of iterations	20
Water content tolerance	0.0001
Pressure head tolerance	$1x10^{-5}$
Lower optimal iteration range	3
Upper optimal iteration range	7
Lower time step multiplication factor	1.3
Upper time step multiplication factor	0.7

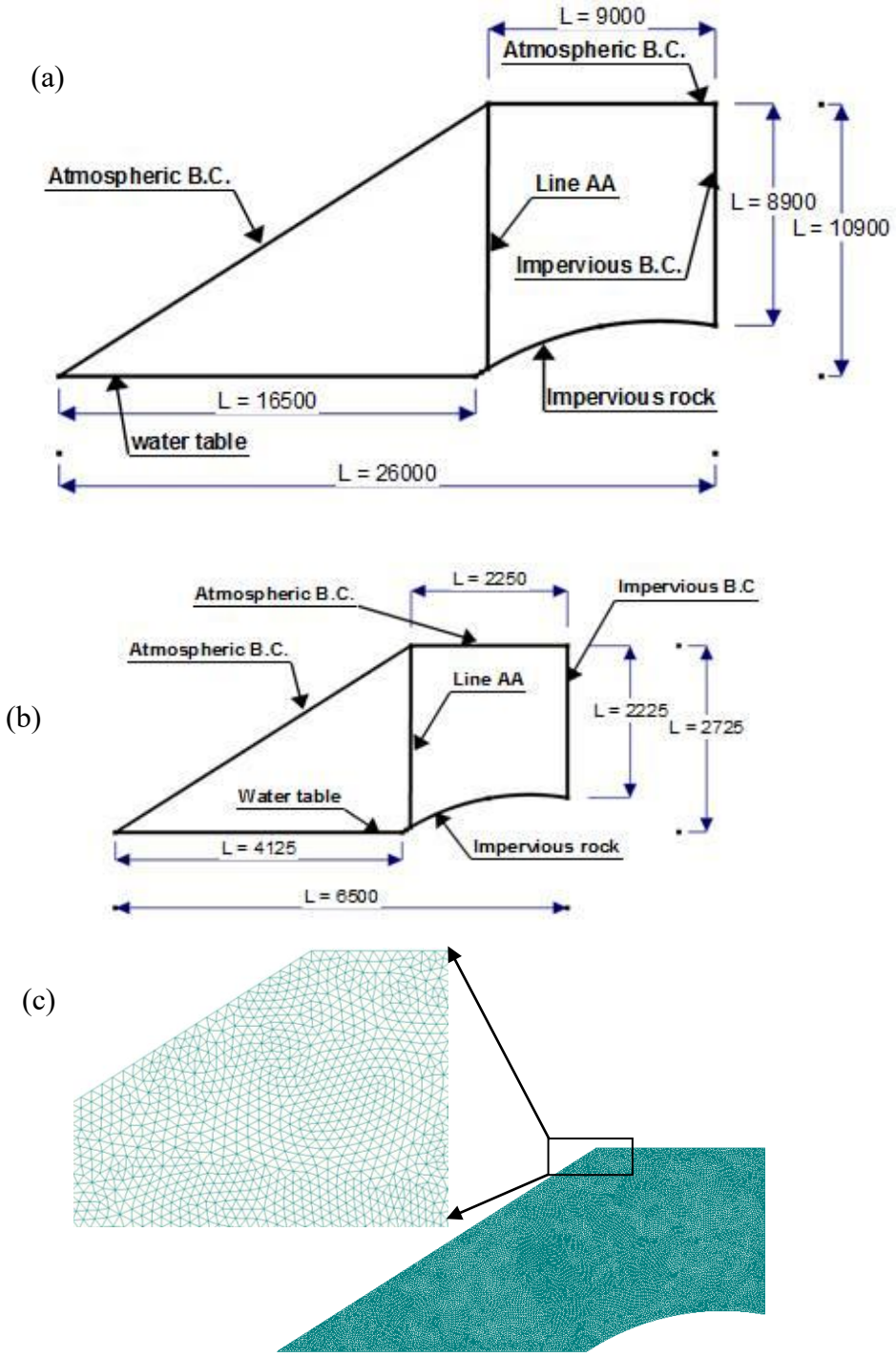

Figure 1: (a) Geometry and boundary conditions (B.C.) for the large waste rock pile, (b) Geometry and boundary conditions for the small waste rock pile and (c) example of a finite elements mesh; all dimensions are in cm.

Three types of materials are used to represent different fractions (or types) of waste rock inside the pile; these can be classified as very coarse (gravely-GRV), coarse (sandy-SBL), and relatively fine (silty-SLT). The materials properties have been obtained from laboratory and field tests conducted on waste rocks and similar materials in recent years (Aubertin et al. 2002 b; 2005; 2008; Bussière et al. 2002, 2011). The hydrogeological parameters for these materials are given in Table 2; these are based on the van Genuchten (1980) model for the water retention curve, and on the Mualem (1976) formulation for the unsaturated hydraulic function. The corresponding equations can be expressed as follows:

$$\theta_e = \frac{\theta - \theta_r}{\theta_s - \theta_r} = \left[\frac{1}{1 + (\alpha_v \psi)^{n_v}} \right]^{m_v} \qquad [2]$$

$$k(\theta_e) = k_s \theta_e^{\ell} \left[1 - \left(1 - \theta_e^{1/m_v} \right)^{m_v} \right]^2 \qquad [3]$$

In these equations, θ_e is the effective volumetric water content; θ_s is the saturated volumetric water content (equals the porosity n of the incompressible materials); θ_r is the residual volumetric water content; α_v, m_v and n_v (with $m_v = 1\text{-}1/n_v$) are the van Genuchten (1980) model parameters; $k(\theta_e)$ is the unsaturated hydraulic conductivity that depends on the water content (L/T); k_s is the saturated hydraulic conductivity; ℓ is a pore conductivity factor ($\ell = 0.5$). The parameters values given in Table 2 indicate that there are large differences in the hydraulic properties between the three types of materials. Figures 2 and 3 show the water retention curves and hydraulic conductivity functions for the three materials. The climatic conditions (i.e. cycles of precipitation – evaporation) used in this study are based on the monthly average values measured at the Latulipe, Quebec (Canada) monitoring station (P1-E), and (for the more humid regime) at Addis-Ababa, in Ethiopia, (P2-E). The monthly distributions are presented in Figure 4:

Table 3: The Mualem (1976) - van Genuchten (1980) model parameters for the materials used in the numerical simulations performed with HYDRUS-2D

Material	θ_r	θ_s	α_v (cm^{-1})	n_v	k_s (cm/s)
GRV	0	0.39	149.6	1.45	$4.7x10^{-1}$
SBL	0.01	0.29	0.03	3.72	$5.1x10^{-2}$
SLT	0.034	0.46	0.016	1.37	$6.9x10^{-5}$

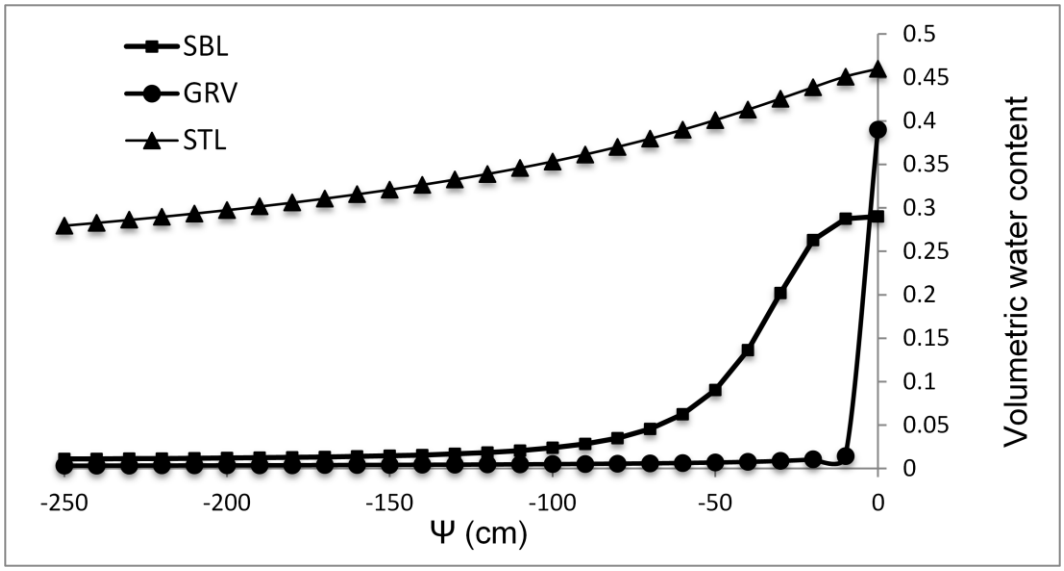

Figure 2: Water retention curves for the sandy (SBL), silty (STL) and gravelly (GRV) materials.

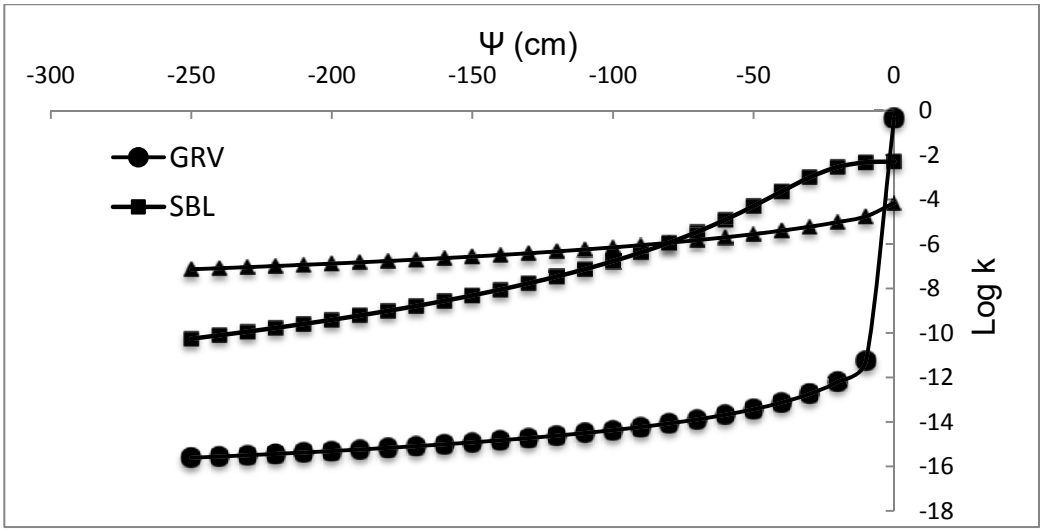

Figure 3: Hydraulic conductivity functions for the sandy (SBL), silty (STL) and gravelly (GRV) materials; the k values are expressed in cm/s.

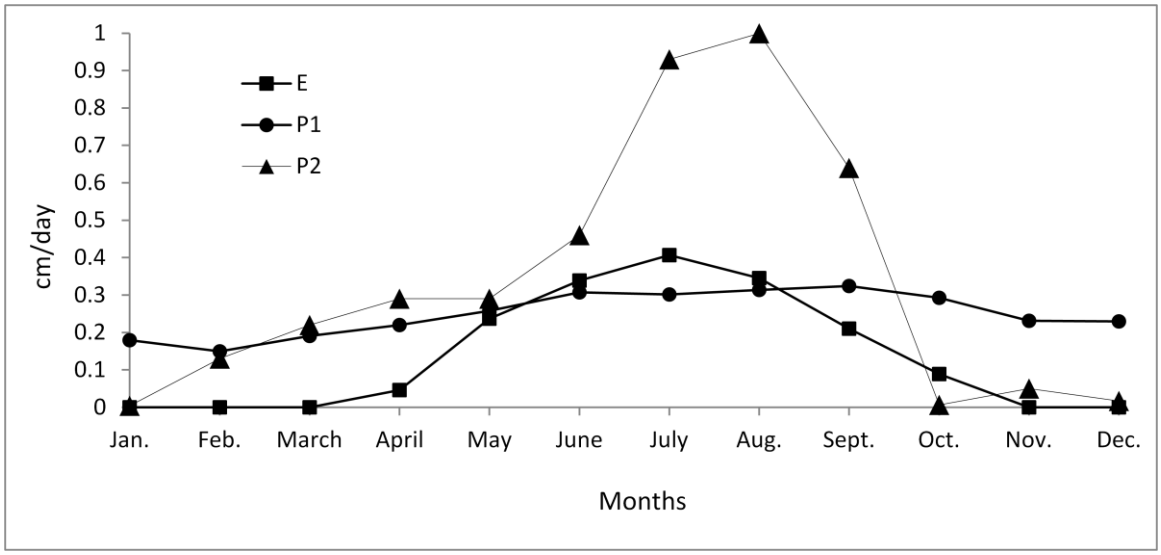

Figure 4: Cycles of Precipitation – Evaporation used in the simulations. P1: precepitation values at Latulipe; E: evaporation values at Latulipe, P2: precepitation values at Addis-Ababa.

3. SIMULATIONS RESULTS

3.1 Base Cases

3.1.1 Simulation S1 (GRV)

The gravely (GRV) material has been used in simulation S1 to model a homogeneous pile over a period of 10 years. Results at the end of December of the 10^{th} year are shown in Figure 5, which shows the contour distribution and the vertical profile (at line AA) of the volumetric water content θ. It is seen that the values of θ are less than 0.1 (it was nil at the beginning of the simulation: $\theta_{ini} = \theta_r = 0$). After 10 years, water dose not reach the bottom of the pile near its core (above the impervious rock). Figure A1, in Appendix A, shows the contours and the vertical profile (at line AA) of the volumetric water content at different times (end of December of the 2^{nd}, 4^{th}, 6^{th} and 8^{th} years). This figure shows that the values of θ are always around 0.1, but water tends to go deeper with time. It can also be noticed that near the inclined surface of the pile (left hand side of Figures 5 and A1), the infiltrating water is reach the water table faster, as can be expected due to the short vertical distance between the surface and the base

(compared with the distance near center of the pile). Also, the volumetric water content in the regions close to the surface is typically higher than in the rest of the pile due to the direct exposure to the infiltrating water. Contours distribution and vertical profiles (at line AA) of water velocity at the end of December of the 2nd, 4th, 6th, 8th, and 10th year are shown in Figure B1 (in Appendix B). This figure shows that water velocity varies between 0 and 0.035 cm/hr and that it follows the distribution of the volumetric water content. These results indicate that the infiltrating water front has traveled about 65 m near the center of the pile over 10 years.

3.1.2 Simulation S2 (SBL)

The conditions applied to simulation S1 are repeated in simulation S2, but the gravely material (GRV) is replaced by the sandy material (SBL); this reflects the fact that some piles (or portions of piles) have hydrogeological properties similar to those of sandy soils. Figure 6 shows simulation results at the end of December of the 10th year. It is seen that the θ values are less than 0.05 in the pile, except just above the impervious rock where the volumetric water content is around 0.13. Additional results show that water front reaches the base of the pile, at its core, after about 6 years (see Figure A2, in Appendix A). The contours distributions and vertical profiles (at line AA) of water velocity v shown in Figure B2 (Appendix B) indicate that this velocity remains under 0.012 cm/hr, except just above the impervious rock at the base where v can reach 0.8 cm/hr. Figures A2-G, A2-H, B2-C, B2-D, and B2-E in Appendixes A and B indicate that the values of θ and v evolve during the year, but these are repeated monthly each year after the 6th year of simulation (for the same recharge). To illustrate this aspect, the contours of θ at the end of March, June, September and December of the 10th year are selected and shown in Figure 7. It is seen that the values of θ are different from month to other, while these are the same for a specific month after the 6th year of simulation. The comparison between the results of simulation S1 (GRV) and simulation S2 (SBL) shows that the θ values in the GRV are larger than in

the SBL; this tendency is due to the larger porosity (Table 2) and lower unsaturated hydraulic conductivity (Figure 3) of the gravely material. Also, in simulation S2 (SBL), the main wetting front reaches the base (near the center of the pile) after 6 years, while it does not reach the base of the pile in simulation S1 (GRV) after 10 years.

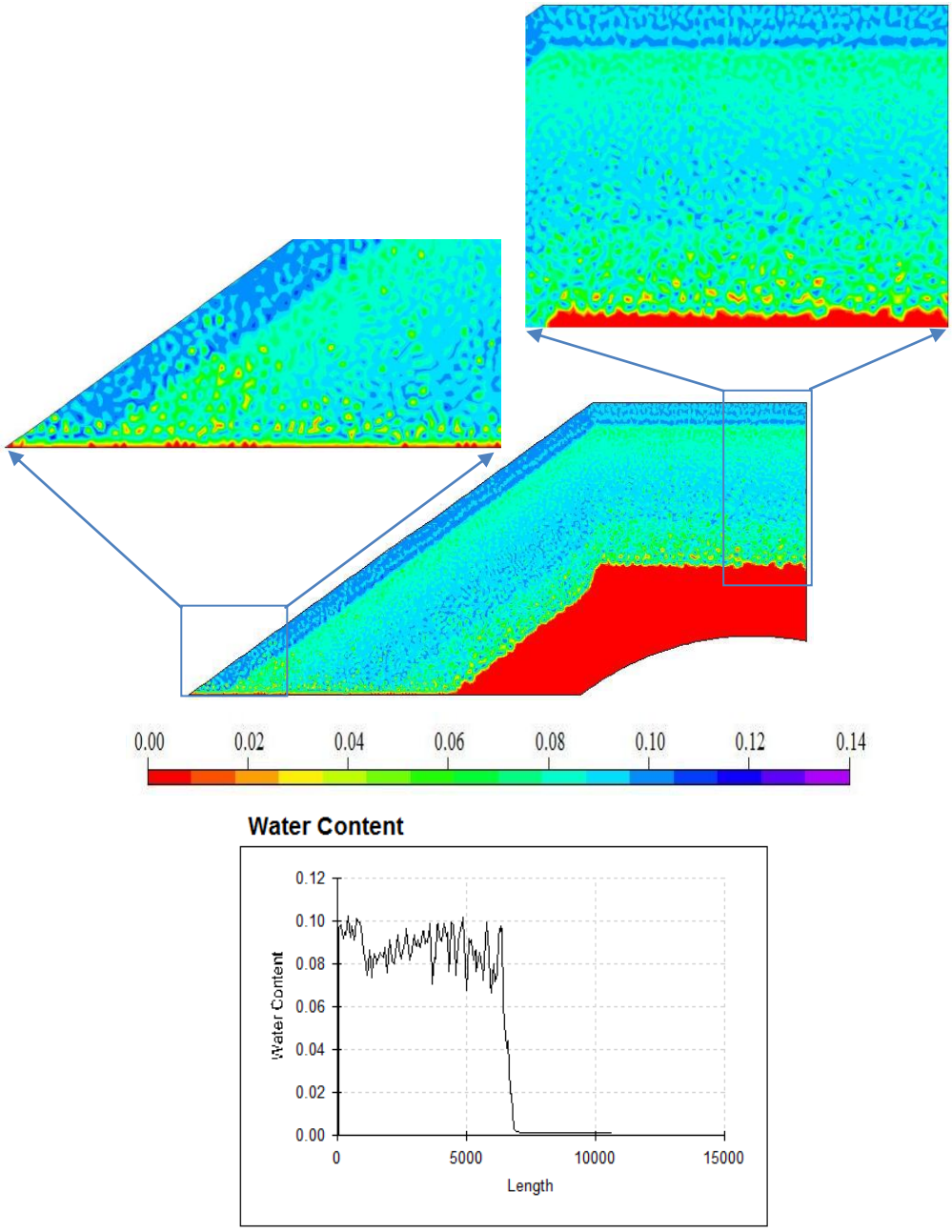

Figure 5: Contours and vertical profile (at line AA) of the volumetric water contents for simulation S1 (GRV) at the end of December of the 10th year

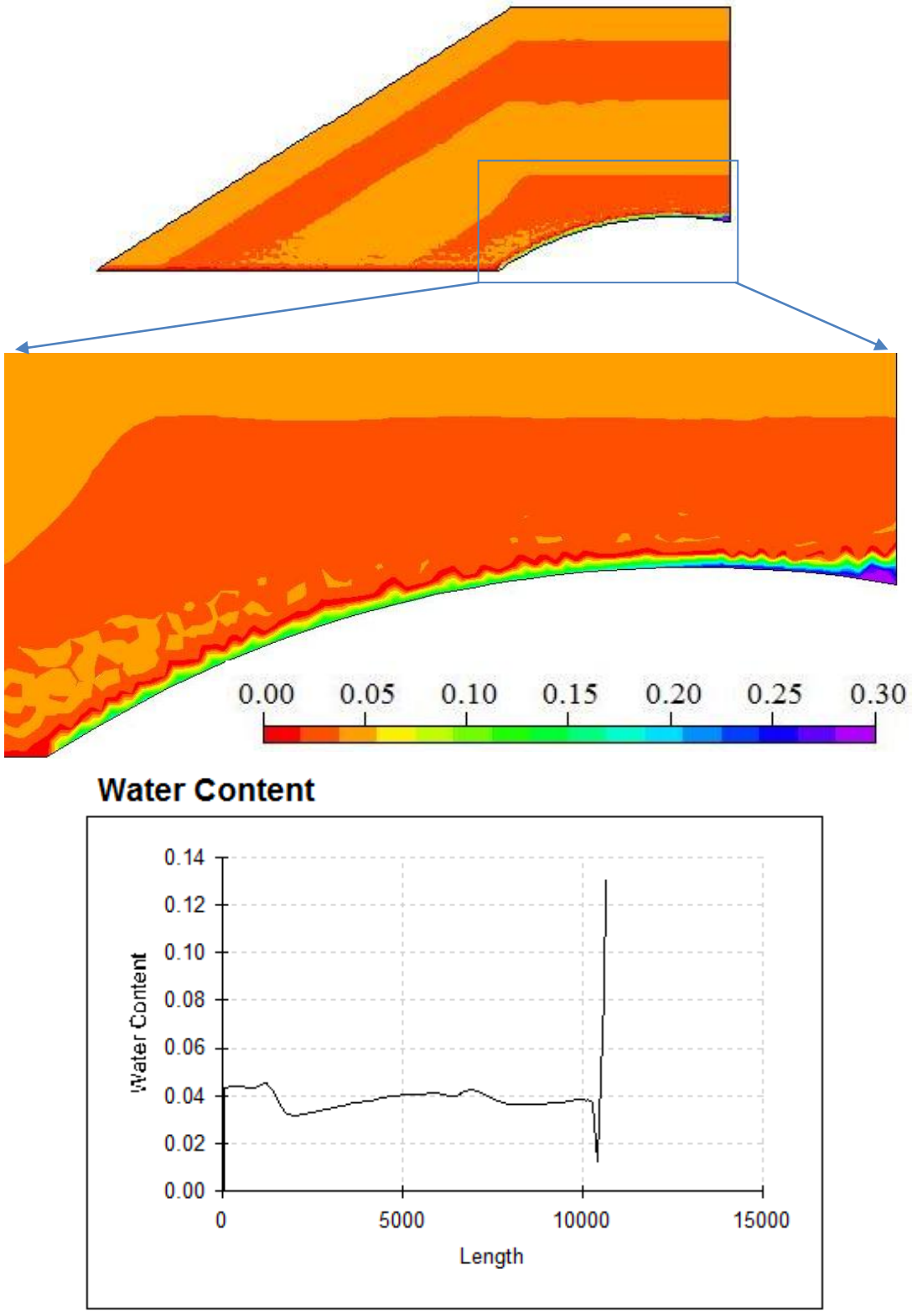

Figure 6: Contours and vertical profile (at line AA) of the volumetric water contents for simulation S2 (SBL) at the end of December of the 10th year

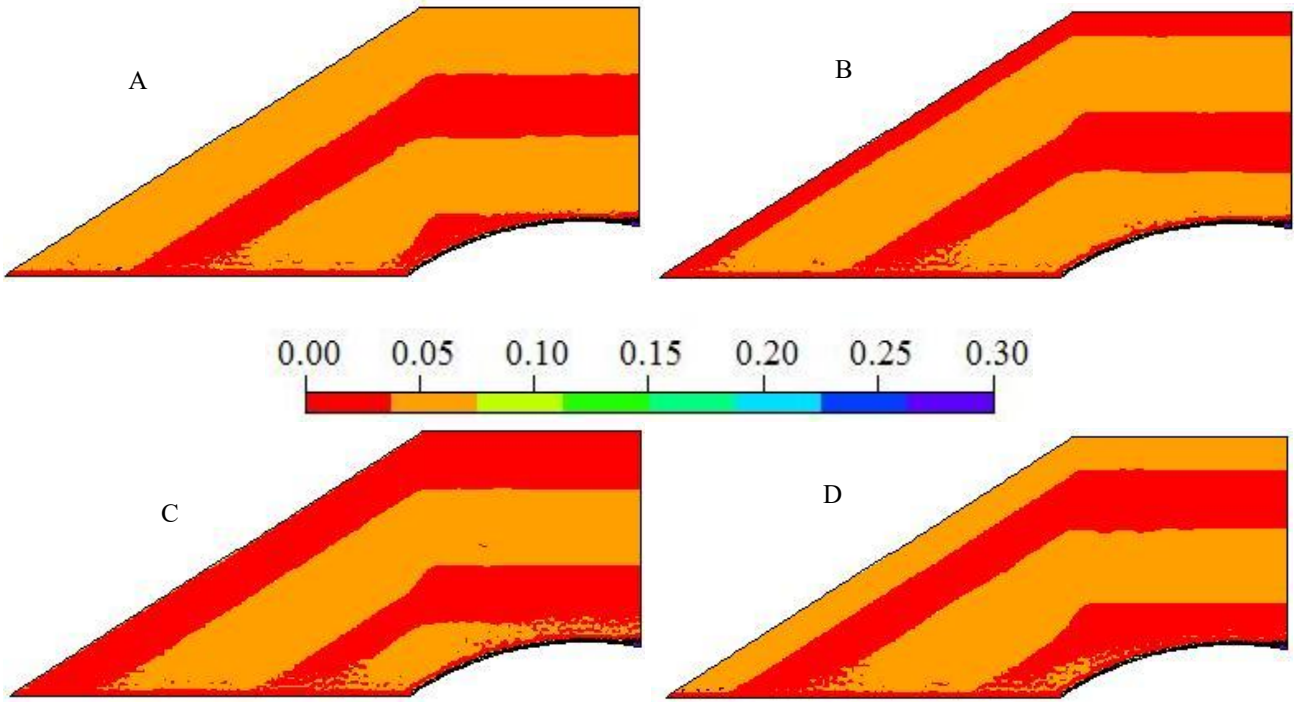

Figure 7: Results from Simulation S2: Contour distribution of the volumetric water content at different months at the 10th year: A) March, B) June, C) September and D) December.

3.2 Effect of Recharge

Two different annual precipitation-evaporation cycles (figure 4) have been used to assess the influence of surface recharge on the movement and distribution of water through the waste rock pile. Simulation S1 is repeated in simulation S3, replacing the precipitation cycle of Latulipe with that of Addis-Ababa (which increases the recharge by about 35 %). The results of simulation S3 are shown in Figure 8. It is seen that the volumetric water content along line AA is typically close to 0.1 down to a depth 87 m, beyond which it drops to almost zero. Figure 8 and Figure A3 in Appendix A also show that there are no significant differences in the values of θ for cases S1 and S3, except for the depth traveled inside the pile by the wetting front (larger for S3). Water velocity shown in Figure B3 in Appendix B indicates that v reaches up to 0.035 cm/hr in some locations inside the pile, although it generally remains low (< 0.05 cm/hr) . This result demonstrates that the magnitude of the recharge (infiltration)

has an impact on the arriving time of water at the base of the pile. This is due to the increased hydraulic conductivity associated with higher volumetric water content. Larger precipitations can thus be expected to transport contaminants more quickly to the groundwater system in such homogenous pile.

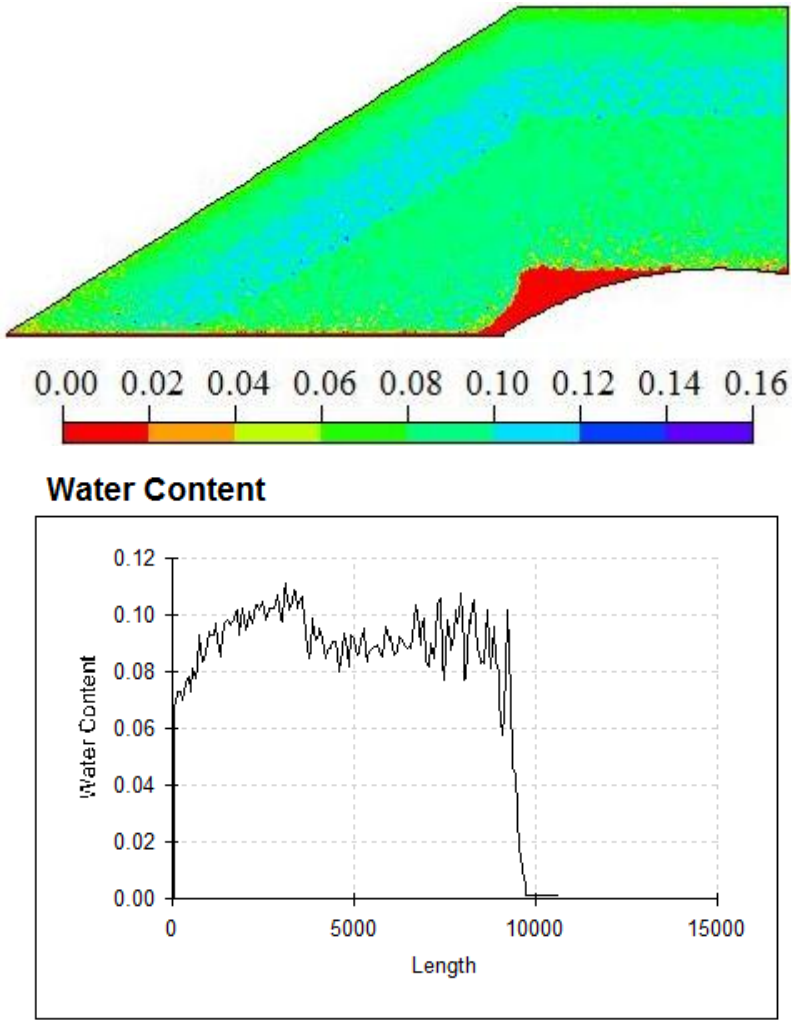

Figure 8: Contours and vertical profile (at line AA) of the volumetric water contents for simulation S3 (GRV, precipitation cycle P2-E) at the end of December of the 10th year

3.3 Effect of Fine Grained Material Layers

Previous calculations have shown that compacted layers, made with denser and finer materials, tend to modify the transient flow of water inside a 25 m high waste rock pile (Fala et al. 2003, 2005). This aspect is investigated here for the much larger pile shown in Figure 1a. It should be noted that the layers added on top of and (in some cases) inside the pile have in irregular interface with the coarser material of the pile; this can favor water accumulation in local troughs that exist along the contact between the finer and coarser materials, which can then lead to localized flow, as will be shown below (see also Fala et al. 2005, 2005, 2006).

3.3.1 Number of Layers

A layer of sandy material (SBL), 0.5 m thick, was added on top of the pile made of GRV material in simulation S4. This horizontal layer represents the effect of surface compaction due to the heavy equipments (Aubertin et al. 2002b, 2005). The calculations were conducted with the same initial and boundary conditions as used above (Figure 1 and Tables 1 and 2). Figure 9 shows the distribution of the volumetric water contents (θ) at the end of December of the 10^{th} year. It is seen that θ values are higher in the sand layer, due in part to the creation of a capillary barrier effect between the finer and coarser material layers on top of the pile. However, Figures 9 and A4 (Appendix A) also show that there is little effect of this sand layer on water transport inside the pile itself. The horizontal sand layer causes a local accumulation of water that eventually escapes downward, causing more localised flow zones in the pile. Figures 9 and A1 show that the θ value in the sandy layer (90 m long and 0.5 m thick) is varying between 0.05 and 0.25, while it is around 0.1 in the rest of the pile. Figure B1 (Appendix B) shows that the water velocity in the sandy layer is varying between 0.005 to 0.01 cm/hr, while it is between 0 and 0.03 cm/hr elsewhere. The comparison between the base case (S1, GRV) and simulation

S4 (GRV with a sand layer) indicate that some of the water reaches the base of the pile faster in the latter case due to the localized (preferential) flow zones.

Two horizontal sandy material layers are added to the pile in simulation S5: one on top (90 m long and 0.5 m thick) and one at mid-height (185 m long, with the same thickness) to represent the effect of a previously compacted surface. The results of the simulation after 10 years (end of December) are shown in Figures 10, A5, and B5 (Appendixes A and B). The vertical profile of the volumetric water content along line AA shows the creation of capillary barrier effects due to the different hydraulic properties of the sandy (SBL) and gravelly (GRV) materials, and an increased number of localized flow paths. The volumetric water content in the upper sand layer is varying between 0.04 and 0.15 and it varies between 0.06 and 0.18 in the mid-height sand layer, while the value of θ in the rest of the pile stays below 0.12. Water velocities in the top sandy layer are varying between 0.005 cm/hr (near the upper surface of the layer) and 0.1 cm/hr (near the lower surface of the layer). Also, at mid-height layer, water velocities are varying between 0 and 0.07 cm/hr, while it is under 0.035 cm/hr for the rest of the pile.

Three horizontal sandy layers (90 m, 136 m and 182 m long, respectively, with a thickness of 0.5 m) were added at regular intervals in the pile in simulation S6. The volumetric water content distribution with three layers also indicates the presence of capillary barriers effects (Figures 11 and A6). The volumetric water content value in the top layer varies between 0.05 and 0.15.In the second and third sandy layers, the value of θ varies between 0.01 and 0.014, while it is lower than 0.12 in the rest of the pile. Figure B6 (Appendix B) shows that water velocity after ten years is varying between 0 and 0.08 cm/hr in the top layer (near the upper and lower surfaces of the layer, respectively), between 0 and 0.06 in the second layer (near the upper and lower surfaces of the layer, respectively), and between 0 and 0.04 cm/hr in the third layer (near the upper and lower surfaces of the layer, respectively) and in the rest of the pile.

Four horizontal sandy layers (90 m, 124 m, 159 m and 194 m long, with the same thickness) were added at regular intervals in the pile in simulation S7. The volumetric water content distribution within the four layers also indicates the presence of capillary barriers effects (see Figures 12 and A7). The volumetric water content in the first and second sandy layers varies between 0.04 and 0.15. In the third sandy layers, the θ value varies between 0.04 and 0.17; in the fourth sandy layer, the value of θ varies between 0.06 and 0.2; in the rest of the pile, θ varies between 0.01 and 0.12. Figure B7 in Appendix B shows that vertical velocity at the end of December of the 10^{th} year varies between 0 and 0.07 cm/hr for the entire pile (including the fine-grained material layers).

Comparison between the results from simulations S4, S5, S6, S7 (Figures 9, 10, 11, and 12) with the base case (S1, Figure 5, with only the GRV material) shows that water trends to accumulate inside the compacted layers and then move down along preferential flow path created below the SBL-GRV interfaces. This type of horizontal layers tends to cause a more rapid flow of water, deeper inside the pile, and creates preferential flow zones. The same observations were made following short term simulations of water flow inside a smaller pile with horizontal layers (Fala et al. 2003, 2005). As such layers are expected to exist in actual waste rock piles (Dawood et al. 2011), these results suggest that the water flow in large piles is largely influenced by the internal structure, with water moving deeper and faster in layered piles than within idealised homogeneous piles (as is the case in smaller piles; Fala et al. 2003, 2005).

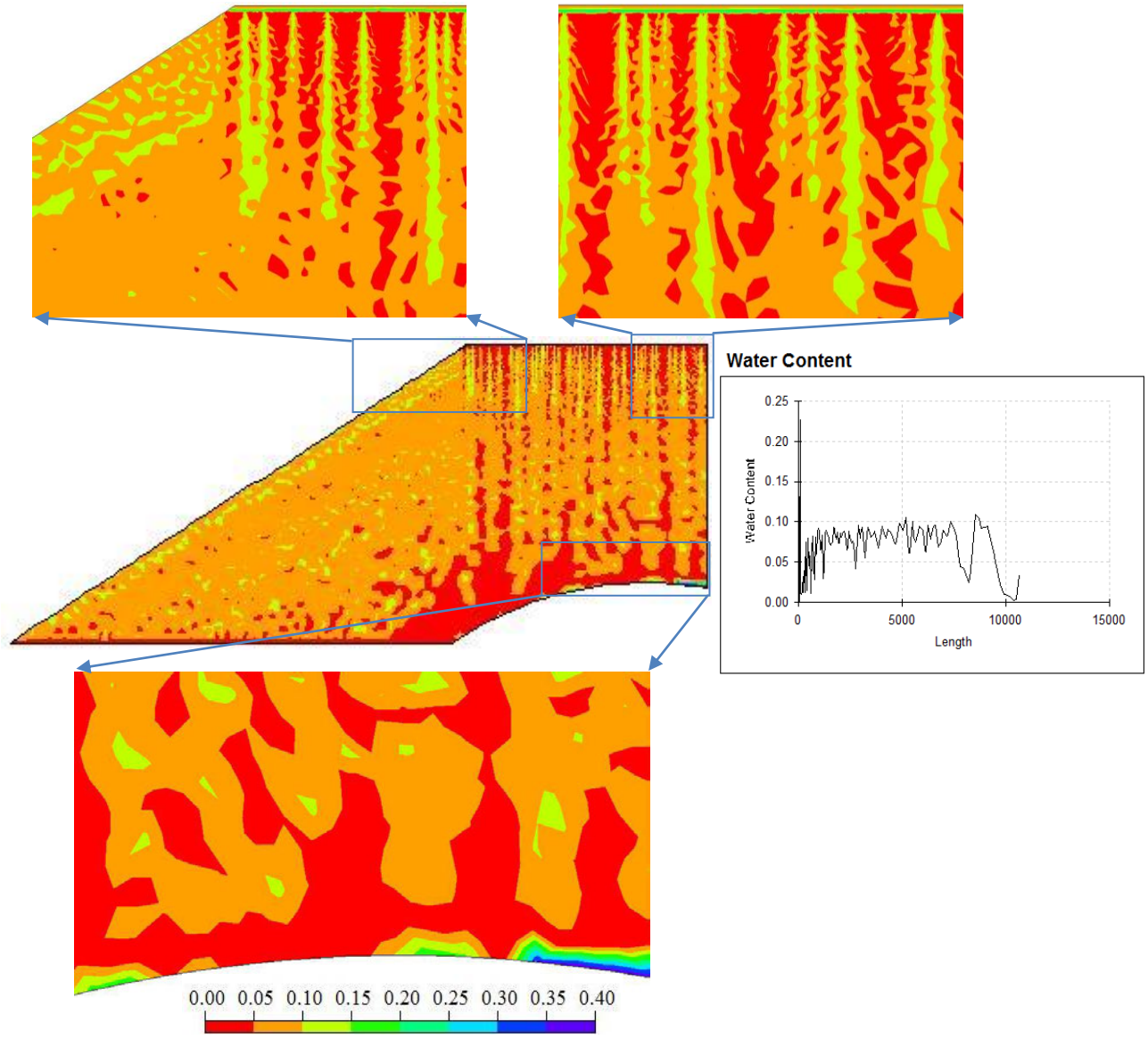

Figure 9: Contours and vertical profile (at line AA) of the volumetric water contents for simulation S4 at the end of December of the 10th year. One sand layer is added on top of the pile.

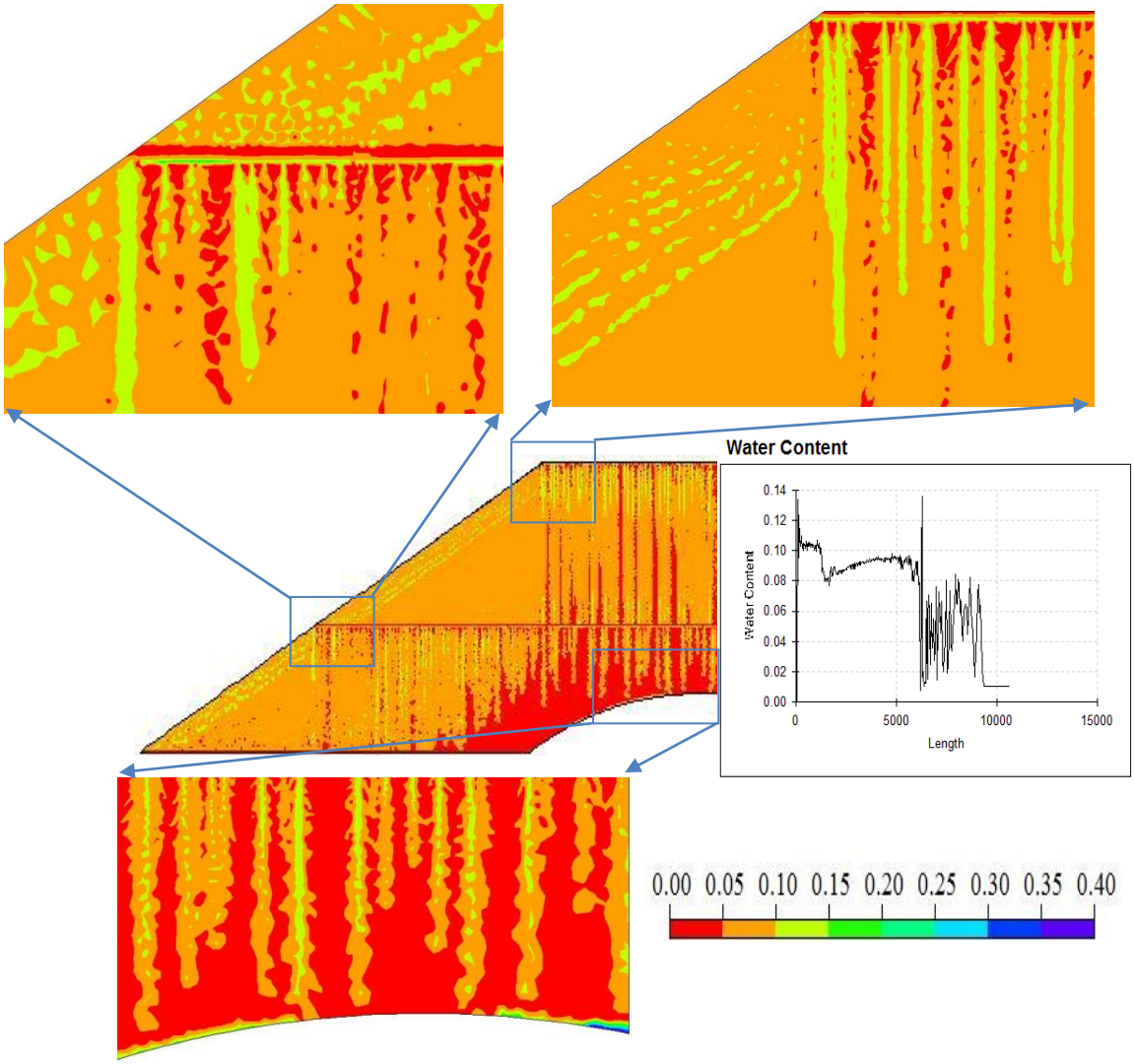

Figure 10: Contours and vertical profile (at line AA) of the volumetric water contents for simulation S5 at the end of December of the 10th year. Two sand layers are added on top and at mid-height of the pile.

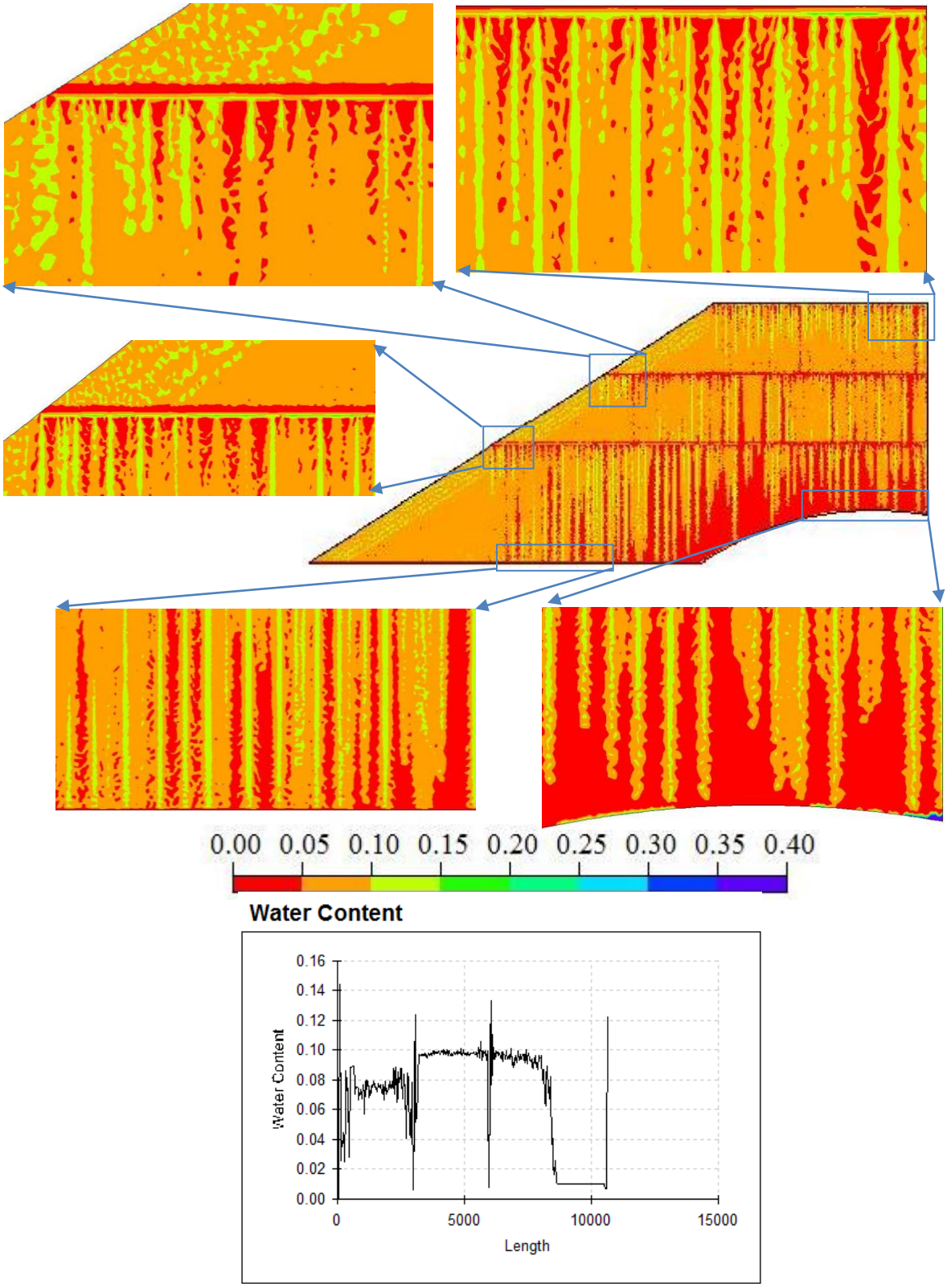

Figure 11: Contours and vertical profile (at line AA) of the volumetric water contents for simulation S6 at the end of December of the 10th year. Three sand layers are added on top and inside the pile.

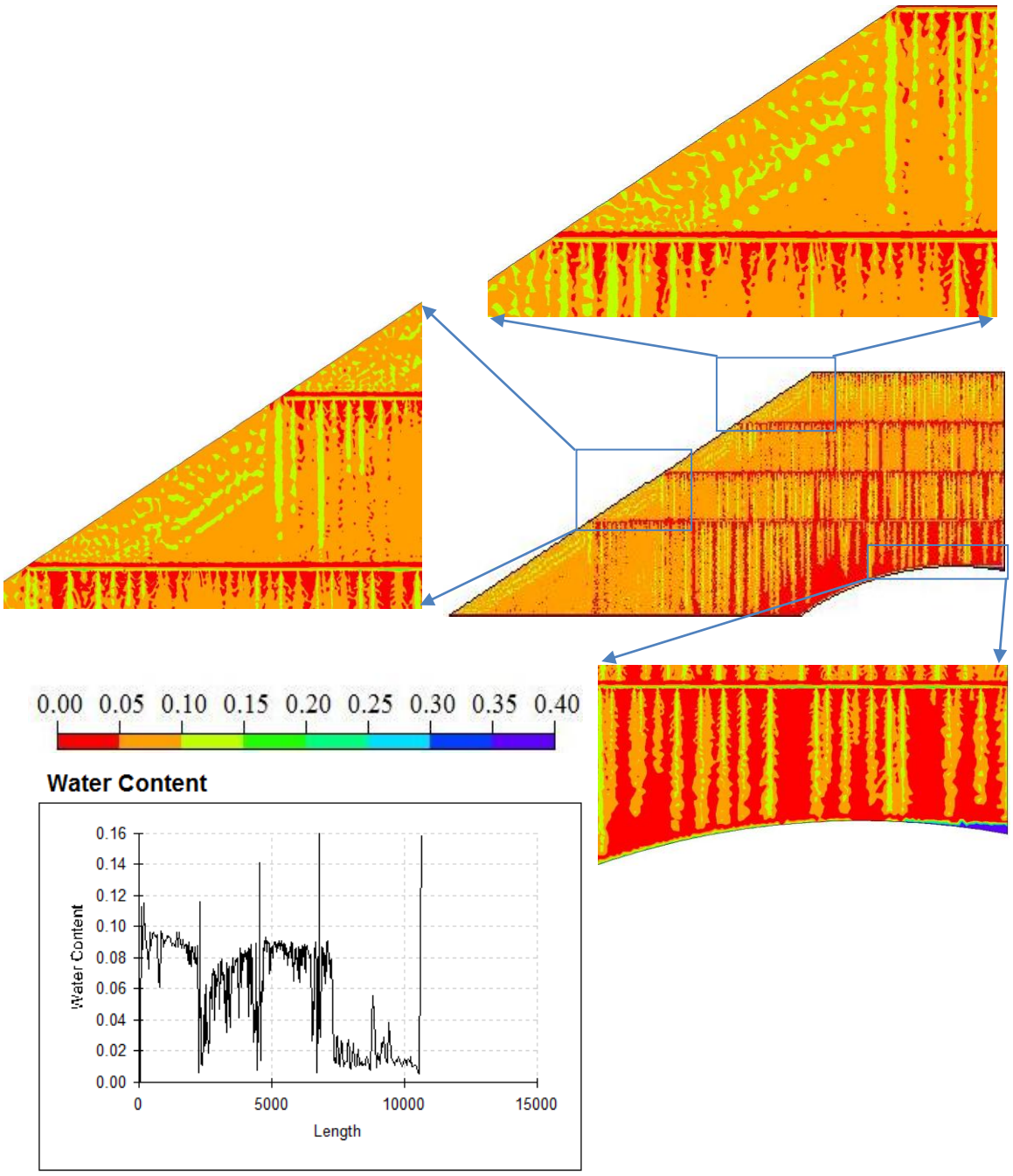

Figure 12: Contours and vertical profile (at line AA) of the volumetric water contents for simulation S7 at the end of December of the 10th year. Four sand layers are added on top and inside the pile.

3.3.2 Inclined Layers

Earlier simulation results (Fala, 2002; Fala et al. 2003, 2005, 2006; Molson et al. 2005) have shown that fine-grained (sandy) material layers can be used to reduce water flow deep inside a relatively small pile when these layers are inclined outward. In the next simulations, two sandy layers (S8 and S9) are introduced with inclinations of 5% and 10% to assess their effect on the movement of water through the large pile modeled here.

- *Slope of 5%*

Two sandy layers (located on top and at mid height of the pile) are inclined at 5% outward (simulation S8). The results after 10 years (at the end of December) are shown in Figure 13. The volumetric water content in the first layer varies between 0.04 and 0.27 and in the second layer between 0.04 and 0.24, while it is under 0.12 for the rest of the pile. Also, Figure B8 in Appendix B shows that the vertical velocity varies between 0.001 and 0.7 cm/hr (near the upper and lower surfaces of the layer, respectively), for the first layer, and between 0.001 and 0.3 cm/hr for the second layer (near the upper and lower surfaces of the layer, respectively), while it is under 0.05 cm/hr for the rest of the pile. More results on the volumetric water content and water vertical velocity for simulation S8 are shown in Figures A8 and B8 (Appendices A and B), respectively.

- *Slope of 10%*

An additional simulation (S9) was conducted with sandy layers inclined at 10%. The results shown in Figures 14 and A9 indicate that that the volumetric water content varies between 0.04 and 0.12 in the top sand layer, and between 0.04 and 0.16 in the second sand layer, while it is below 0.10 in the rest of the pile. Water velocity is ranging between 0.001 and 0.05 cm/hr in the top layer (near the upper and lower surfaces of the layer, respectively), and between 0.001 and 0.14 cm/hr in the second layer (near the upper and lower surfaces of the layer, respectively), while it is below 0.03 cm/hr in the rest of the

pile. More results on the volumetric water content and water velocity for simulation S9 are shown in Figures A9 and B9 (Appendices A and B), respectively.

Table 3 shows a comparison between the results of simulations S5, S8 and S9. Comparing results from simulation S5 (Figure 10, with two horizontal sandy layers) with those from simulation S8 indicates that the 5% inclination of the two sandy layers increased the volumetric water content along the interface between the SBL layers and the rest of the pile. It is also seen that water is moving preferentially toward the external boundary (left hand side) of the pile within the sandy layers.

These tend to show that inclined layers can help control the flow in piles, by creating areas (in the core of the pile) where there is less water and a lower velocity. However, these results are not fully conclusive for the case of this large pile, when the base of the layers has an irregular geometry (instead of a flat contact area).

The comparison of the results from simulation S8 with those from S9 shows that the θ value in the first sandy layer inclined at 10% is smaller than in the case of a 5% inclination. The same tendency is observed for the second sandy layer. Also, water vertical velocity in the two sandy layers in the case of 10% inclination is smaller than in the case of 5% inclination. This comparison indicates that a more pronounced inclination of the two sandy layers (at 10%) can help reduce the values of θ and v inside the pile, more efficiently than with the 5% inclination.

The comparison of the results from simulations S8 and S9 with those obtained from simulation S5 (two horizontal SBL layers) also indicates that the inclination of the finer material layers tends to increase water content and velocity in these layers, hence favoring water flow in the direction of the external boundary of the pile. The inclined layers also create areas with a lesser water content in the pile, especially in the case of a 10 % inclination. However, the irregular shape of the interfaces between the finer and coarser materials and the relatively large spacing between the inclined layers limits the effects of these layers on water flow. These two geometrical factors need to be assessed further.

Table 4. Comparison between simulations S5, S8 and S9

		Simulation S5 (2 horizontal SBL layers)	Simulation S8 (2 SBL layers inclined at 5%)	Simulation S9 (2 SBL layers inclined at 10%)
1st layer	θ	0.04 – 0.15	0.04 – 0.27	0.04 – 0.12
	v (cm/hr)	0.001 – 0.1	0.001 – 0.7	0.001 – 0.05
2nd layer	θ	0.04 – 0.18	0.04 – 0.24	0.05 – 0.16
	v (cm/hr)	0.001 – 0.07	0.001 – 0.3	0.001 – 0.14
Rest of the pile	θ	< 0.12	< 0.12	< 0.1
	v (cm/hr)	< 0.035	< 0.05	< 0.03

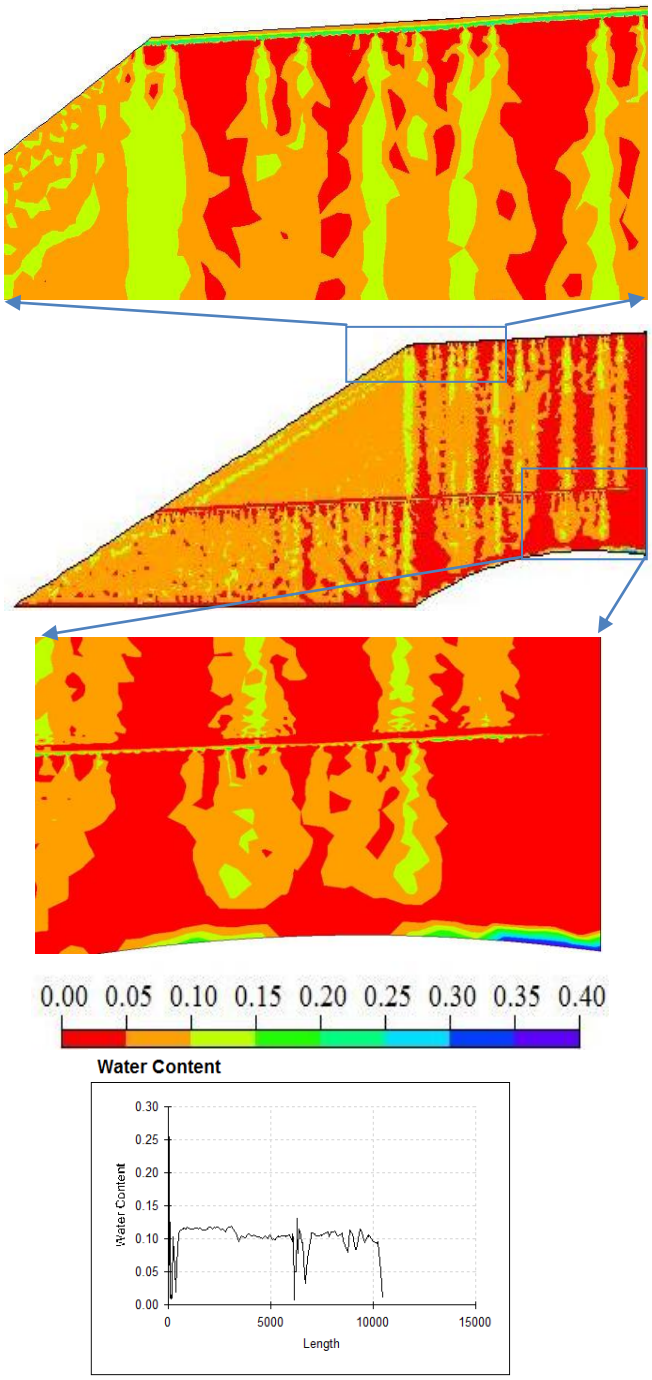

Figure 13: Contours and vertical profile (at line AA) of the volumetric water contents for simulation S8 at the end of December of the 10th year. The two sand layers added on top and at mid-height of the pile are inclined at 5%.

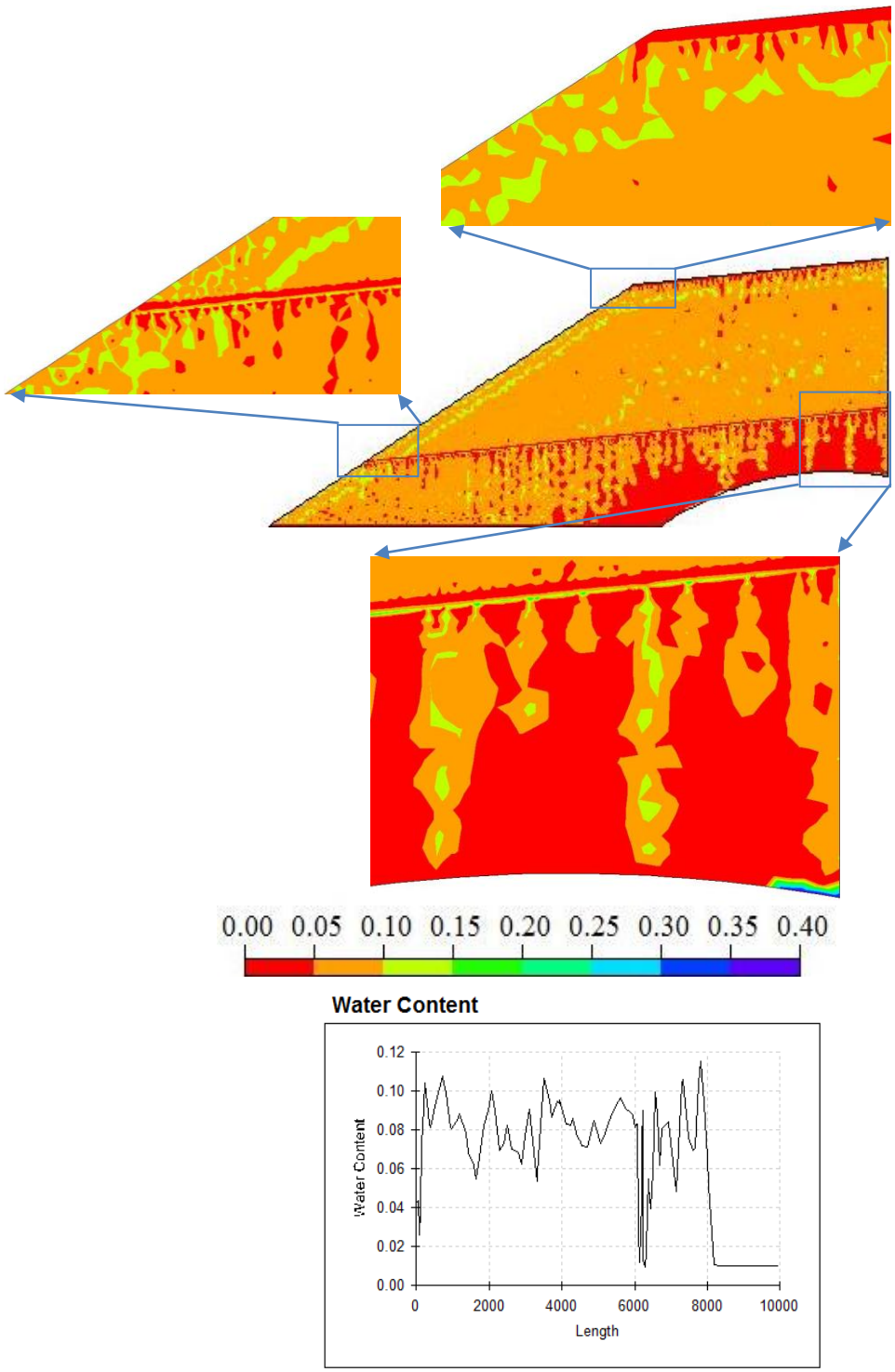

Figure 14: Contours and vertical profile (at line AA) of the volumetric water contents for simulation S9 at the end of December of the 10th year. The two sand layers added on top and at mid-height of the pile are inclined at 10%.

3.3.3 ***Properties of the Fine Grained Material Layers***

In the next simulations, the sandy material SBL (used in simulations S8 and S9) was replaced with a finer (silty) grained material, in order to increase the contrast in hydraulic properties between the gravely waste rock and the compacted layers. The hydraulic properties of the silty (SLT) material layers are given in Table 2. This material has a lower saturated conductivity and a larger air entry value (AEV) than the SBL (and GRV). Figure 15 shows the results of simulation S10 when two silty material layers (inclined at 5%) are used. The comparison of these results with those obtained from simulation S8 indicates that the volumetric water contents in the inclined layers are increased from 0.27 (SBL layers) to 0.4 (SLT layers), while it is around 0.12 in the rest of the pile for both cases. The maximum vertical velocity in the first layer decreased from 0.7 cm/hr (for S8) to 0.02 cm/h (for S10) and from 0.3 cm/hr (for S8) to 0.017 cm/hr (for S10), while it is about 0.014 cm/hr in the rest of the pile in both cases (see Figures A8 and A10 in Appendix A for more results).

Two silty layers inclined at 10% are included in the pile with simulation S11. The results shown in Figure 16 indicate that the volumetric water content in the silty layers is around 0.4, while it is less than 0.12 in the rest of the pile. Figure B11 shows that water vertical velocity in the two SLT layer varies between 0 and 0.035 cm/hr, while it is below 0.014 cm/hr for the rest of the pile. More results are shown in Figure A11 and B11 in Appendices A and B, respectively. These results indicate that the silty layers inclined at 10 % can be more efficient in creating areas inside the pile with lower volumetric water content and velocity.

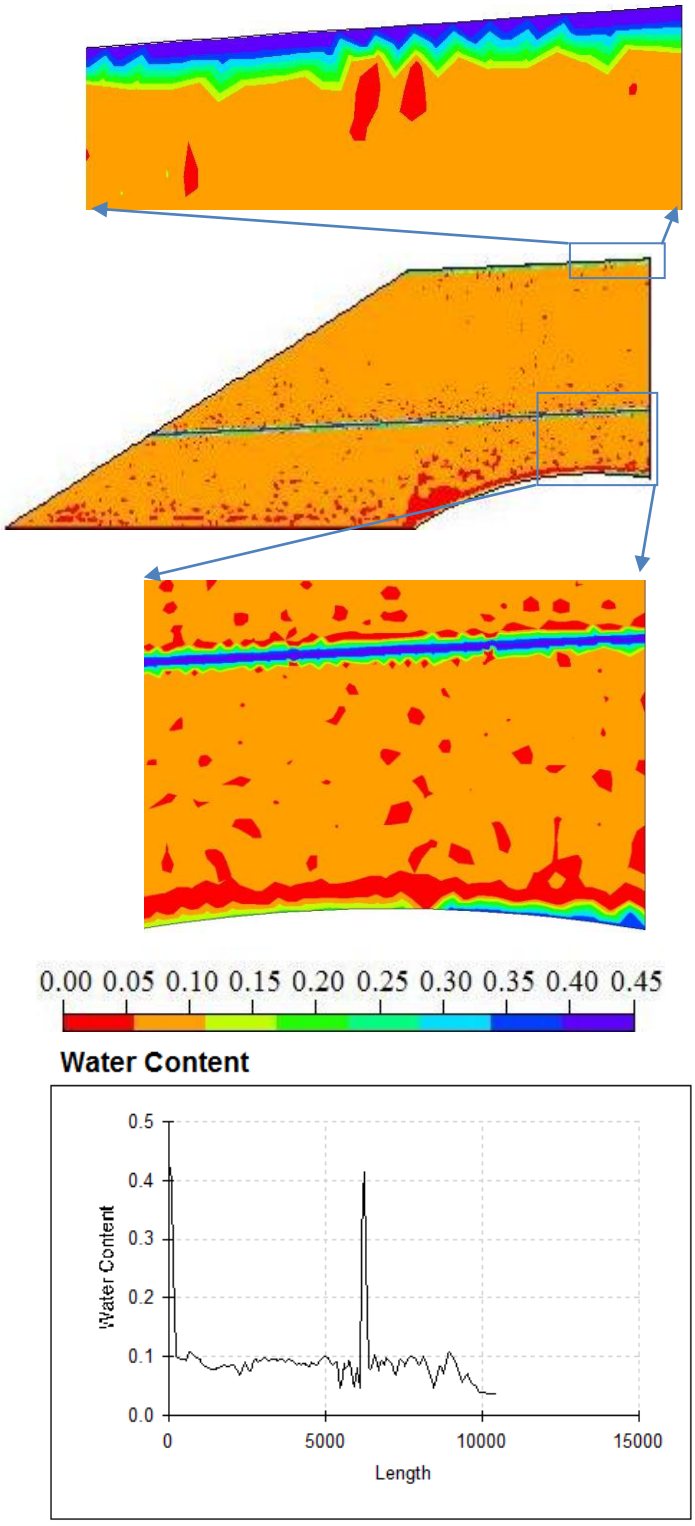

Figure 15: Contours and vertical profile (at line AA) of the volumetric water contents for simulation S10 at the end of December of the 10th year. The two silt layers added on top and at mid-height of the pile are inclined at 5%.

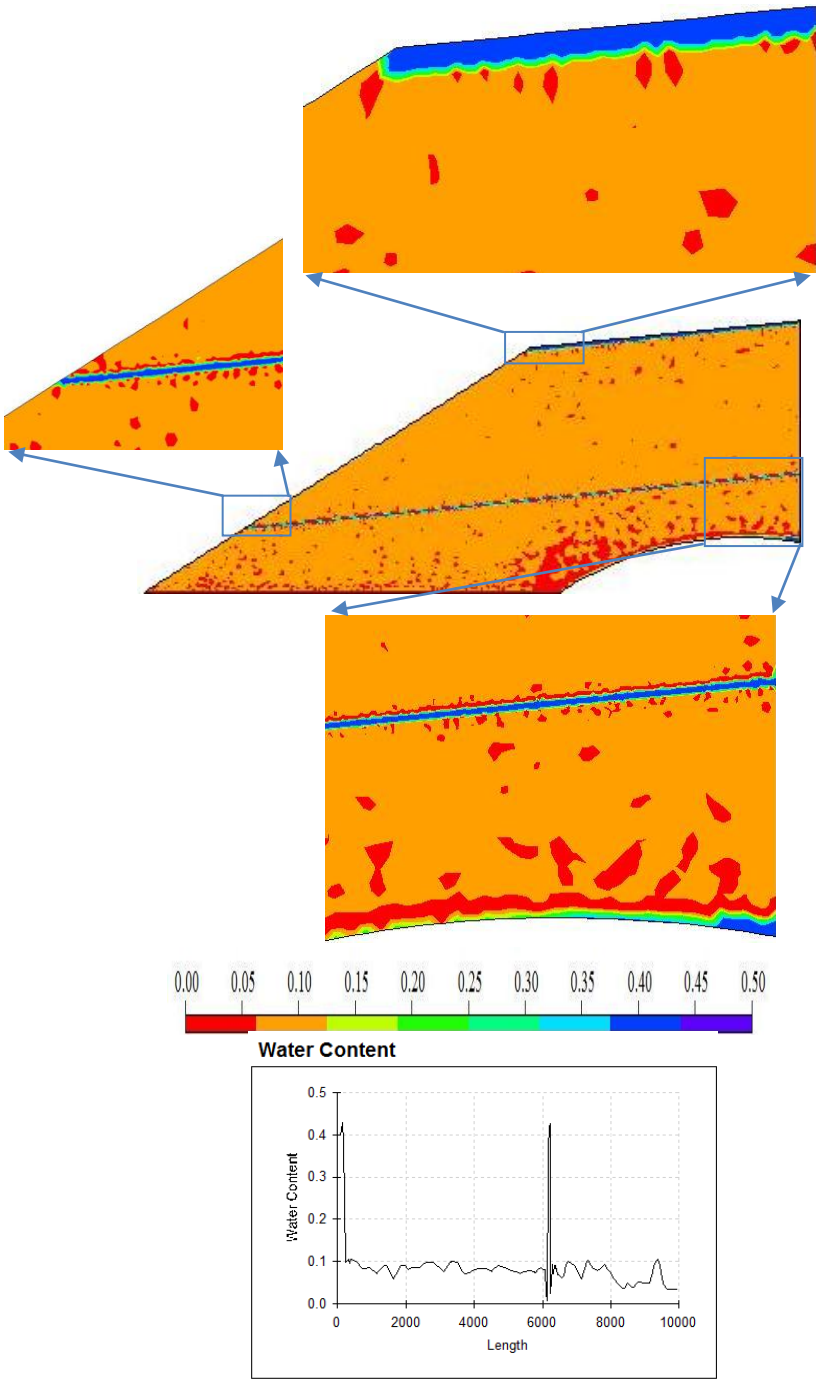

Figure 16: Contours and vertical profile (at line AA) of the volumetric water contents for simulation S11 at the end of December of the 10th year. The two silt layers added on top and at mid-height of the pile and inclined at 10%.

3.4 Effect of Pile Size

The size of the waste rock pile may affect its hydrogeological (and environmental) behaviour. Simulations were conducted on a smaller pile, 65 m in width and 27.25 m in height (which represents 1:4 of the large pile, Figure1b) to assess the influence of the size. Simulations S2, S5, S8, S9, S10, and S11 were repeated in S12, S13, S14, S15, S16, and S17 using the smaller pile size with the same boundary and initial conditions.

The comparison between the results of simulations S2 and S12 (Figures 6 and 17) shows that there is no significant difference for the two piles (large and small) made with the GRV material in terms of the volumetric water content and vertical water velocity along line AA and in the entire pile ($\theta \approx 0.04$ and $v \approx 0.012$ cm/hr), and also just above the impervious rock ($\theta \approx 0.14$ and $v \approx 0.8$ cm/hr).

The effects of two horizontal sandy layers are about the same in the small and large pile (S5 and S13). Figures 10 and 18 show that the volumetric water content is similar in both cases (under 0.1 in the waste rock and above 0.1 in the sand layers). Figures 13 and 19 show that inclining of the two sandy layers at 5% (in the small pile, S14), also produces similar θ and v values to those obtained with simulation S8 (for the large pile), It is also seen that in the right hand side of the pile (Figure 13), close to the imposed flow boundary, there are larger areas where θ is close to θ_r (i.e. water does not flow in these areas). Hence, the two sandy layers inclined at 5% produce more favorable effects, by creating areas inside the pile with limited or no water flow. The inclination of the sandy layers at 10% (simulation S15, for the small pile) leads to even larger areas with limited water flow on the right hand side of the pile, as shown in Figure 20. The comparison between simulations S9 and S15 (Figures 14 and 20, for the large and small piles, respectively) shows that the 10% inclination of the sandy layers is more effective to control water flow inside the small pile than with the larger pile. The same observation applies to the comparison between simulations S10 and S11 (for the large pile) and S16 and S17 (for the small pile),with two silty layers inclined at 5% and 10% (as shown in Figures 15, 16,

21 and 22, respectively). It can thus be concluded that the effect of the fine material layers on water flow inside a waste rock pile depends on its size, the inclination angle of the layers, and their vertical spacing (when the same materials and boundary conditions are used). It is also seen that the wetting front in the smaller pile reaches the base faster, leading to increased volumetric water content and water velocity near the bottom of the pile. Also, the distribution of water inside the pile is different but the magnitude of θ remains relatively similar in both cases (large and small piles). Figures A12 to A17 in Appendix A are additional results on the distribution of the volumetric water content (inside the small pile) for simulations S12 to S17 at the end of December of the 2nd, 4th, 6th and 8th year. Also, Figures B12 to B17 in Appendix B show more results about water vertical velocity for simulations S12 to S17 (for the small pile) at the end of December of the 2nd, 4th, 6th and 8th year.

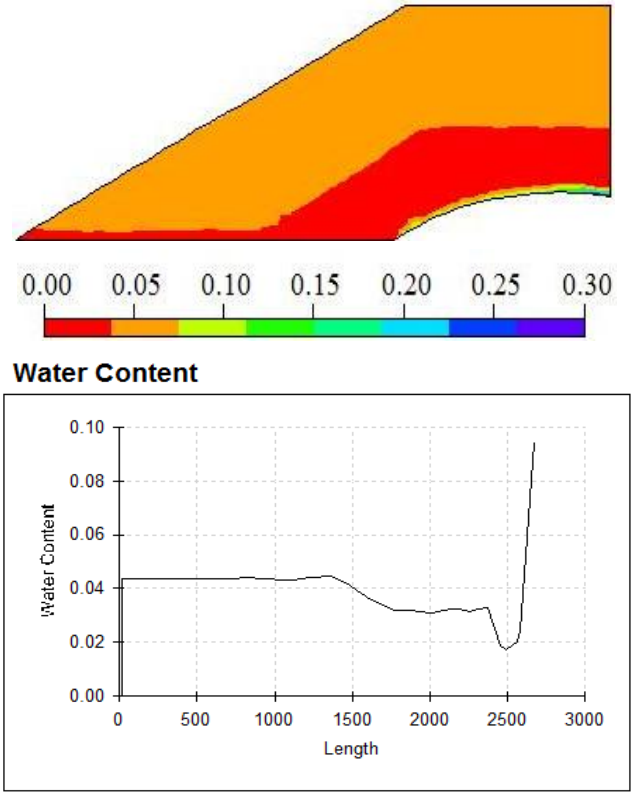

Figure 17: Contours and vertical profile (at line AA) of the volumetric water contents for simulation S12 (SBL) at the end of December of the 10th year; small pile.

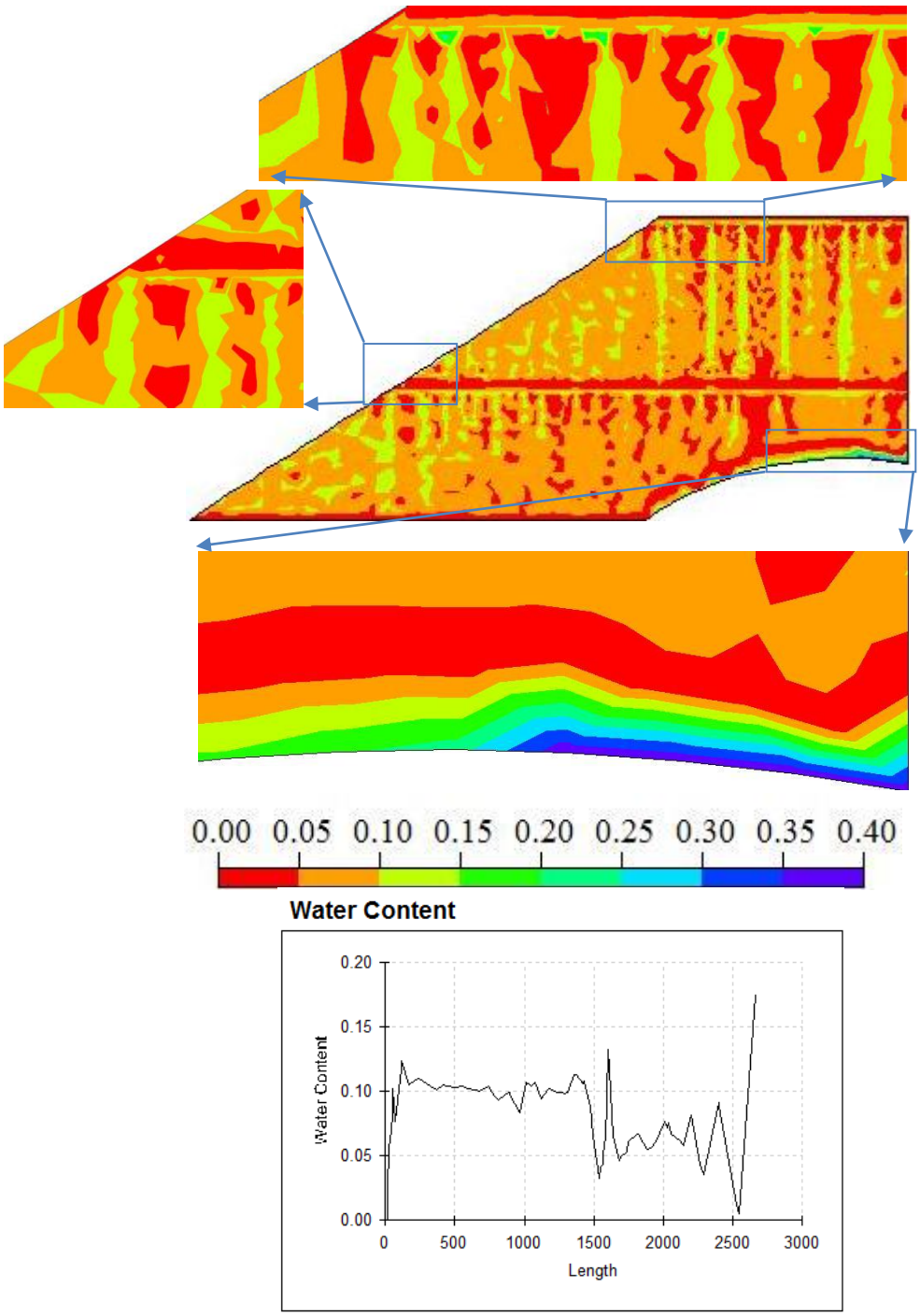

Figure 18: Contours and vertical profile (at line AA) of the volumetric water contents for simulation S13 (GRV with two horizontal SBL layers) at the end of December of the 10th year; small pile

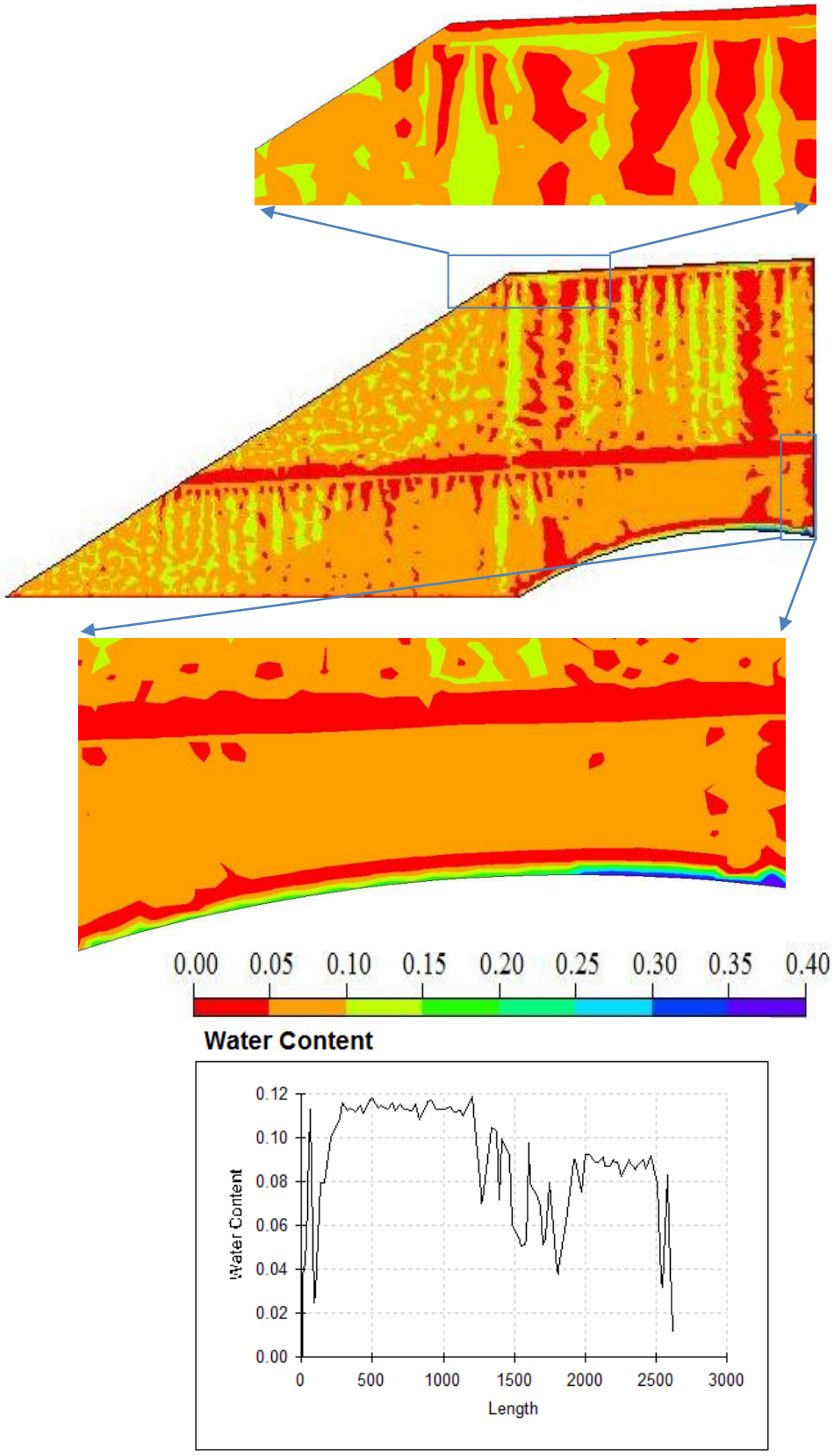

Figure 19: Contours and vertical profile (at line AA) of the volumetric water contents for simulation S14 (GRV with two SBL layers inclined at 5%) at the end of December of the 10th year; small pile

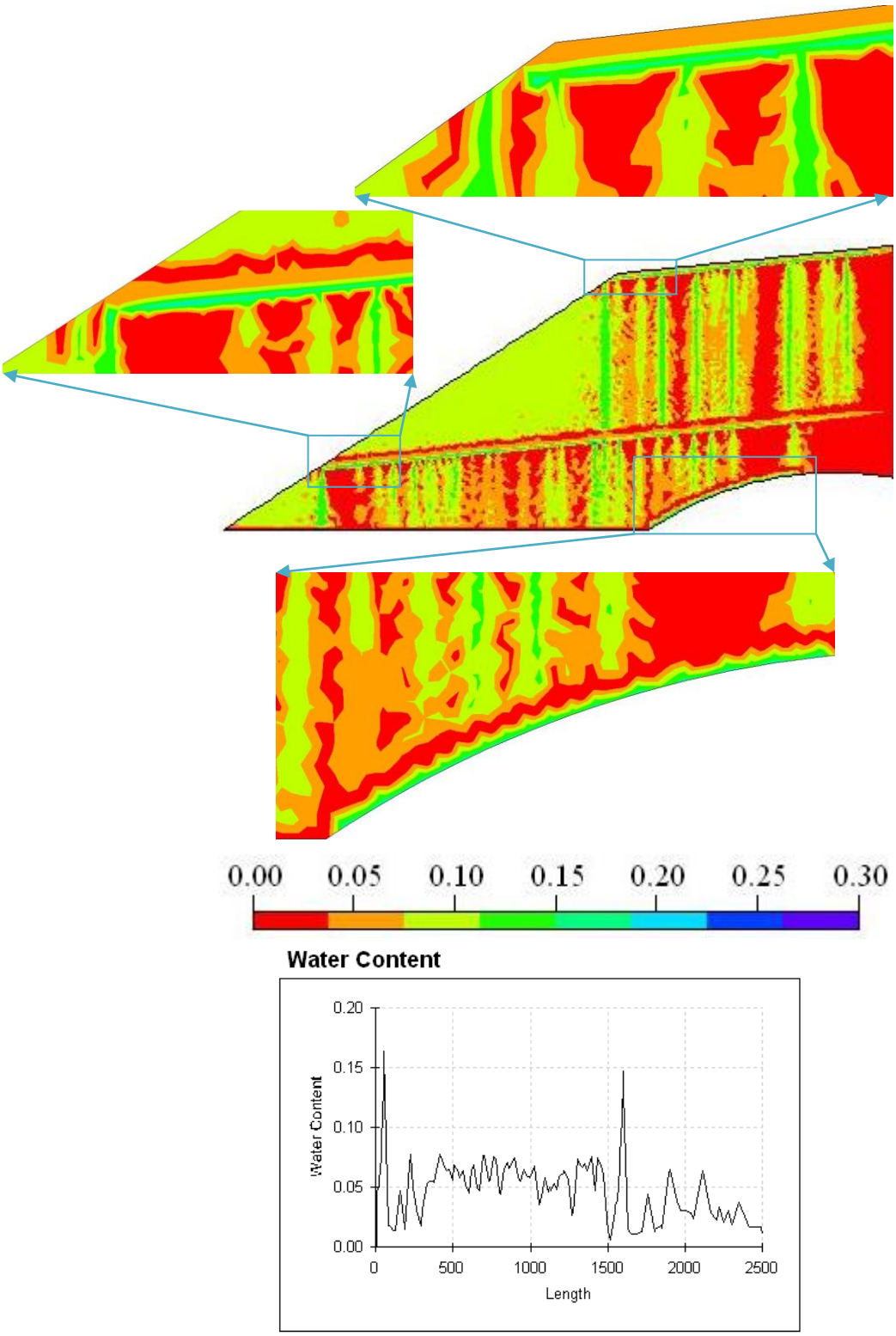

Figure 20: Contours and vertical profile (at line AA) of the volumetric water contents for simulation S15 (GRV with two SBL layers inclined at 10%) at the end of December of the 10th year; small pile.

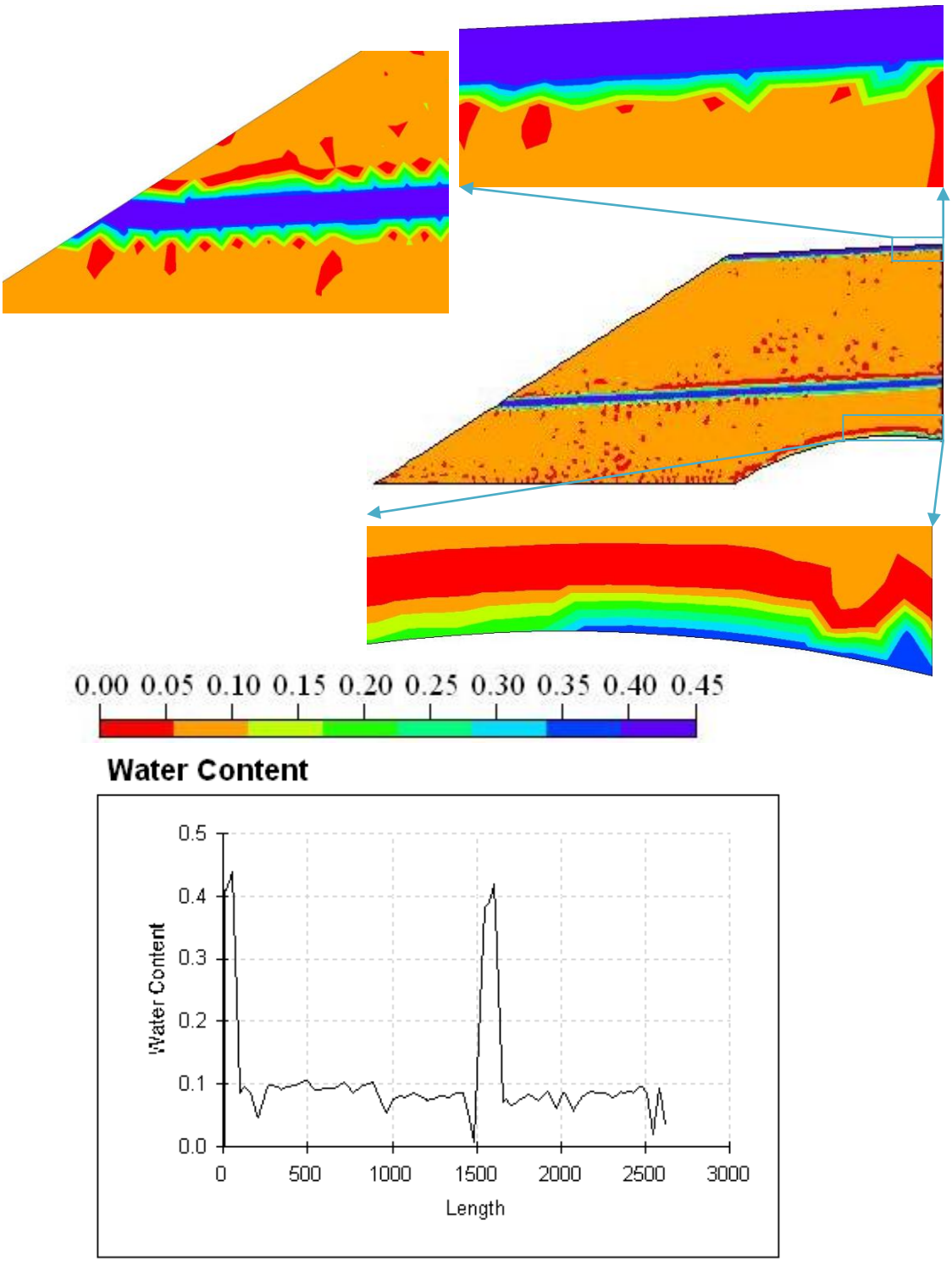

Figure 21: Contours and vertical profile (at line AA) of the volumetric water contents for simulation S16 (GRV with two SLT layers inclined at 5%) at the end of December of the 10th year; small pile.

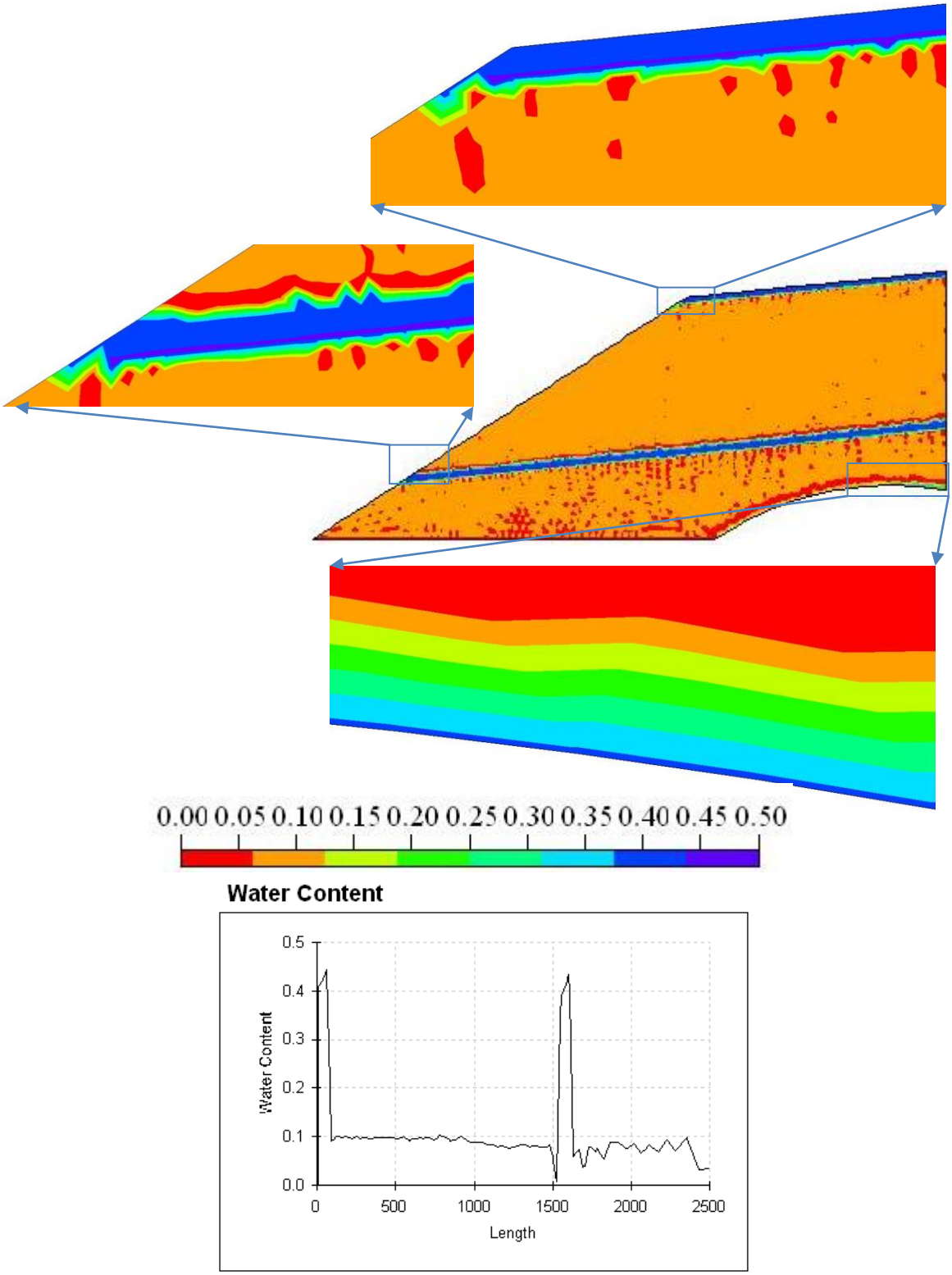

Figure 22: Contours and vertical profile (at line AA) of the volumetric water contents for simulation S17 (GRV with two SLT layers inclined at 10%) at the end of December of the 10th year; small pile.

4. DISCUSSION

Results from several simulations were presented to illustrate the hydrogeological behaviour of a large size waste rock piles under different conditions, based on the movement and distribution of water inside the unsaturated pile. The results for the gravely (GRV) waste rock shows that the wetting front (which always remain unsaturated) does not reach the base of the 109 m - high pile after ten years; in this case, the degree of saturation remained very low (usually around 10%), thus reducing the hydraulic conductivity of the waste rock in the entire pile. This hydrogeological behaviour would provides a favourable condition to gas exchanges with the atmosphere, in terms of air movement under the influence of advection, convection and diffusion (Lefebvre et al. 2001; Molson et al. 2005). Under these conditions, air can easily travel inside the pile, providing the oxygen needed for oxidation reactions.

In the case of sandy material (SBL), the simulations show that seepage may reach a quasi-stationary state in less than 10 years, in terms of water content and suction, with the wetting front reaching to base of the pile. After this state is reached, only the zones near the surface undergo significant changes following recharge, depending on the external climatic conditions, whereas the situation within the pile remains almost unchanged from one year to the other (with a cycle that nonetheless changes during the year).

The simulations that include horizontal layers of denser and finer materials in the gravely waste rock indicate that water flows differently in the various zones of the pile. Water tends to accumulate in the finer grained material because of their higher water retention capacity, and the creation of capillary barriers effect at the interfaces with the coarser waste rock. As the water content increases in these fine grained material, the base of these layer can become almost fully saturated. When the suction at an interface reaches the water entry value (WEV) on the water retention curve of the coarse GRV material, the capillary barrier effect tends to disappear (Aubertin et al. 2009), and water can then

infiltrate more deeply in the form of localized flow zones (Fala et al. 2003, 2005). The wetting zones associated with such fingering infiltration areas develop gradually downwards and laterally. The degree of saturation in these localized zones of infiltration is higher than in adjacent areas in the gravelly waste rock (i.e. up to 40% vs. less than 10%), so that water velocity is much larger in the former than in the latter.

Simulations were also performed with inclined (sandy or silty) layers to assess the possibility of controlling the appearance of localized infiltration zones in the core of the large waste rock pile. Results indicate that infiltrating water tends to follow the interfaces between the fine grained material layers and the underlying coarse waste rock (e.g. Bussière et al. 2003; Fala et al. 2003, 2005; Aubertin et al. 2009). Layers inclined at 5% and 10% tend to maintain the center of the pile dryer as the water is channelled to the outer portion due to the capillary barrier effects that develop between the fine and coarse grained materials, so the external portion of the pile becomes more highly saturated than the central core. The magnitude of the effect of inclined layers depends on several factors including the hydrogeological properties of the adjacent materials, the thickness of the layers and their inclination angle, the amount of precipitation (recharge), the lateral dimension of the pile and its shape. The geometry of the interfaces (flat versus irregular) between the waste rock and compacted layers is also expected to influence the motion of water inside the finer grained material, and the presence of localized water flow areas beneath the layers; this aspect is being investigated further.

Several simulations were also conducted to assess the effect of the pile size on water movement, using a size reduced by a factor of 4 (27 m vs 109 m). The results of this comparison between the small and the large piles shows that water (in the wetting front) arrives at the base of the smaller pile much faster than in the large pile in most cases. Table 3 shows the water arrival times for different simulations.

Table 5: Comparison of time required for water arrival at the base of the waste rock pile (for the different simulations presented here; see details in Table 1).

Simulation	Pile size	Water arrival time at the base of the pile (near the central part)
S1	Large	Doesn't reach the base of the pile after 10 years
S2	Large	Arrives at the base after 5 years
S3	Large	10 years
S4	Large	10 years
S5	Large	9 years
S6	Large	10 years
S7	Large	9 years
S8	Large	7 years
S9	Large	9 years
S10	Large	10 years
S11	Large	7 years
S12	Small	2 years
S13	Small	3 years
S14	Small	2 years
S15	Small	2 years
S16	Small	3 years
S17	Small	3 years

5. CONCLUSIONS

The results presented above indicate that horizontal sandy layers can have negatively effects on water movement inside a large waste rock piles; the effects do not seem that different when these layers are inclined outward. When the inclined layers are made of a silty material, these may have relatively more positive effect on water movement, which tends to follow the inclination, hence protecting (in part) the core of the pile from extensive wetting; this beneficial effect appears more important when the layers are inclined at 10% rather than 5%. The actual effect of the layers depend on a number of factors, including the height of the pile, the precipitation regime, the number of layers, their inclination, and

material properties. The similarity of the results obtained with a smaller waste rock pile suggests that the same effect would apply to the larger pile under comparable conditions.

Identifying areas where the capillary barrier effects can develop is an essential point in the design and construction of a waste rock pile, because these effects tend to favour the accumulation of water and the appearance of localized flow. These phenomena can occur naturally as a result of the construction method, but they can also be produced voluntarily in the construction of the pile by controlling the position, configuration and properties of the dense layers. The fine material layers (which cause the capillary barrier effects) can help divert water outside the pile and thus improve the quality of the percolating waters (Aubertin et al. 2002b; Fala et al., 2003, 2005, 2006; Molson et al., 2005). It should be emphasized that the design and construction of waste rock piles should be carefully planned. In this sense, various proposals have been put forward over the years to improve the configurations and methods of construction of piles, by including areas promoting controlled drainage and reducing infiltration and water accumulation in the heart of the pile (Fala 2002; Aubertin et al., 2002b; Wels et al., 2003; Williams et al., 2008; Dawood and Aubertin 2009). But such methods are not yet commonly used in practice and the construction of waste rock piles still remains largely dictated by operational and financial considerations, which are mainly based on short-term analysis.

In the longer term however, it is advantageous to plan the construction of piles to minimize the geotechnical and hydro-geochemical problems during and after the operation of the mine. The modeling tools presented above can also be used to study and compare various scenarios to arrive at an optimal design

The effects of other parameters and factors (including non homogeneous material properties; e.g. Fala et al. 2012) are under investigation; the results will be presented elsewhere.

ACKNOWLEDGEMENT

The authors received a financial support from the Industrial NSERC Industrial Polytechnique-UQAT Chair on Environment and Mine Wastes Management (www.polymtl.ca/enviro-geremi) and from the Institut de recherche Robert-Sauvé en santé et en sécurité du travail (IRSST).

REFERENCES

AUBERTIN M., BUSSIÈRE B. and BERNIER L. (2002a). *Environnement et gestion des rejets miniers. Manual on CD-Rom.* Montréal, Québec, Canada: Presses Internationales Polytechnique.

AUBERTIN M., CIFUENTES E., MARTIN V., APITHY S., BUSSIÈRE B., MOLSON J., CHAPUIS R.P. and MAQSOUD A. (2006). An investigation of factors that influence the water diversion capacity of inclined covers with capillary barrier effects. *The Fourth International Conference on Unsaturated Soils. No. 147*, pp. 613-624. Carefree, Arizona: Miller et al., ASCE Geotechnical Special Publication.

AUBERTIN M., FALA O., BUSSIÈRE, B., MARTIN, V., CAMPOS, D., GAMACHE-ROCHETTE, A., CHOUTEAU, M. and CHAPUIS, R. (2002b). Analyse des écoulements de l'eau en conditions non saturées dans les haldes à stériles. *Symposium sur l'Environnement et les Mines* (13 pages). Rouyn-Noranda: CD-Rom. CIM.

AUBERTIN M., FALA O., MOLSON J., CHOUTEAU M., ANTERRIEU O., HERNANDEZ M. A., CHAPUIS P.R., BUSSIÈRE B., LAHMIRA B. and LEFEBVRE R. (2008). Caractérisation du comportement hydrogéologique et géochimique des haldes à stériles. *Symposium sue l'Environnement et les Mines* (25 pages). Rouyan-Noranda: CD-ROM. CIM.

AUBERTIN M., FALA O., MOLSON J., GAMACHE-ROCHETTE A., LAHMIRA B., MARTIN V., LEFEBVRE R., BUSSIÈRE B., CHAPUIS R.P., CHOUTEAU M. and WILSON G.W. (2005). Évaluation du comportement hydrogéologique et géochimique des haldes à stériles. *Symposium sur l'Environnement et les Mines* (40 pages). Rouyn-Noranda: CD-ROM. CIM.

AUBERTIN M., CIFUENTES E., APITHY S., BUSSIÈRE B., MOLSON J. and CHAPUIS R.P. (2009). Analyses of water diversion along inclined covers with capillary barrier effects. *Canadian Geotechnical Journal , 46*, 1146-1164.

BUSSIÈRE B., AUBERTIN M. and CHAPUIS R.P. (2002). A laboratory set up to evaluate the hydraulic behavior of inclined capillary barriers. In R. Phillips, P. Guo, & R. Popescu. (Ed.), *International Conference on Physical Modelling in Geotechnics* (pp. 391-396). St.Jonh's, Newfoundland: A.A.Balkema, Rotterdam.

BUSSIÈRE B., AUBERTIN M. and CHAPUIS R.P. (2003). The behavior of inclined covers used as oxygen barriers. *Canadian Geotechnical Journal , 40* (3), 512-535.

BUSSIÈRE B., AUBERTIN M., ZAGURY G.J., POTVIN R. and BENZAAZOUA M. (2005). Principaux défis et pistes de solution pour la restauration des sites miniers abandonnés générateurs de drainage minier acide. *Symposium sur l'Environnement et les Mines* (29 pages). Rouyn-Noranda: CD-ROM. CIM.

BUSSIÈRE B., DEMERS I., DAWOOD I., PLANTE B., AUBERTIN M., PEREGOEDOVA A., PEPIN G., LESSARD G., INTISSAR R., BENZAAZOUA M., MOLSON J.W., CHOUTEAU M., ZAGURY G.J., MONZON M. and LAFLAMME L. (2011). Comportement géochimique et hydrogéologique des stériles de la mine LAC TIO. *Symposium sur l'Environnement et les Mines* (26 pages). Rouyand-Noranda: CD-ROM. CIM.

DAWOOD I. and AUBERTIN M. (2009). A numerical investigation of the influence of internal structure on the unsaturated flow in a large waste rock pile. *GeoHalifax'2009: 62nd Canadian Geotechnical Conference and 10th Joint CGS/ IAH-CNC Groundwater Specialty Conference*, (pp. 1534-1541). Halifax, Nova Scoia, Canada.

DAWOOD I., AUBERTIN M., INTISSAR R. and CHOUTEAU M. (2011). A combined hydrogeological–geophysical approach to evaluate unsaturated flow in a large waste rock pile. *Pan-Am CGS Geotechnical Conference* (8 pages). Toronto, ON, Canada.

FALA O. (2002). *Étude des écoulements non saturés dans les haldes à stériles à l'aide de simulations numériques.* Mémoire de maîtrise. École Polytechnique de Montréal, Montréal, Québec, Canada.

FALA O., AUBERTIN M., BUSSIÈRE B., CHAPUIS R. and MOLSON J. (2008). Stochastic numerical simulations of long term unsaturated flow in waste rock piles. *GeoEdmonton 2008, 61st Canadian Geotechnical Conference and 9th Joint CSG/IAH-CNC Groundwater Conference* (pp. 1492-1498). Edmonton, Canada: Canadian Geotechnical Society, International Association of Hydrogeologists-CNC, Geotechnical Society of Edmonton.

FALA O., AUBERTIN M., MOLSON J.W., BUSSIÈRE B., WILSON G.W., CHAPUIS R.P. and MARTIN. V. (2003). Numerical modeling of unsaturated flow in uniform and heterogeneous waste rock pile. *Sixth International Conference on Acid Rock Drainage (ICARD)* (pp. 895-902). Carin, Australia: Australian Institute of Mining and Metallurgy.

FALA O., MOLSON J., AUBERTIN M., BUSSIÈRE B. and CHAPUIS R.P. (2006). Numerical simulations of long term unsaturated flow and acid mine drainage at waste rock piles. In R. Barnhisel (Ed.), *the 7th International Conference on Acid Rock Drainage (ICARD)* (pp. 582-597). St. Louis, Missouri: The American Society of Mining and Reclamation.

FALA O., MOLSON J.W., AUBERTIN M. and BUSSIÈRE, B. (2005). Numerical modelling of flow and capillary barrier effects in unsaturated waste rock piles. *Mine Water & Environment , 24* (4), 172-185.

FALA O., MOLSON J., AUBERTIN M., DAWOOD I., BUSSIÈRE B. and CHAPUIS R. (2012). A numerical modelling approche to assess long term unsaturated flow and geochemical transport in a waste rock pile. (T. &. Francis, Ed.) *International Journal of Mining, Reclamation and Environment (ID: 644473 DOI:10.1080/17480930.2011.644473)* .

LEFEBVRE R., HOCKLEY D., SMOLENSKY J. and LAMONTAGNE A. (2001). Multiphase transfer processes in waste rock pile producing acid mine drainage, 2: Applications of numerical simulations. *Journal of Contaminant Hydrology , 52* (1-4), 165-186.

MARTIN V., AUBERTIN M., ZHAN G., BUSSIÈRE B. and CHAPUIS R.P. (2005). An investigation into the hydrological behaviour of exposed and covered waste rock dumps. *SME Transactions , 318*, 139-146.

MOLSON J.W., FALA O., AUBERTIN M. and BUSSIÈRE B. . (2005). Numerical simulations of pyrite oxidation and acid mine drainage in unsaturated waste rock piles. *Journal of Contaminant Hydrology , 78* (4), 343-371.

MUALEM Y. (1976). A new model predicting the hydraulic conductivity of unsaturated porous media. *Journal of Water Resources Research* , 513-522.

RICHARDS L.A. (1931). Capillary conduction of liquids through porous mediums. *Journal of Physics , 1*, 318-333.

RITCHIE A.I.M. (2003). Oxidation and gas transport in pile of sulfidic material (Chapter 4). *Environmental Aspects of Mine Wastes , 31* , 73-94. (J. Jambor, D. Blows, & A. Ritchie, Eds.) Mineralogical Association of Canada.

SIMUNEK J., SEJNA M., and VAN GENUCHTEN TH.M. (1999). The HYDRUS-2D software package for simulating the two dimensional movement of water, heat, and multiple solutes in variably- saturated media. Version 2.0. U.S. Salinity Laboratory.

SMITH L., LÒPEZ D.L., BECKIE R., DAWSON R. and PRICE W. (1995). *Hydrogeology of waste rock dumps, Final Report to Natural Resources Canada, Contract 23440-4-1317/01-SQ, MEND Report PA-1, Natural Resources Canada.*

SRACEK O., CHOQUETTE M., GELINAS P., LEFEBVRE R. and NICHOLSON R.V. (2004). Geochemical characterization of acid mine drainage from a waste rock pile, Mine Doyon, Québec, Canada. *Journal of Contaminant Hydrology , 69* (1-2), 45-71.

STANTEC CONSULTING LTD. (2004). *Priority assessment of metal leaching in neutral drainage.* Draft report submitted to MEND Initiative. CANMET (Ref. 631-22996).

VAN GENUCHTEN M.TH. (1980). A closed-form equation for predicting the hydraulic conductivity of unsaturated soils. *Soil Science Socity of America Journal , 44*, 892-898.

WELS C., LEFEBVRE R. and ROBERTSON A.M. (2003). An overview of prediction and control of air flow in acid-generating waste rock dumps. *6th International Conference on Acid Rock Drainage (ICARD)* (pp. 639-650). Carins, Australia: The AusIMM, Carlton South.

WILLIAMS D. J., SCOTT P., JOHNSTON D. and LEE G. (2008). Rock dump design to limit potential acid drainage. Rock Dumps 2008. In A. Fourie (Ed.). ACG, Perth.

WILLIAMS D.J. and ROHDE T.K. (2007). Strategies for reducing seepage from surface waste rock pile .during operation and post-closure. *Second International Seminar of Mine Closure*, (pp. 533-542). Santiago, Chili.

ZHAN J. G., AUBERTIN M., MAYER A., BURKE K. and MCMULLEN J. (2001). Capillary cover design for leach pad closure, In: SME Transaction 2001. Vol. 310, pp. 104-110.

APPENDIX A

Contours and vertical profiles (along line AA – see Fig. 1) of the volumetric water content at the end of December of the 2nd, 4th , 6th , and 8th years for simulations S1 to S17

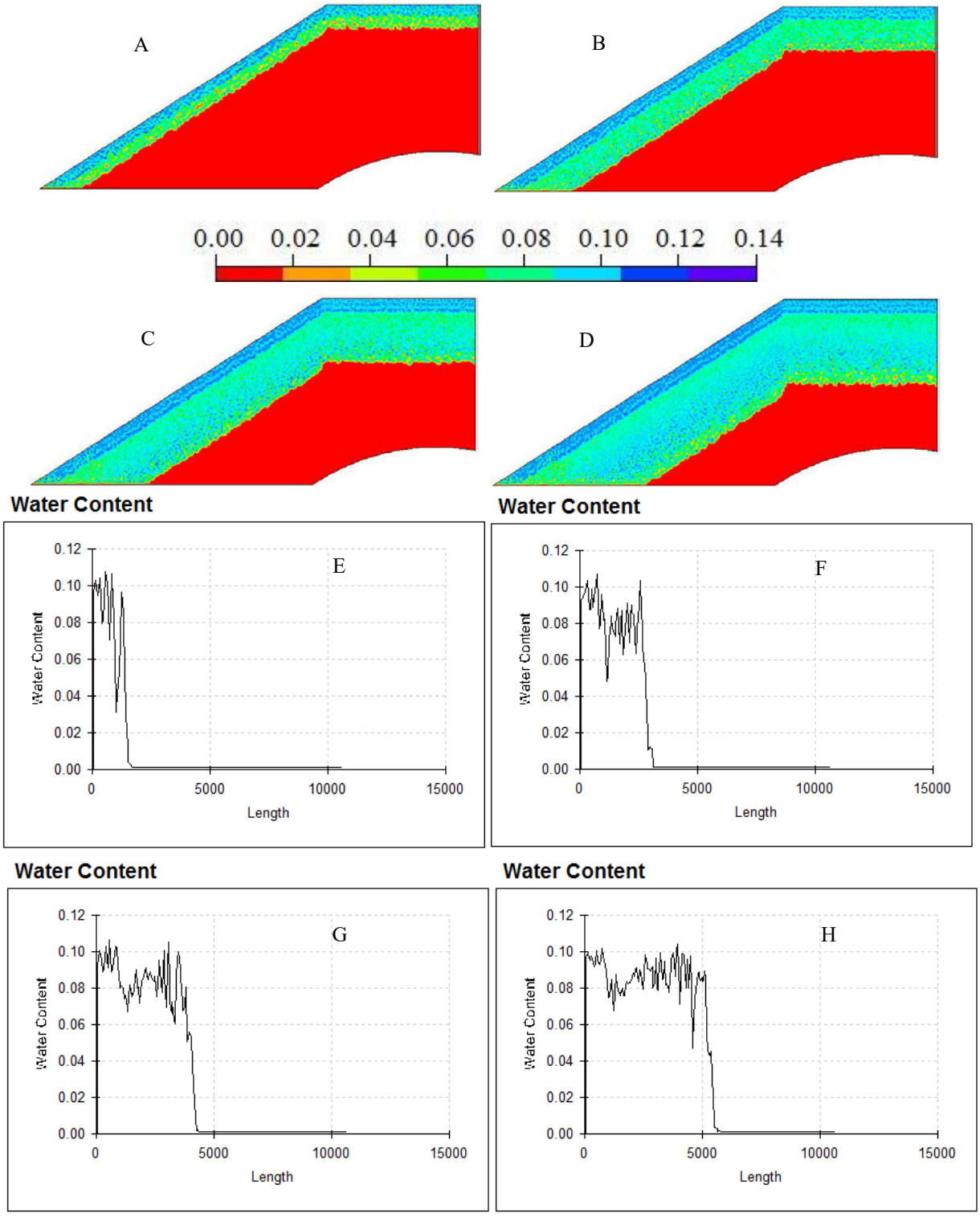

Figure A1: Contours and profiles (at line AA) of the volumetric water content for simulation S1 (base case, GRV only) at the end of December of the A, E) 2nd year; B, F) 4th year; C, G) 6th year; and D, H) 8th year.

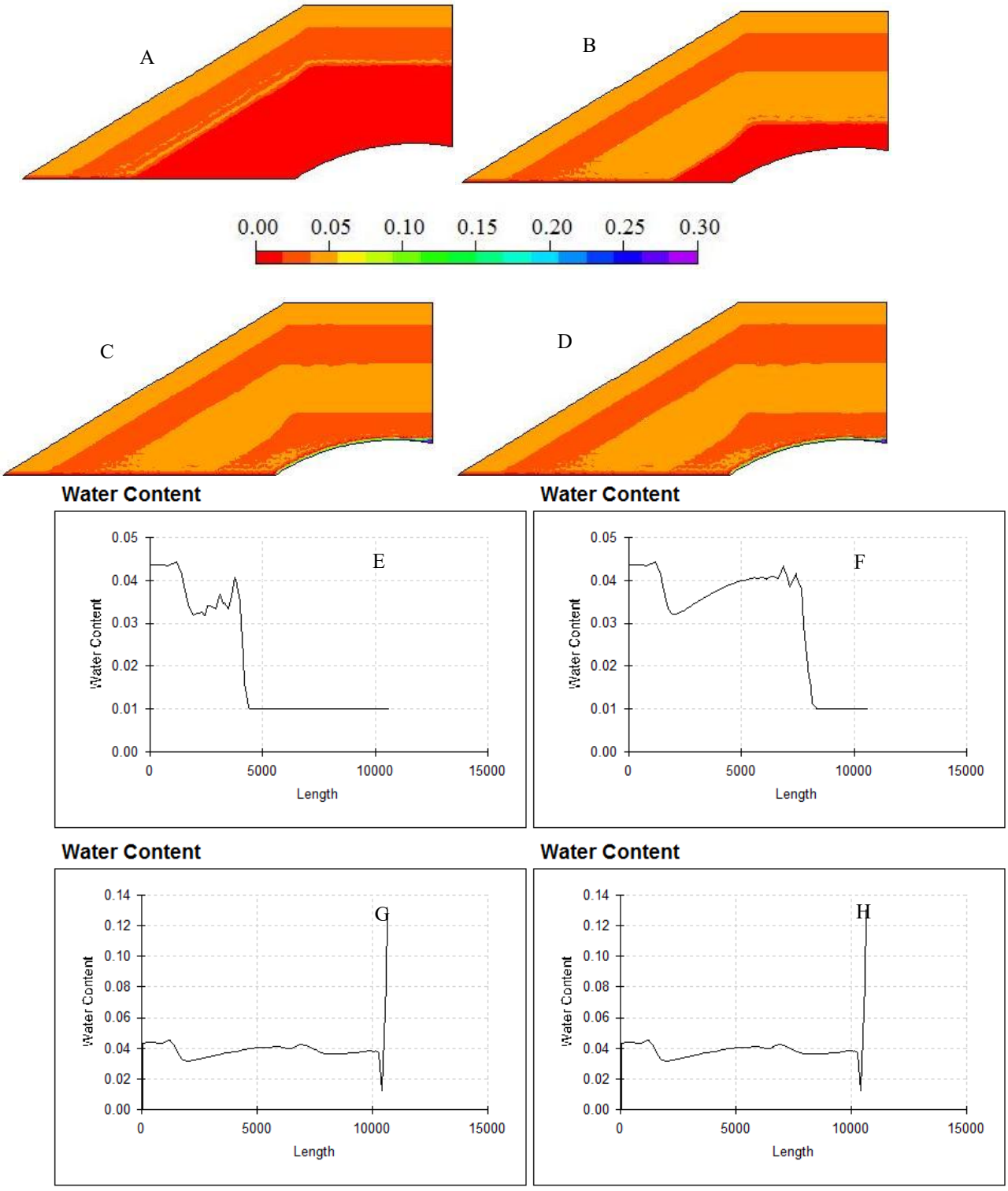

Figure A2: Contours and profiles (at line AA) of the volumetric water content for simulation S2 (base case, SBL only) at the end of December of the A, E) 2nd year; B, F) 4th year; C, G) 6th year; and D, H) 8th year

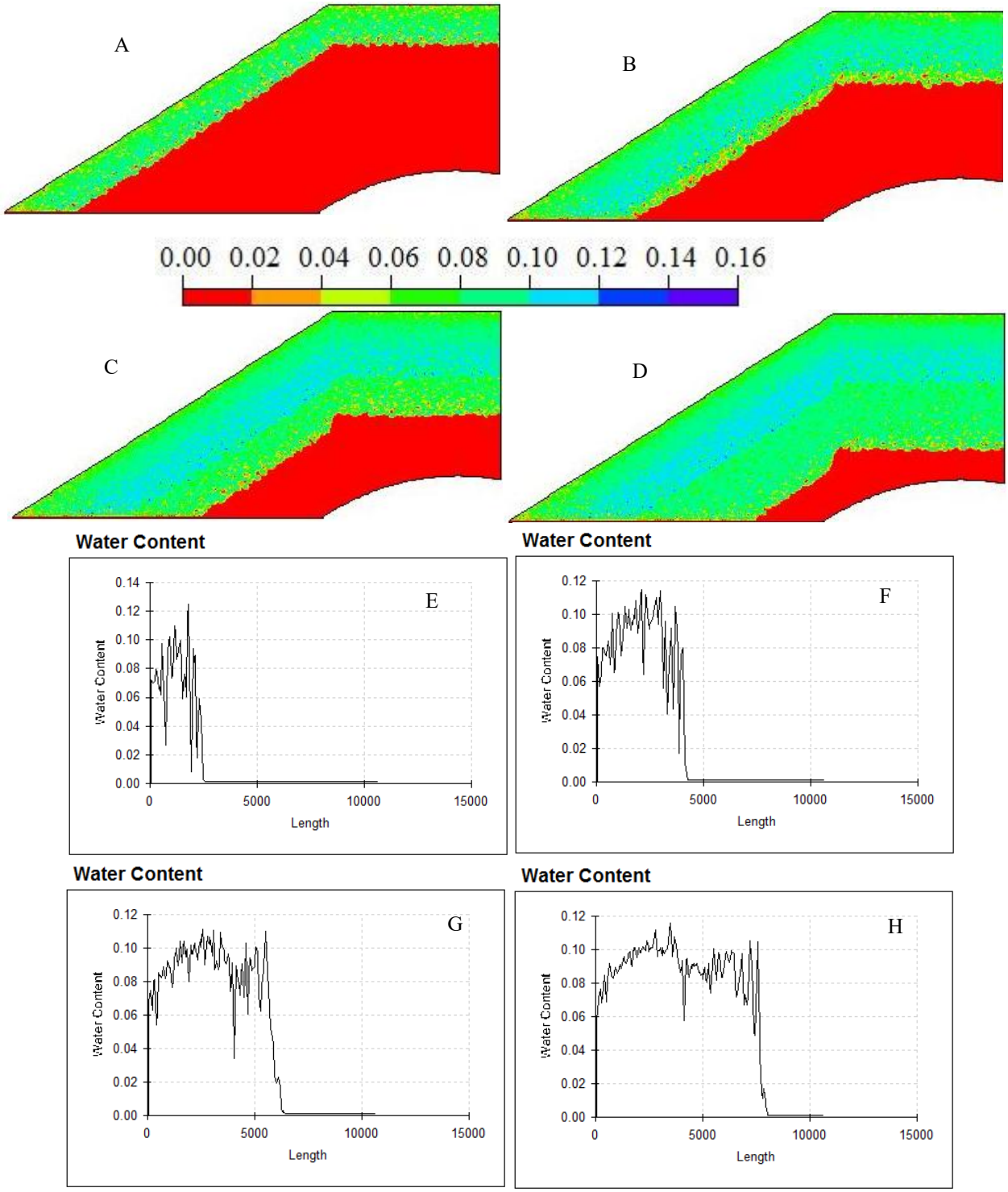

Figure A3: Contours and profiles (at line AA) of the volumetric water content for simulation S3 (GRV only with P2-E precipitation cycle) at the end of December of the A, E) 2nd year; B, F) 4th year; C, G) 6th year; and D, H) 8th year.

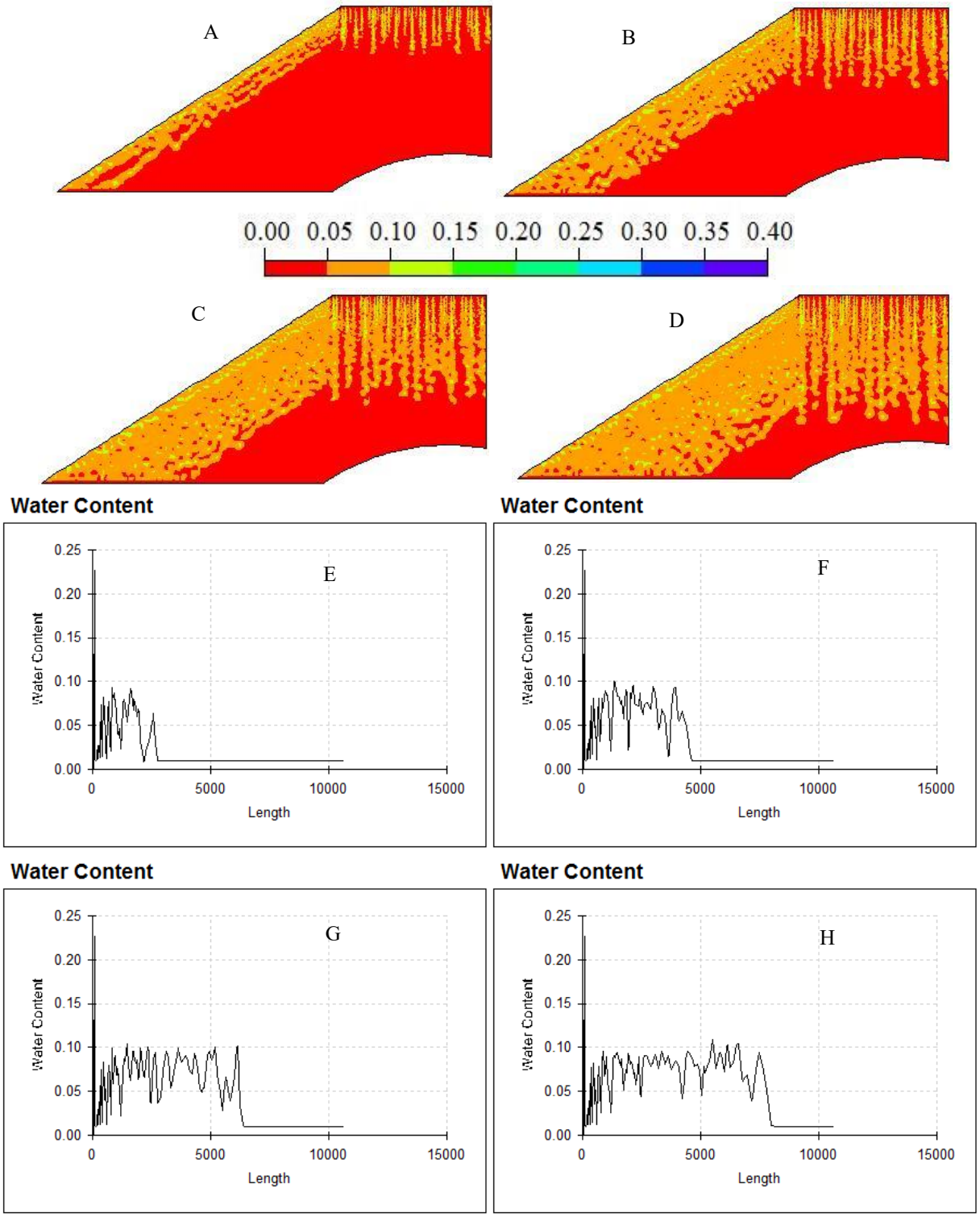

Figure A4: Contours and profiles (at line AA) of the volumetric water content for simulation S4 (GRV with one horizontal SBL layer) at the end of December of the A, E) 2nd year; B, F) 4th year; C, G) 6th year; and D, H) 8th year

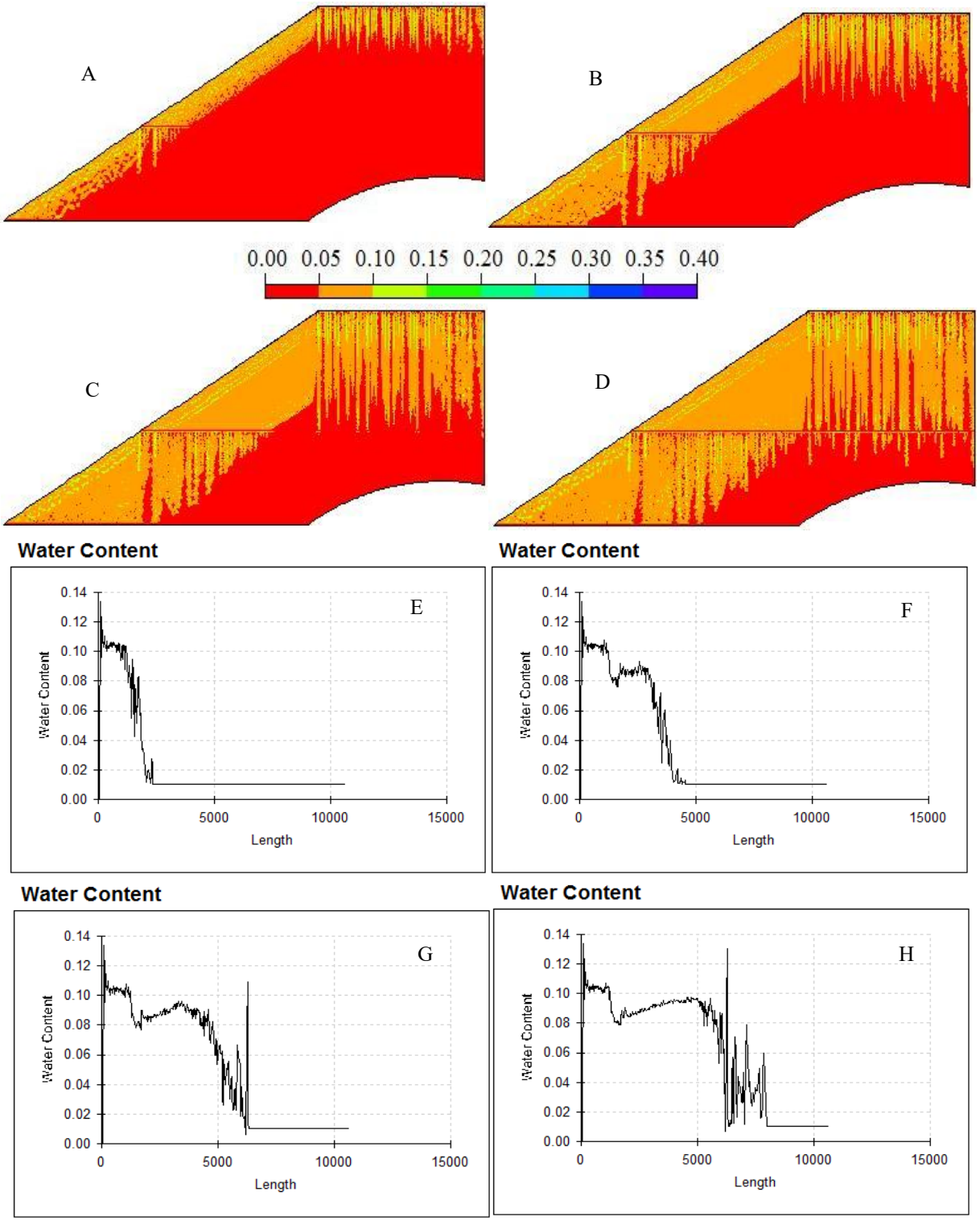

Figure A5: Contours and profiles (at line AA) of the volumetric water content for simulation S5 (GRV with two horizontal SBL layers) at the end of December of the A, E) 2nd year; B, F) 4th year; C, G) 6th year; and D, H) 8th year

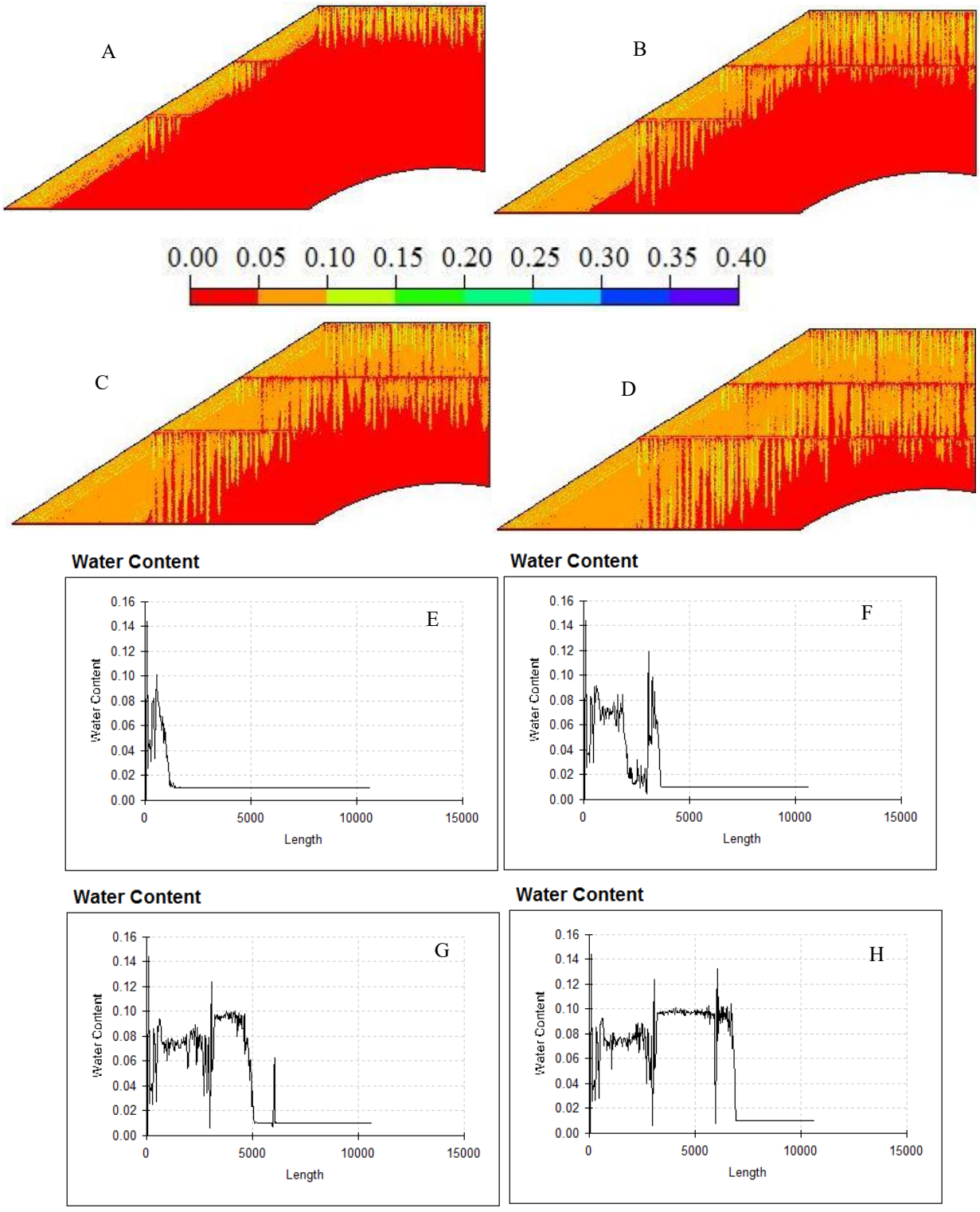

Figure A6: Contours and profiles (at line AA) of the volumetric water content for simulation S6 (GRV with three horizontal SBL layers) at the end of December of the A, E) 2nd year; B, F) 4th year; C, G) 6th year; and D, H) 8th year

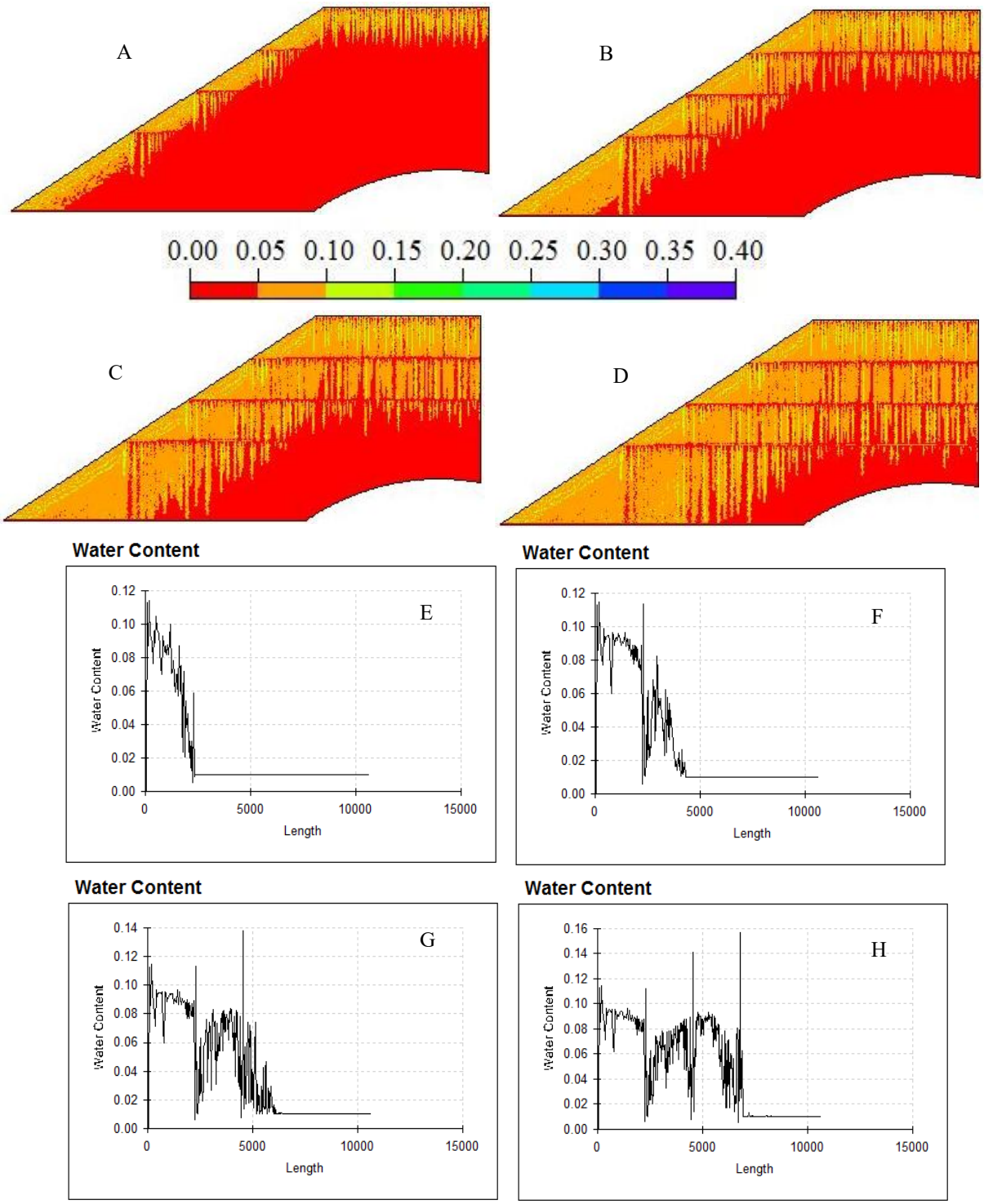

Figure A7: Contours and profiles (at line AA) of the volumetric water content for simulation S7 (GRV with four horizontal SBL layers) at the end of December of the A, E) 2nd year; B, F) 4th year; C, G) 6th year; and D, H) 8th year

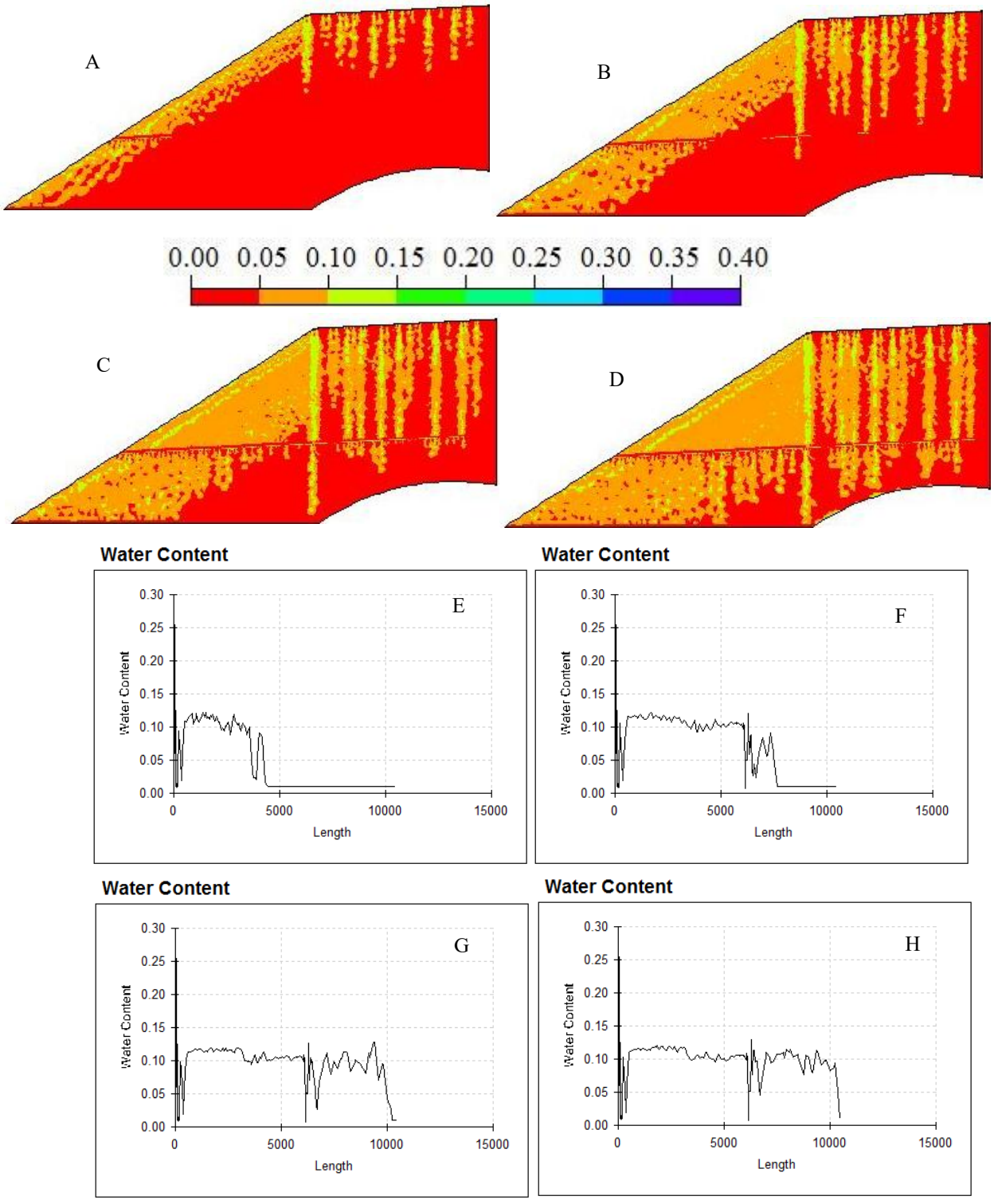

Figure A8: Contours and profiles (at line AA) of the volumetric water content for simulation S8 (GRV with two inclined at 5% SBL layers) at the end of December of the A, E) 2nd year; B, F) 4th year; C, G) 6th year; and D, H) 8th year

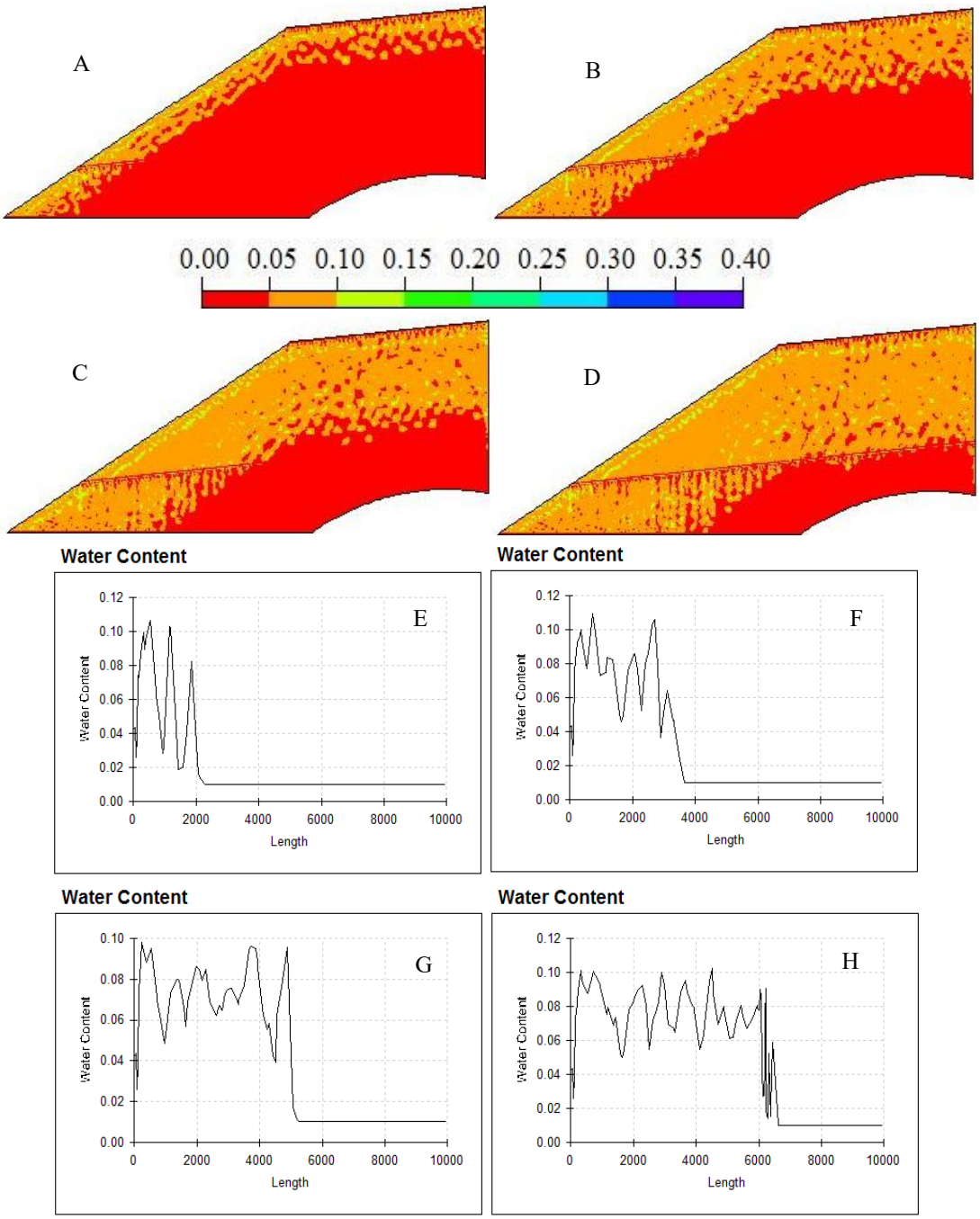

Figure A9: Contours and profiles (at line AA) of the volumetric water content for simulation S9 (GRV with two inclined at 10% SBL layers) at the end of December of the A, E) 2nd year; B, F) 4th year; C, G) 6th year; and D, H) 8th year

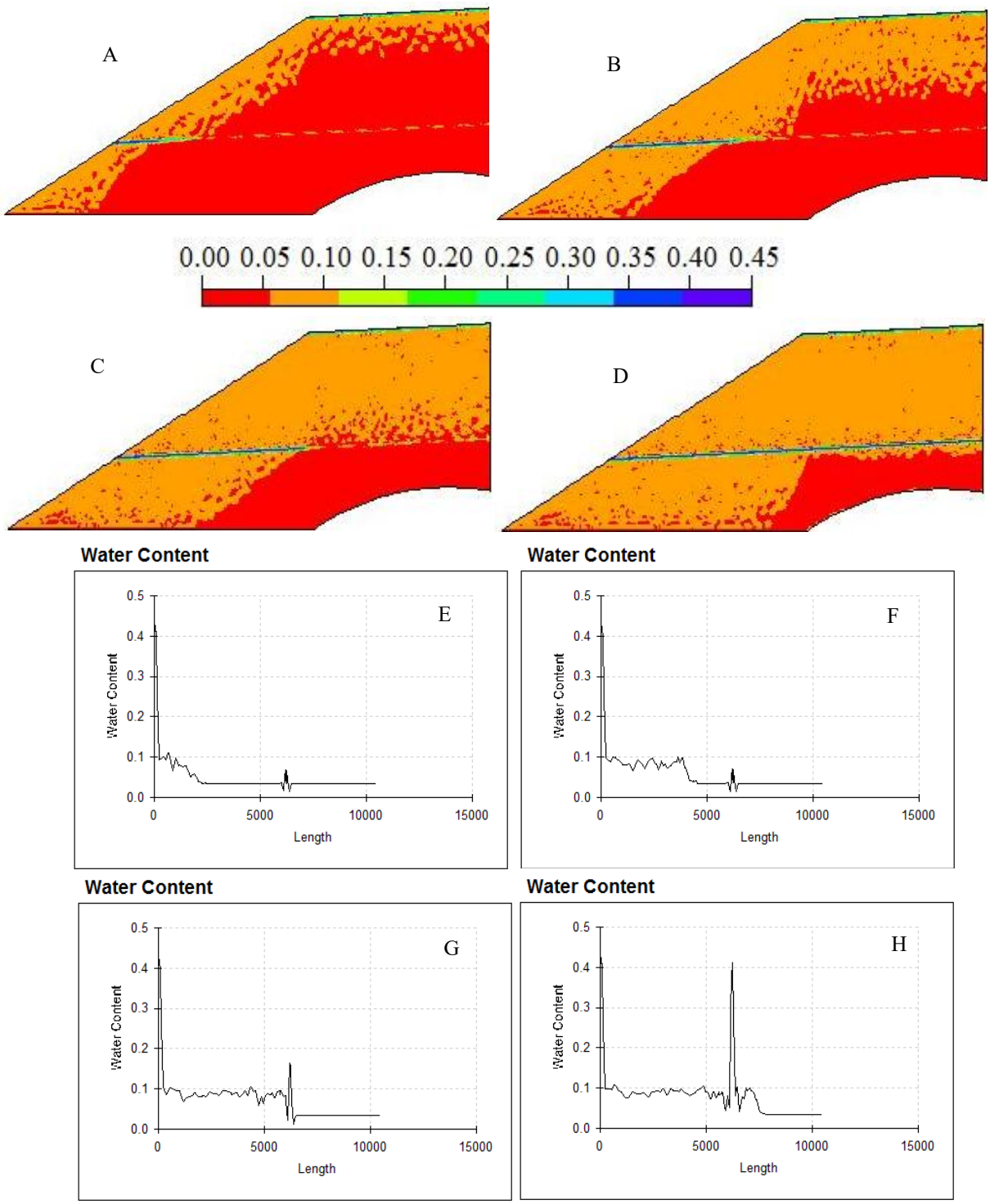

Figure A10: Contours and profiles (at line AA) of the volumetric water content for simulation S10 (GRV with two inclined at 5% SLT layers) at the end of December of the A, E) 2nd year; B, F) 4th year; C, G) 6th year; and D, H) 8th year

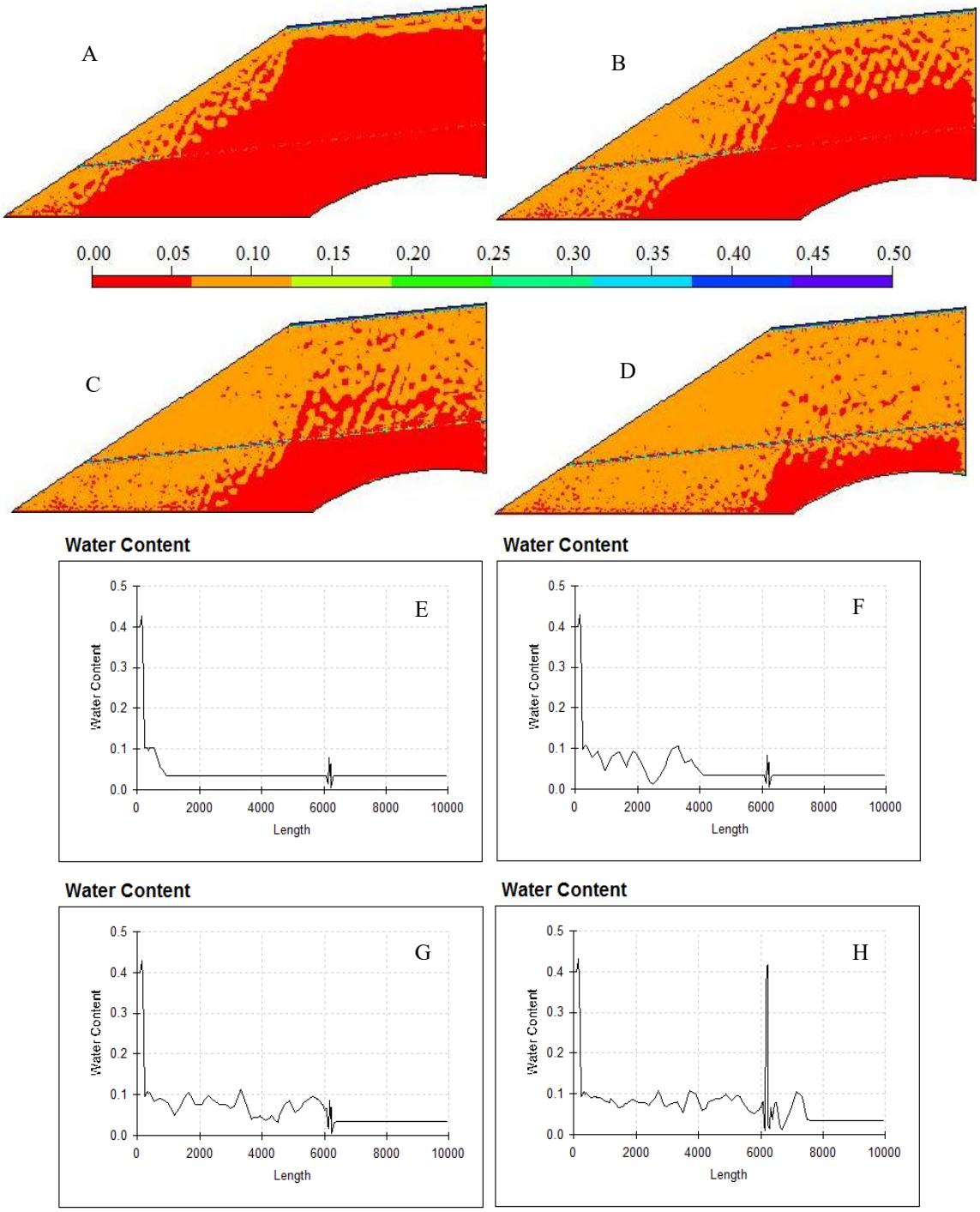

Figure A11: Contours and profiles (at line AA) of the volumetric water content for simulation S11 (GRV with two inclined at 10% SLT layers) at the end of December of the A, E) 2nd year; B, F) 4th year; C, G) 6th year; and D, H) 8th year.

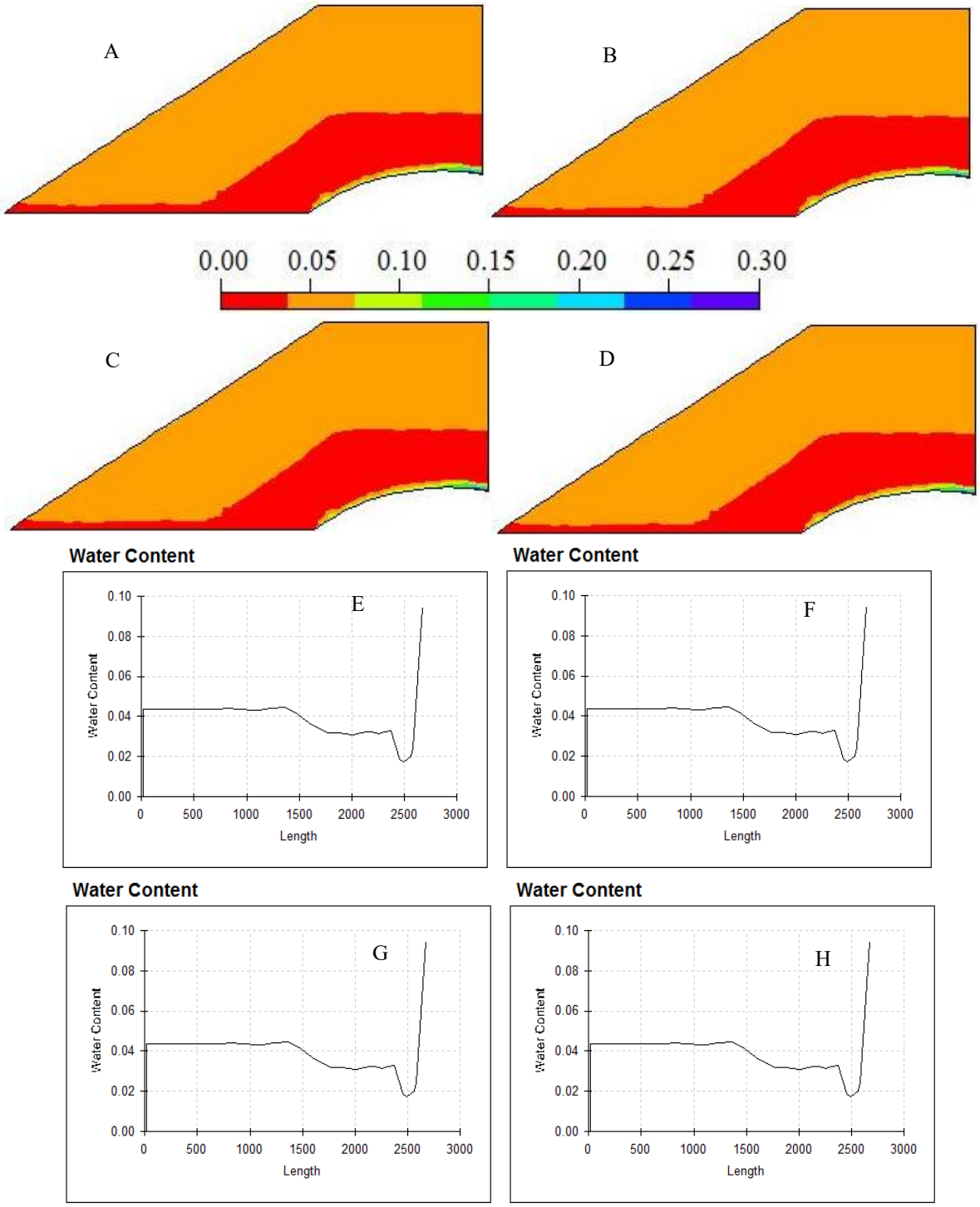

Figure A12: Contours and profiles (at line AA) of the volumetric water content for simulation S12 (base case, SBL only, small size pile) at the end of December of the A, E) 2nd year; B, F) 4th year; C, G) 6th year; and D, H) 8th year.

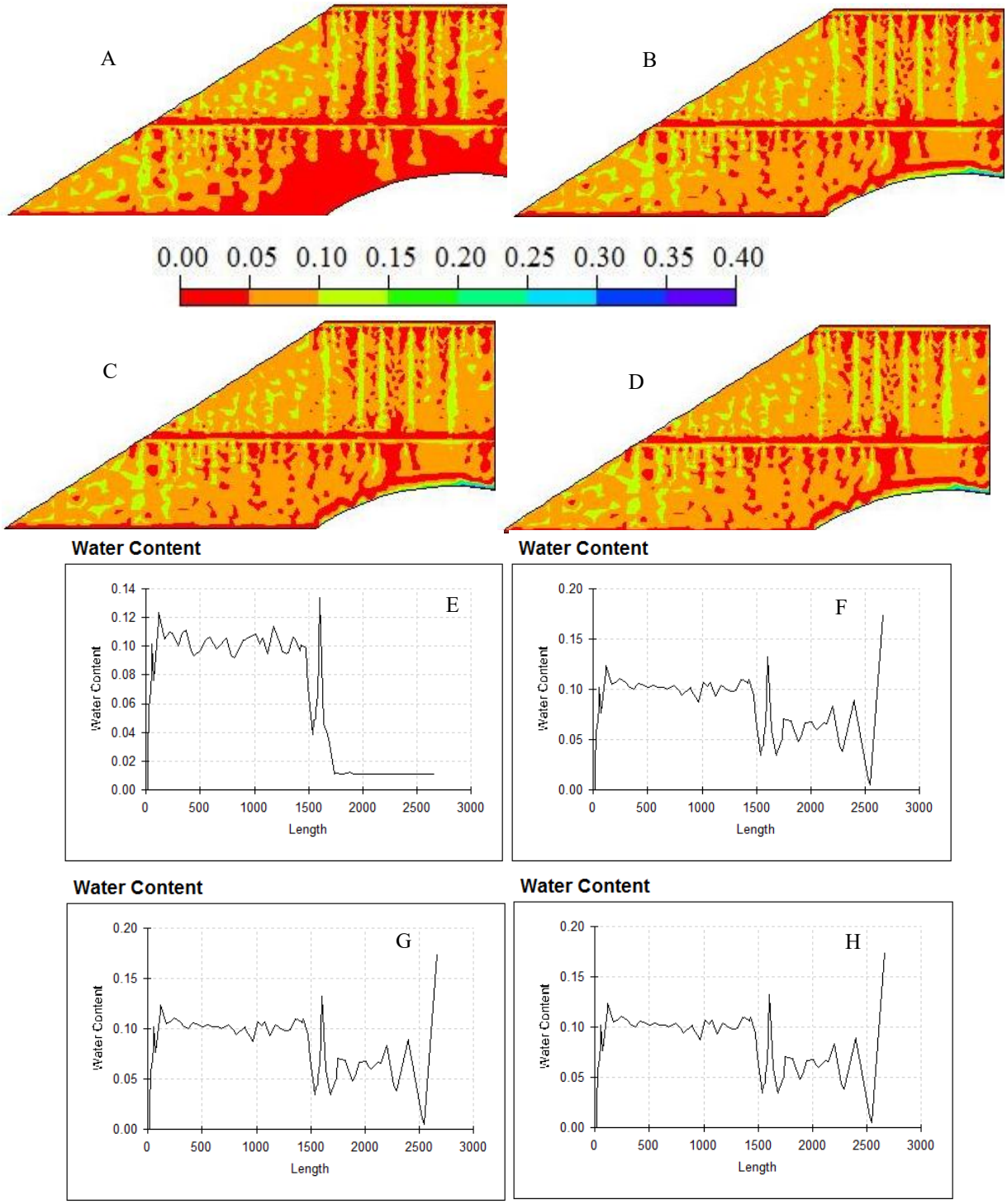

Figure A13: Contours and profiles (at line AA) of the volumetric water content for simulation S13 (GRV with two horizontal SBL layers, small size pile) at the end of December of the A, E) 2nd year; B, F) 4th year; C, G) 6th year; and D, H) 8th year.

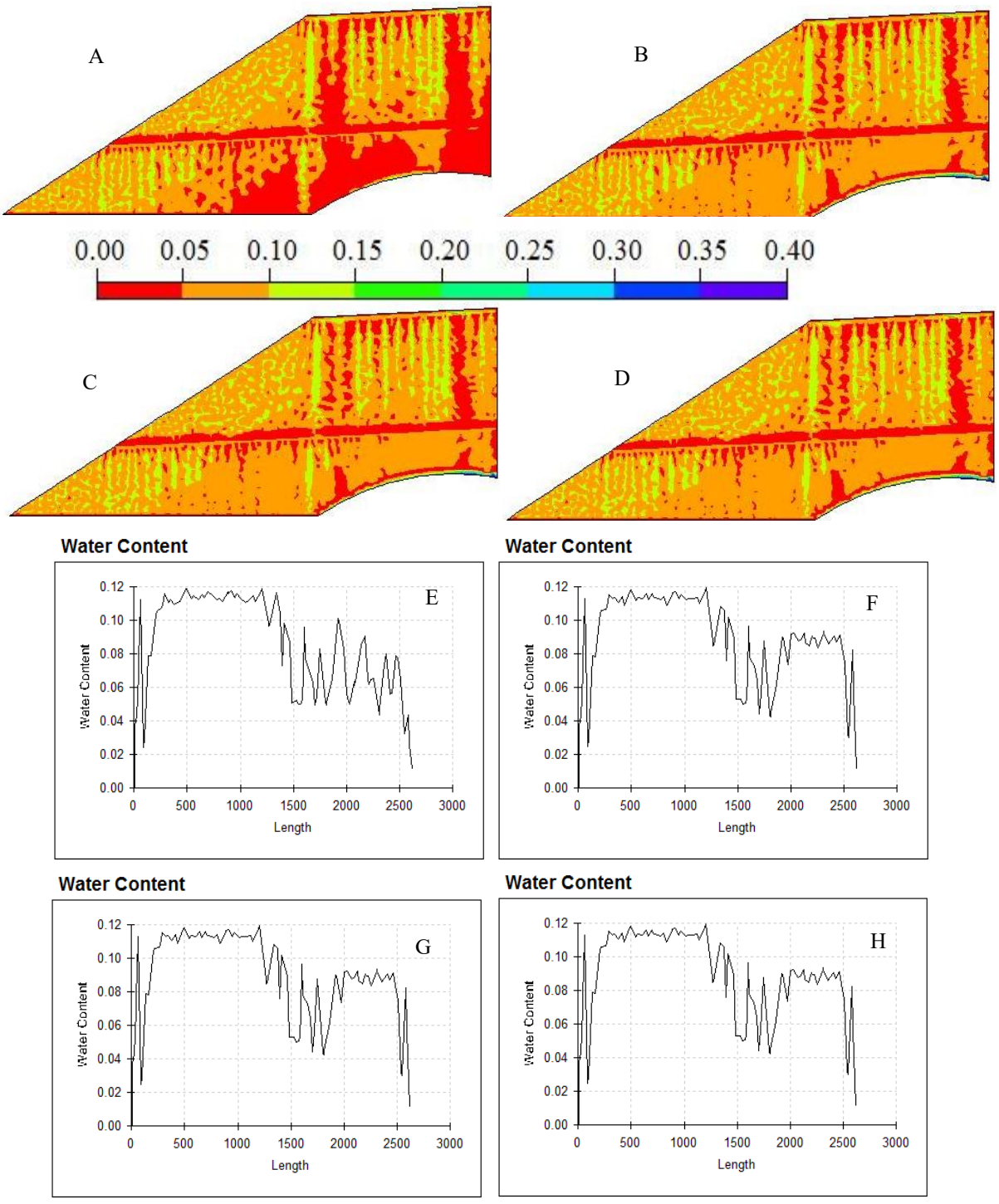

Figure A14: Contours and profiles (at line AA) of the volumetric water content for simulation S14 (GRV with two inclined at 5% SBL layers, small size pile) at the end of December of the A, E) 2nd year; B, F) 4th year; C, G) 6th year; and D, H) 8th year.

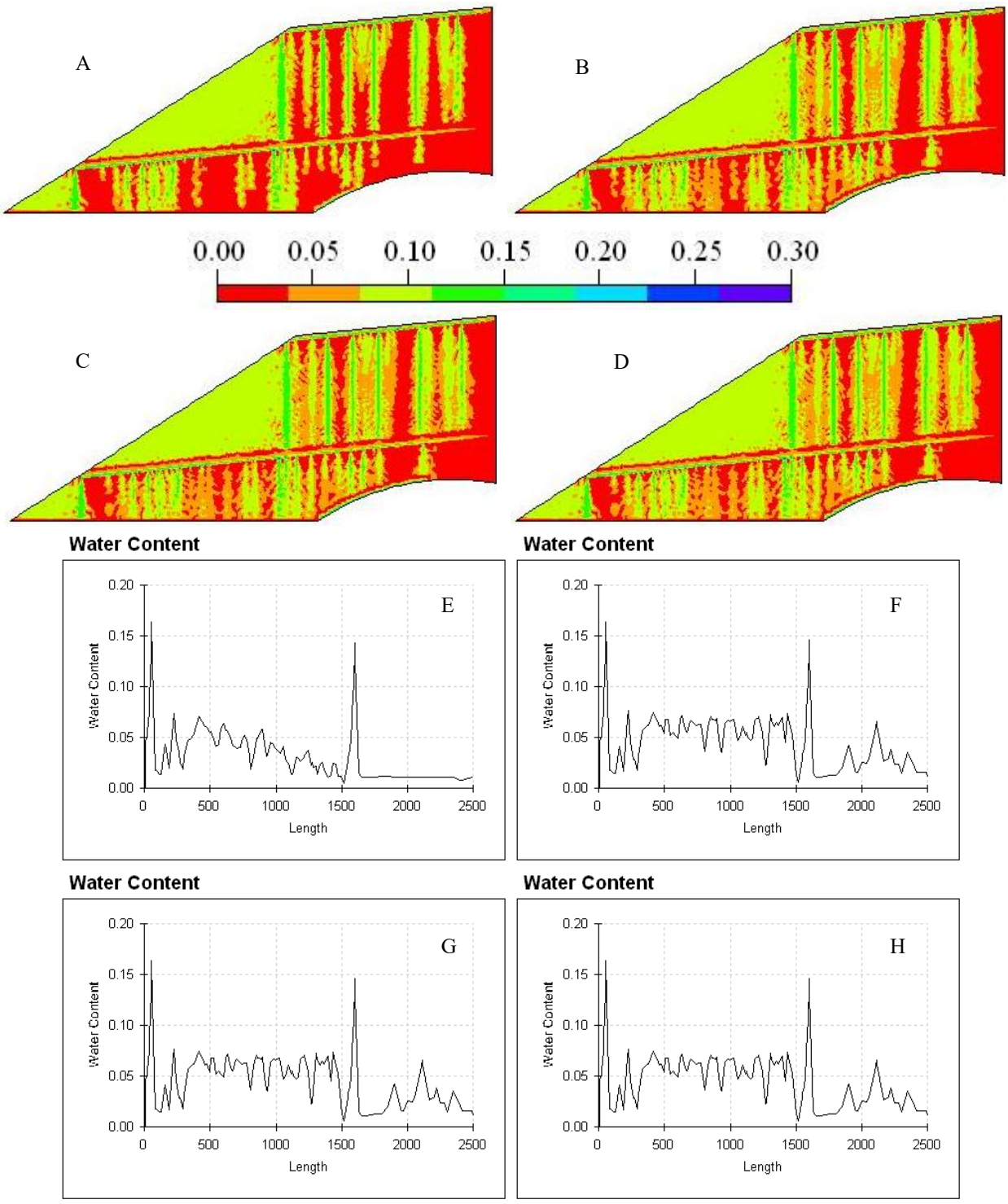

Figure A15: Contours and profiles (at line AA) of the volumetric water content for simulation S15 (GRV with two inclined at 10% SBL layers, small size pile) at the end of December of the A, E) 2nd year; B, F) 4th year; C, G) 6th year; and D, H) 8th year.

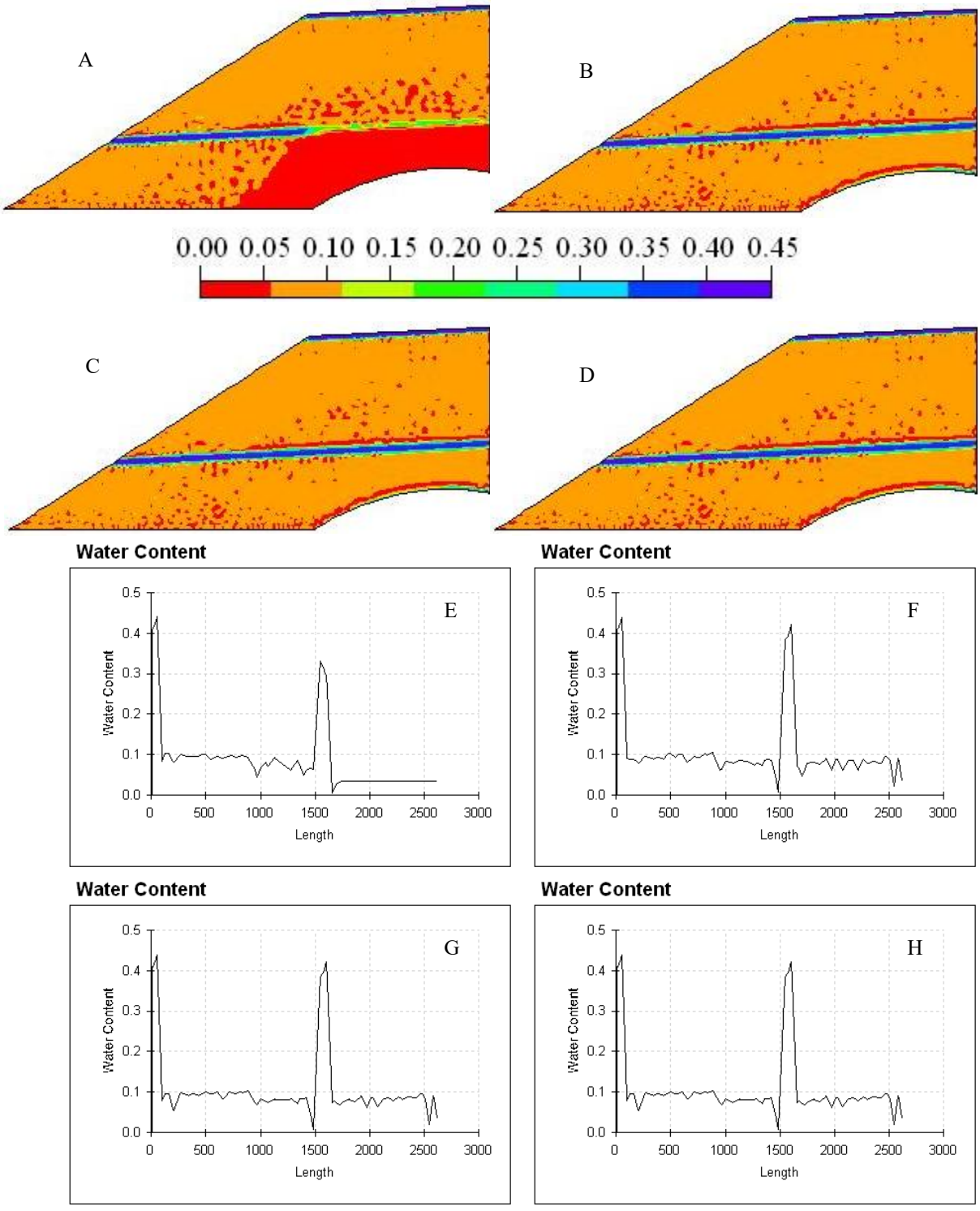

Figure A16: Contours and profiles (at line AA) of the volumetric water content for simulation S16 (GRV with two inclined at 5% SLT layers, small size pile) at the end of December of the A, E) 2nd year; B, F) 4th year; C, G) 6th year; and D, H) 8th year.

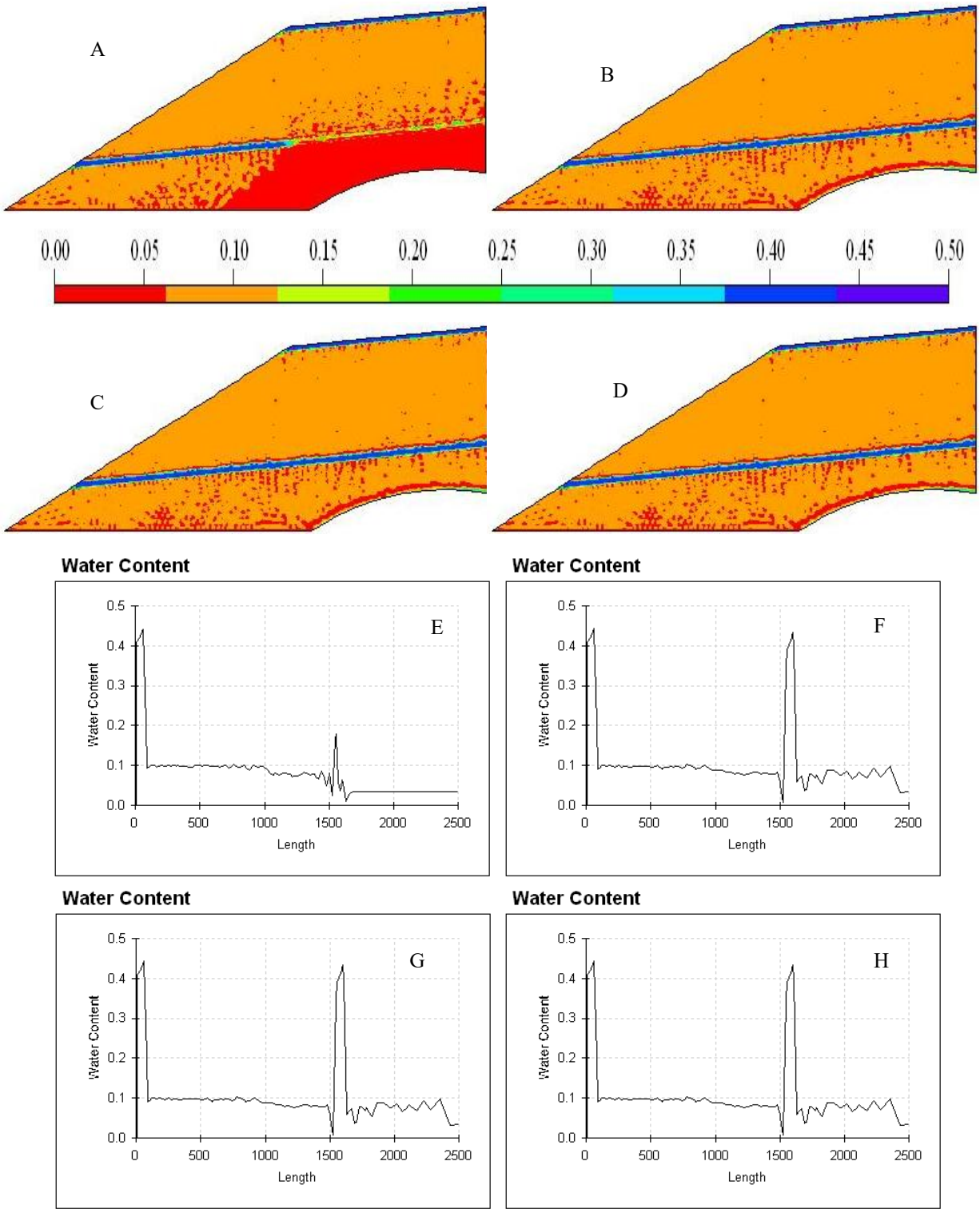

Figure A17: Contours and profiles (at line AA) of the volumetric water content for simulation S17 (GRV with two inclined at 10% SLT layers, small size pile) at the end of December of the A, E) 2nd year; B, F) 4th year; C, G) 6th year; and D, H) 8th year.

APPENDIX B

Contours and vertical profiles (along line AA – see Fig. 1) of the water vertical velocity at the end of December of the 2nd, 4th , 6th , and 8th years for simulations S1 to S17.

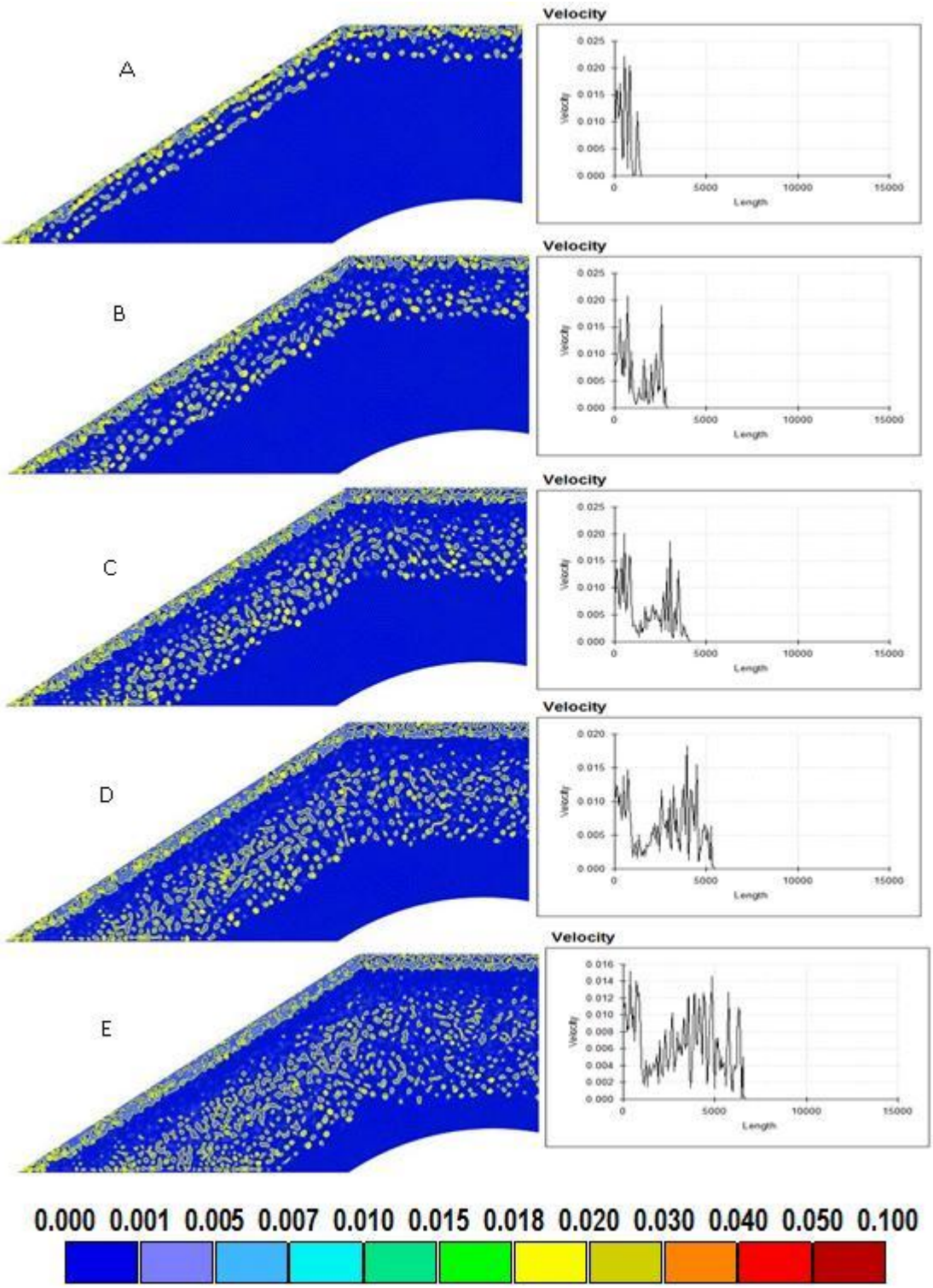

Figure B1: Velocity (cm/hr) contours and profiles (at Line AA) at the end of December of A) 2nd year, B) 4th year, C) 6th year, D) 8th year and E) 10th year for simulation S1 (GRV)

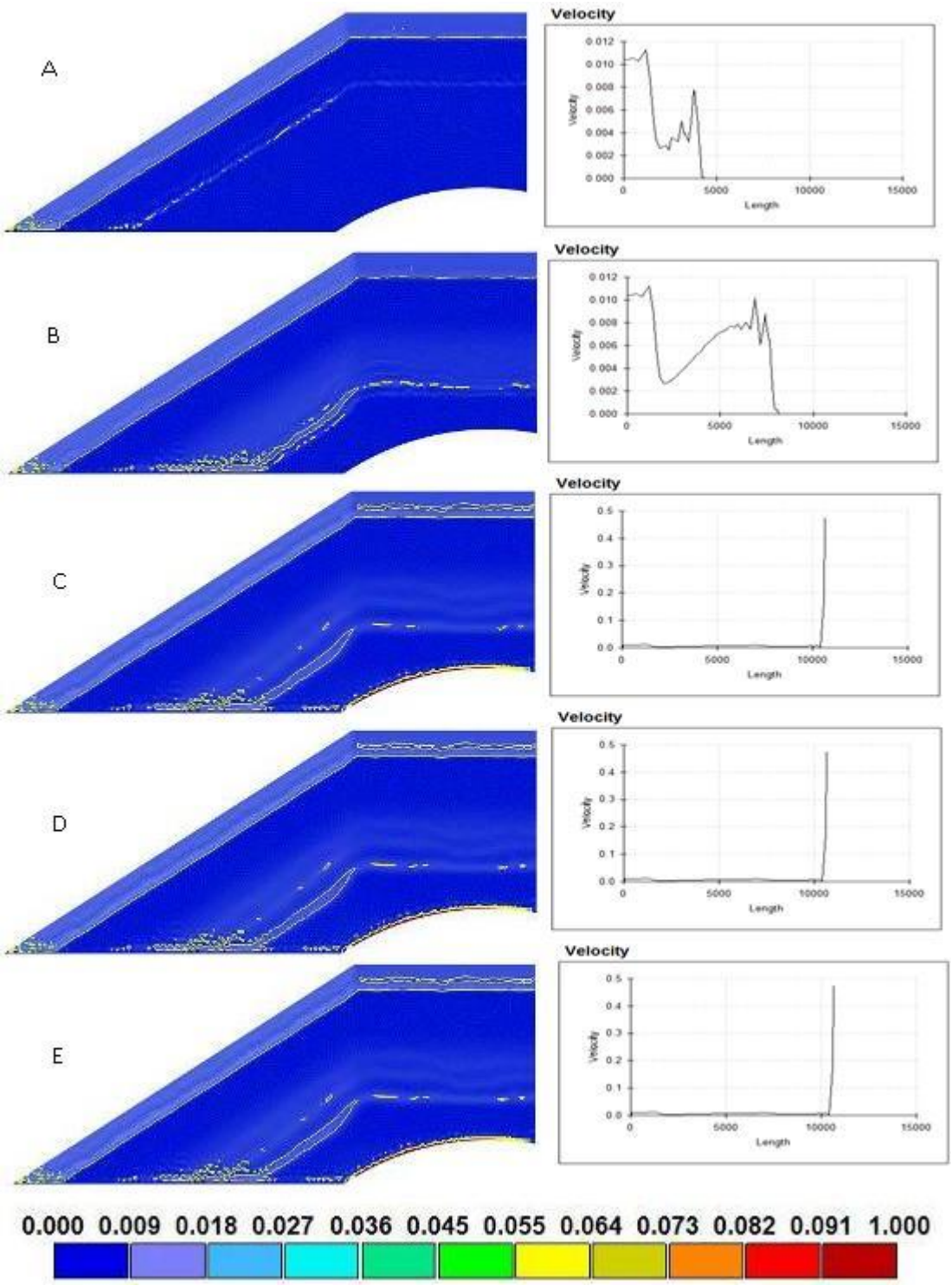

Figure B2: Velocity (cm/hr) contours and profiles (at Line AA) at the end of December of A) 2nd year, B) 4th year, C) 6th year, D) 8th year and E) 10th year for simulation S2 (SBL).

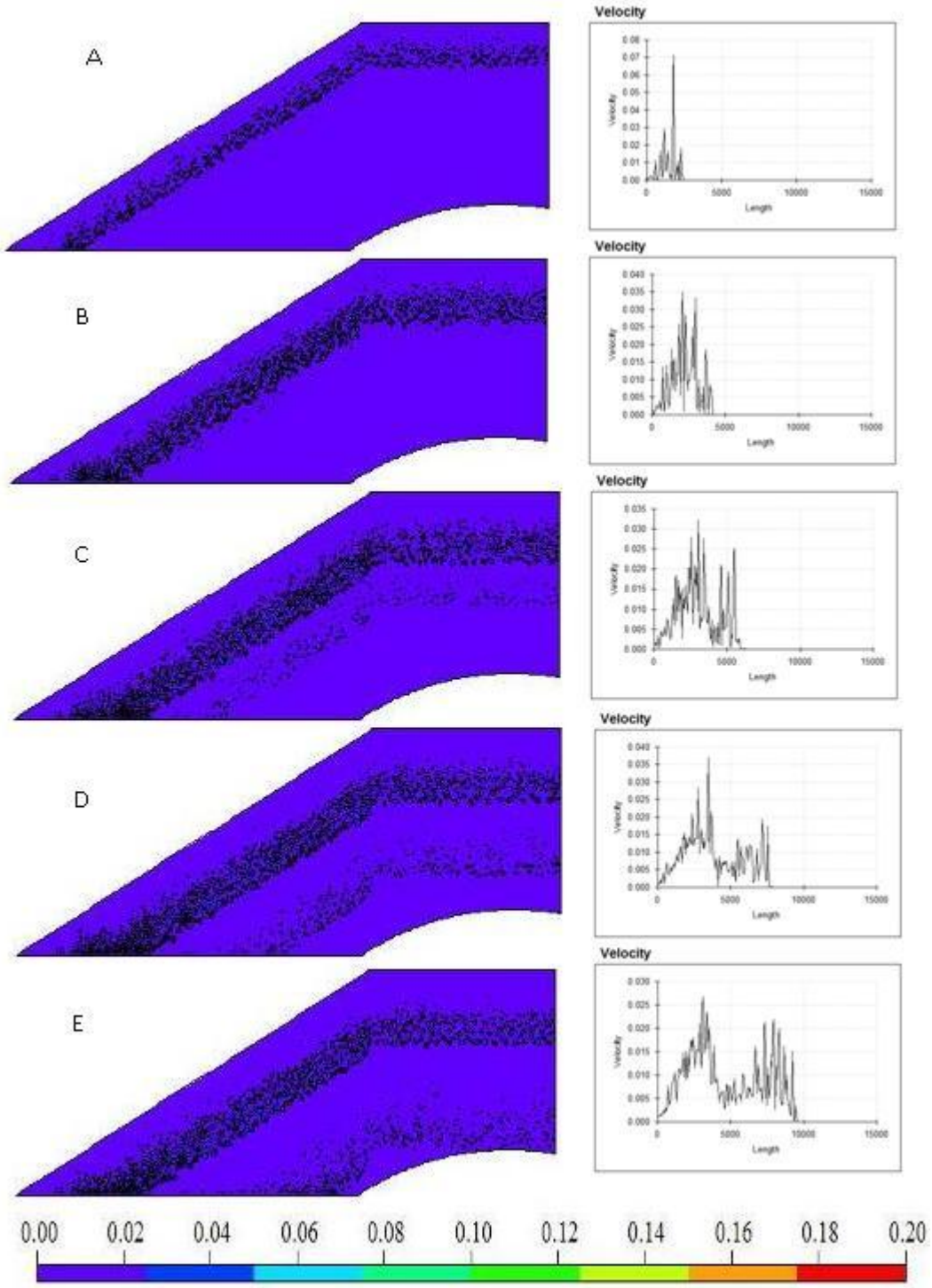

Figure B3: Velocity (cm/hr) contours and profiles (at Line AA) at the end of December of A) 2nd year, B) 4th year, C) 6th year, D) 8th year and E) 10th year for simulation S3 (GRV, precipitation cycle P2-E)

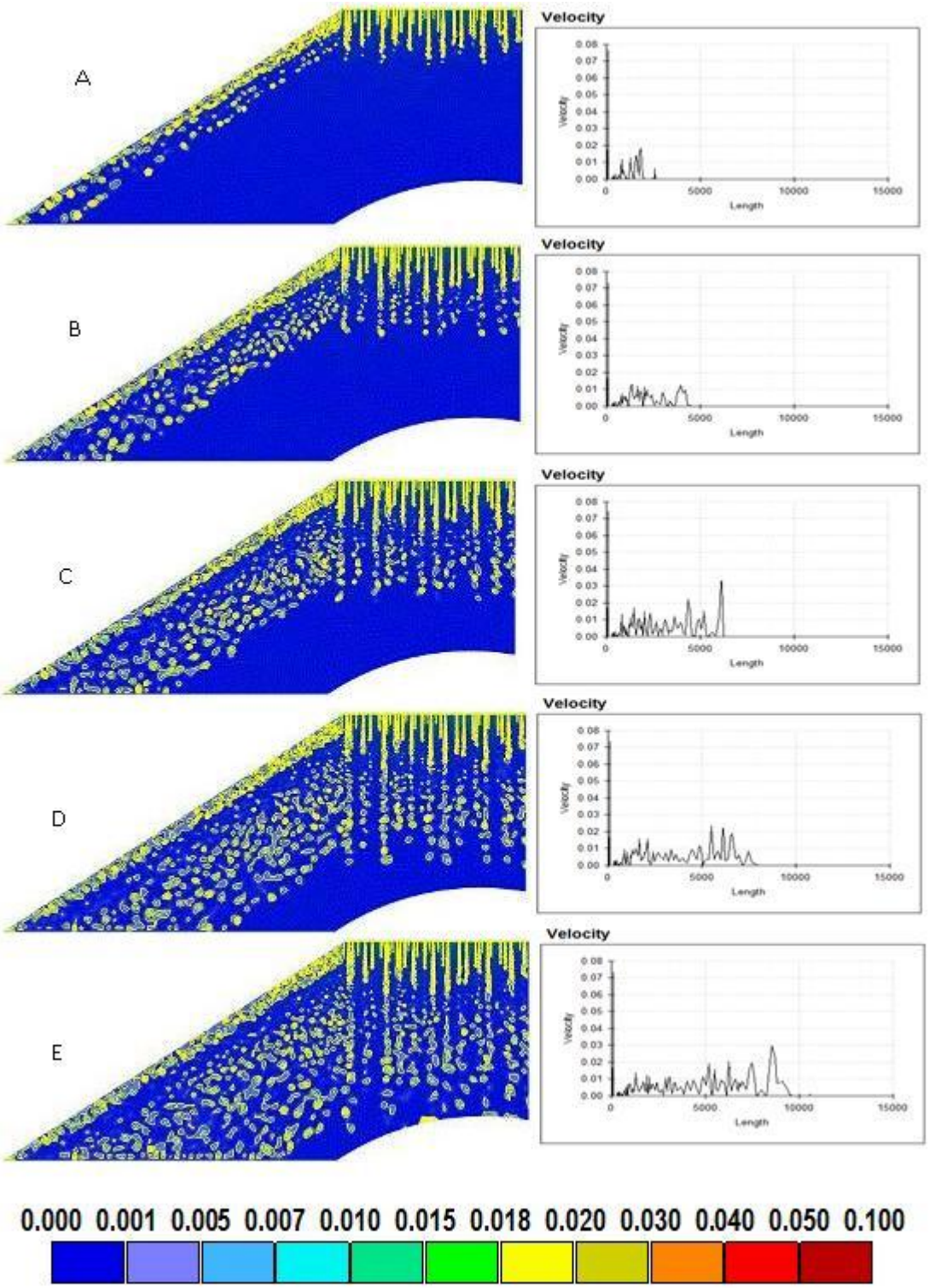

Figure B4: Velocity (cm/hr) contours and profiles (at Line AA) at the end of December of A) 2nd year, B) 4th year, C) 6th year, D) 8th year and E) 10th year for simulation S4 (GRV with one horizontal SBL layer).

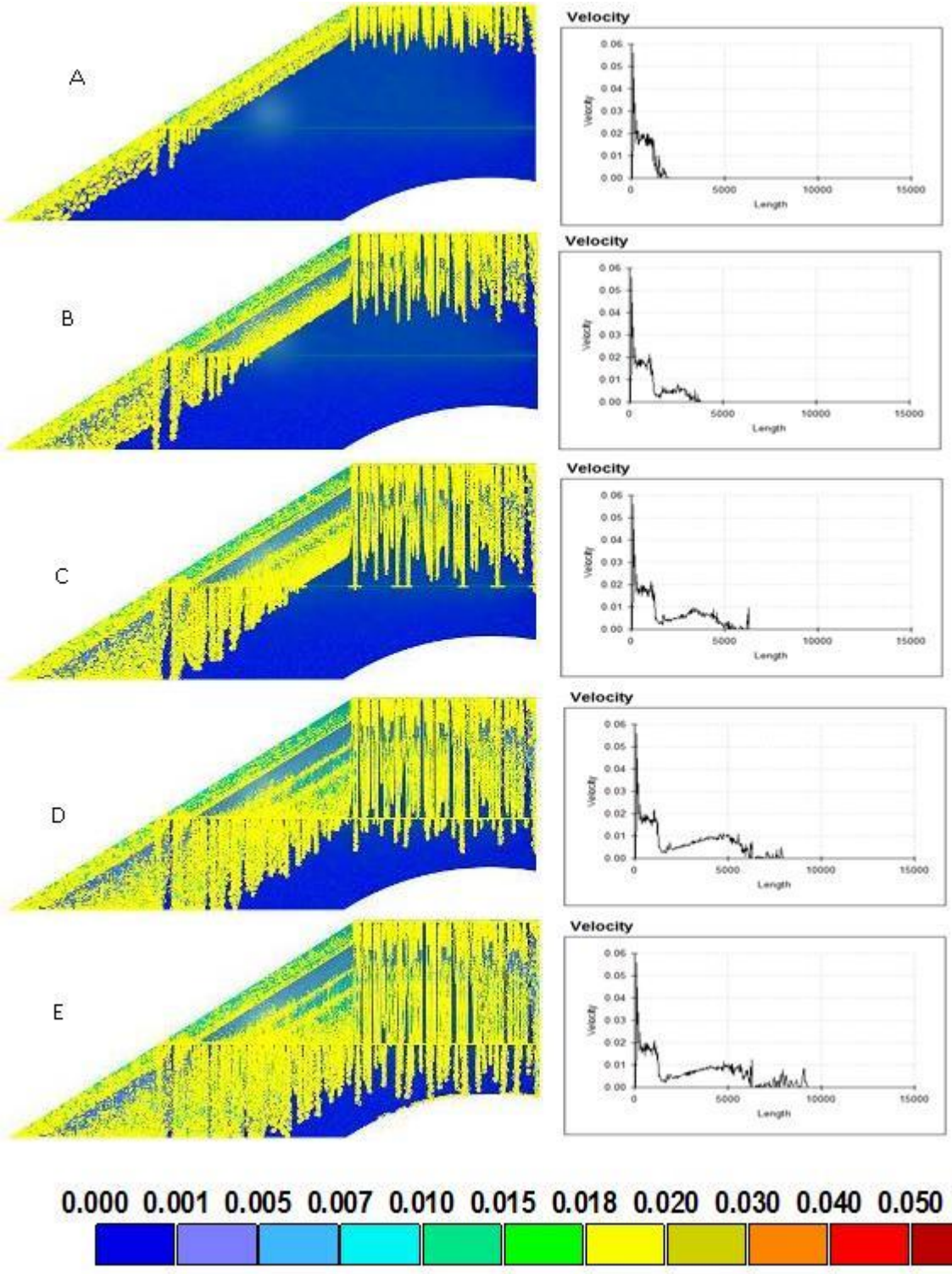

Figure B5: Velocity (cm/hr) contours and profiles (at Line AA) at the end of December of A) 2nd year, B) 4th year, C) 6th year, D) 8th year and E) 10th year for simulation S5 (GRV with two horizontal SBL layers).

.

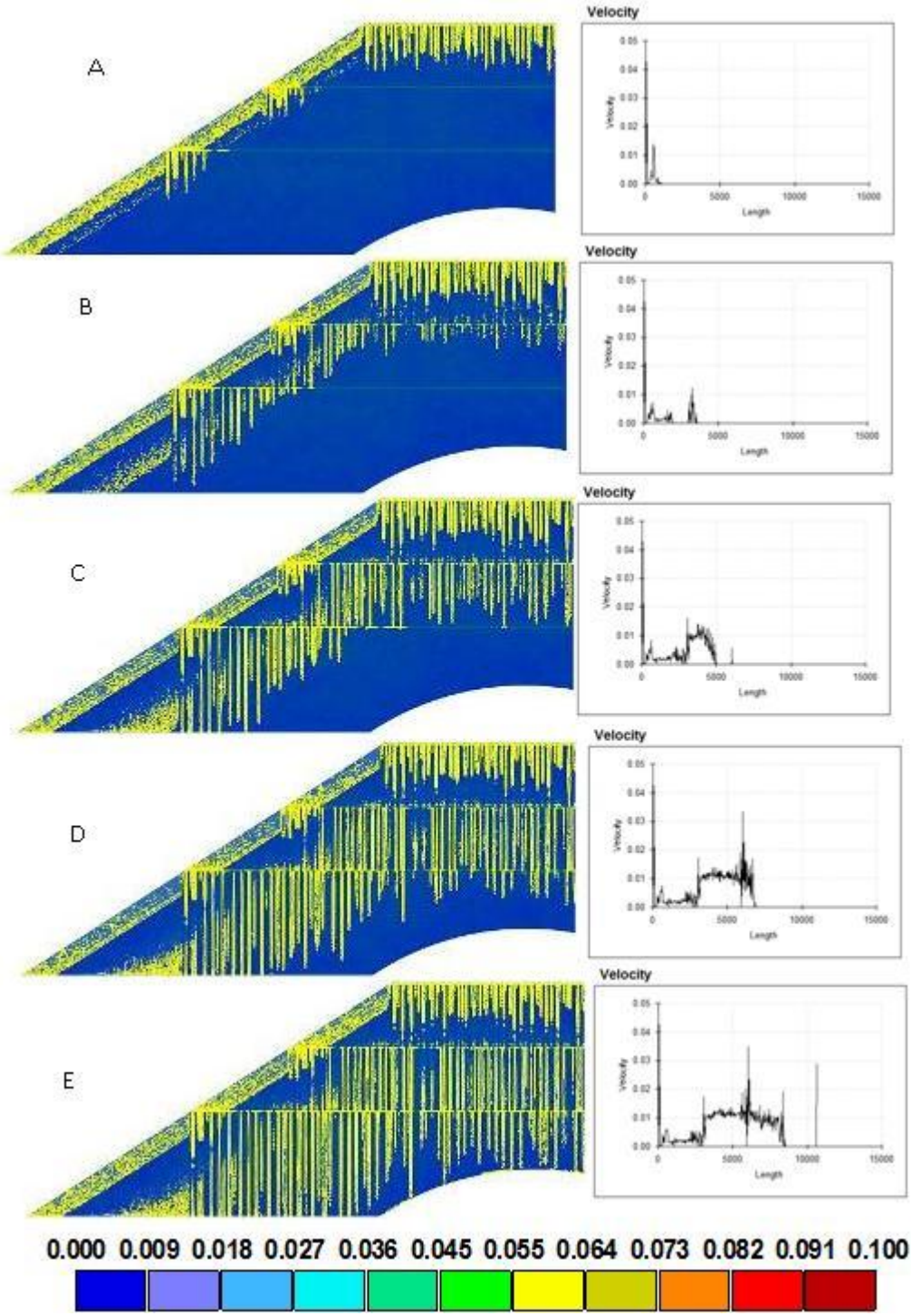

Figure B6: Velocity (cm/hr) contours and profiles (at Line AA) at the end of December of A) 2nd year, B) 4th year, C) 6th year, D) 8th year and E) 10th year for simulation S6 (GRV with three horizontal SBL layers).

.

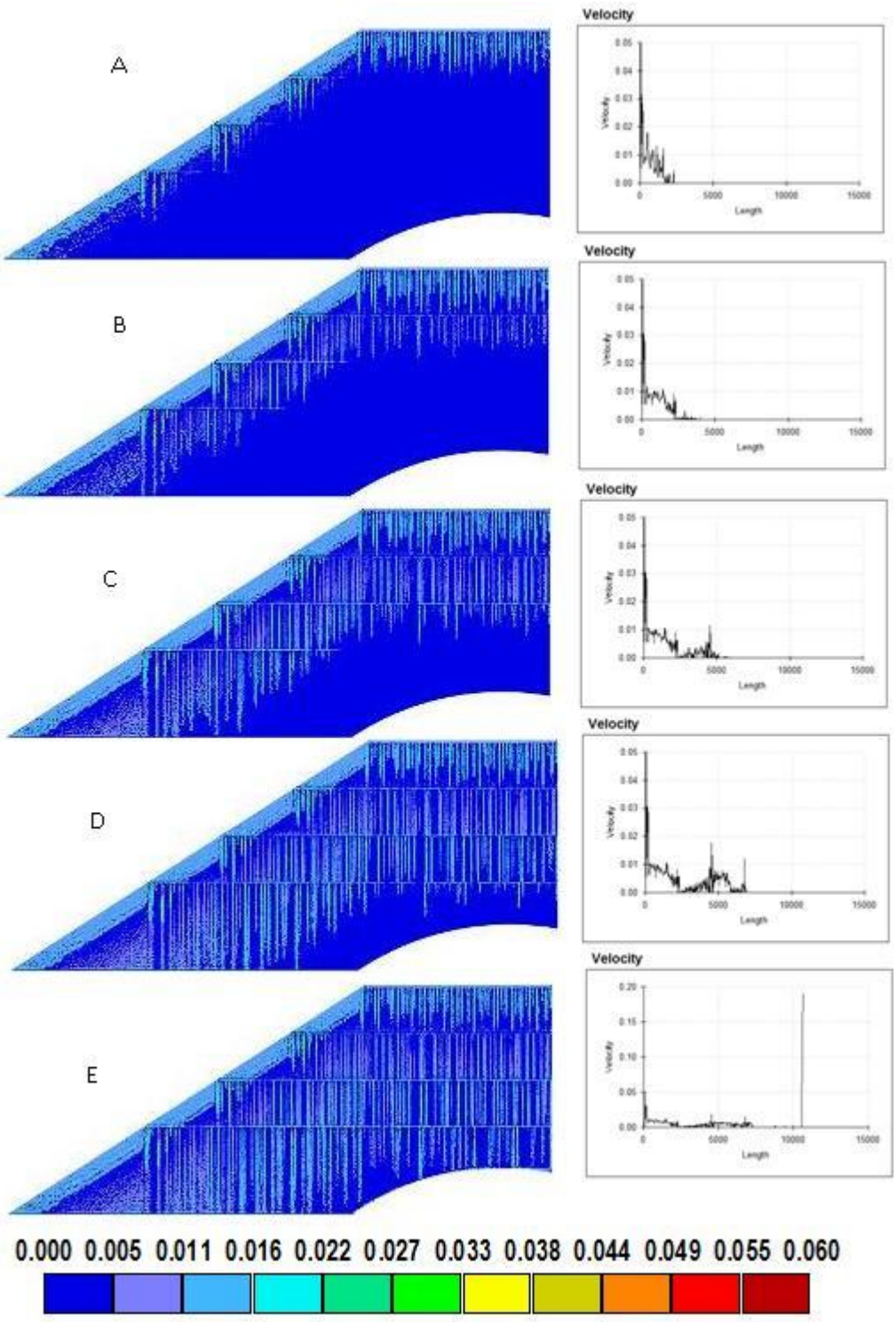

Figure B7: Velocity (cm/hr) contours and profiles (at Line AA) at the end of December of A) 2nd year, B) 4th year, C) 6th year, D) 8th year and E) 10th year for simulation S7 (GRV with four horizontal SBL layers).

.

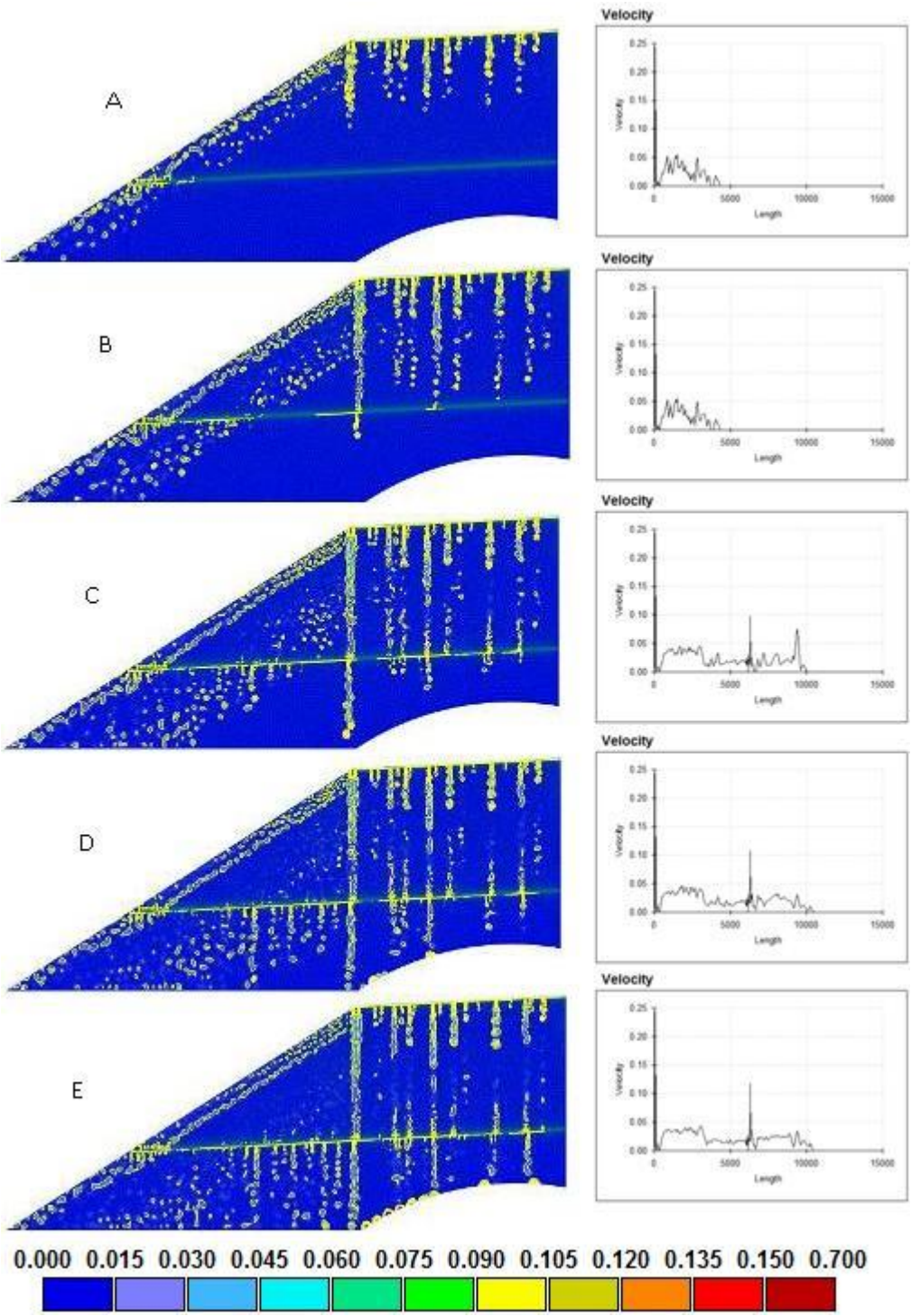

Figure B8: Velocity (cm/hr) contours and profiles (at Line AA) at the end of December of A) 2nd year, B) 4th year, C) 6th year, D) 8th year and E) 10th year for simulation S8 (GRV with two SBL layers inclined at 5%).

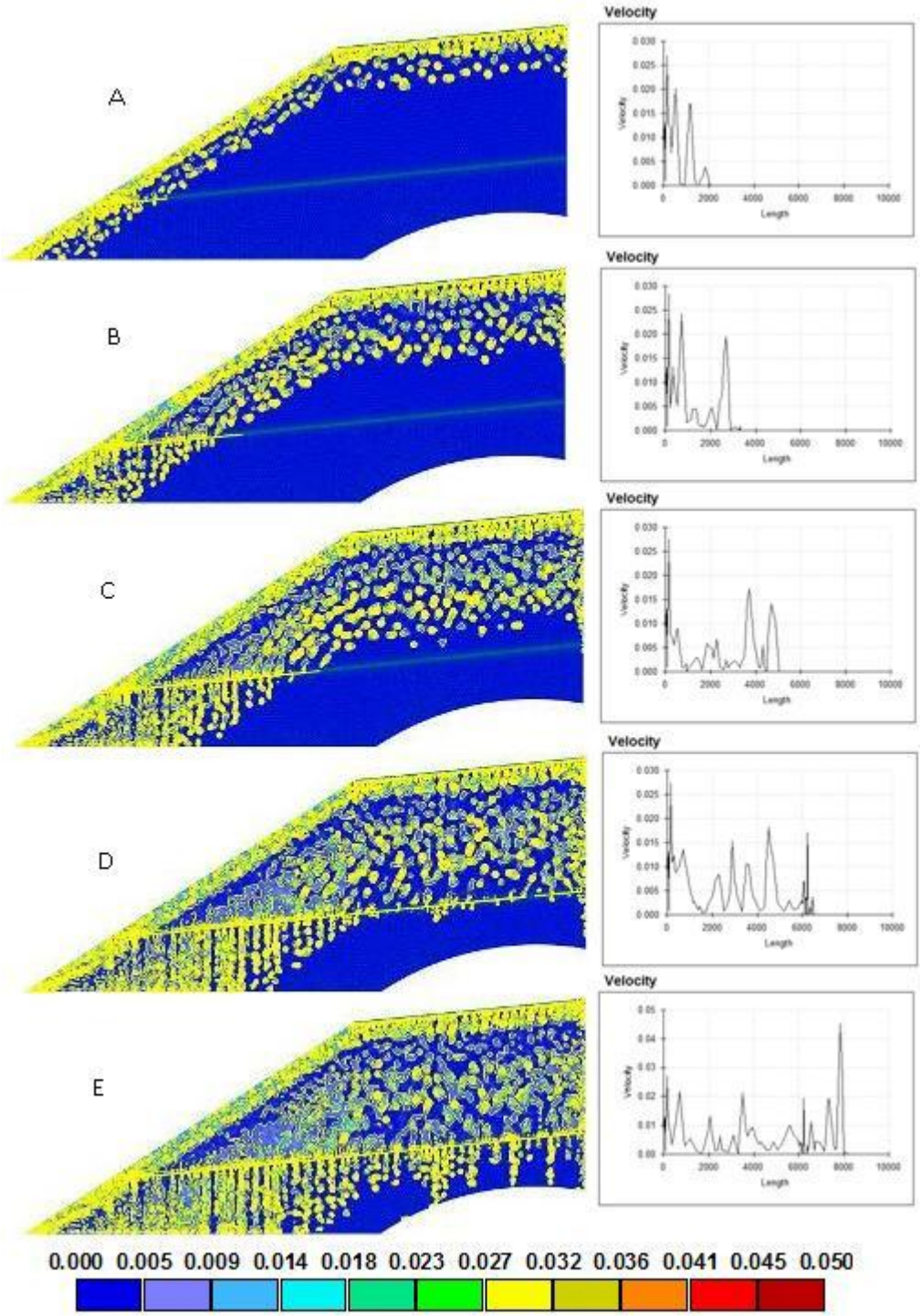

Figure B9: Velocity (cm/hr) contours and profiles (at Line AA) at the end of December of A) 2nd year, B) 4th year, C) 6th year, D) 8th year and E) 10th year for simulation S9 (GRV with two SBL layers inclined at 10%).

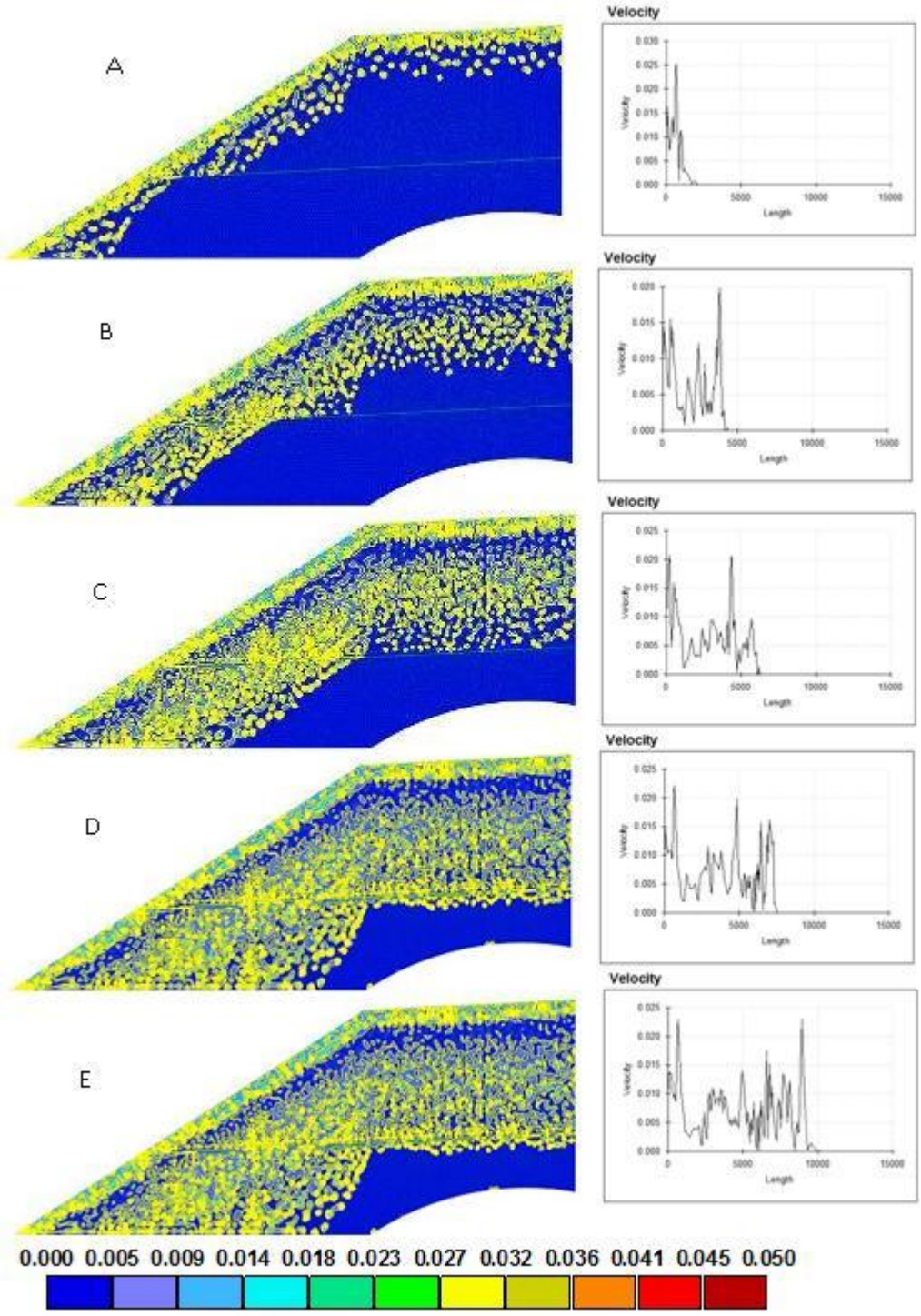

Figure B10: Velocity (cm/hr) contours and profiles (at Line AA) at the end of December of A) 2nd year, B) 4th year, C) 6th year, D) 8th year and E) 10th year for simulation S10 (GRV with two STL layers inclined at 5%).

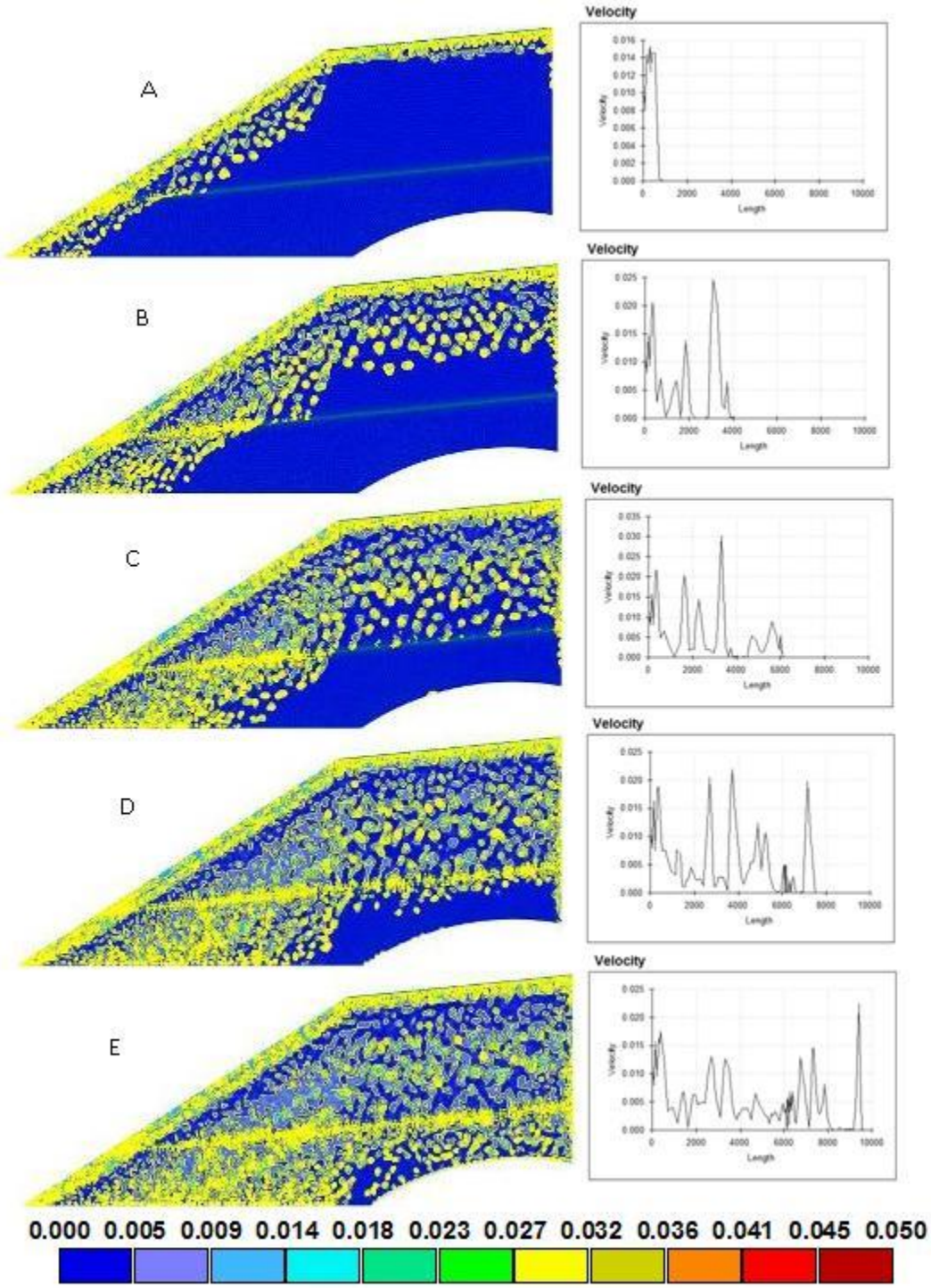

Figure B11: Velocity (cm/hr) contours and profiles (at Line AA) at the end of December of A) 2nd year, B) 4th year, C) 6th year, D) 8th year and E) 10th year for simulation S11 (GRV with two STL layers inclined at 10%).

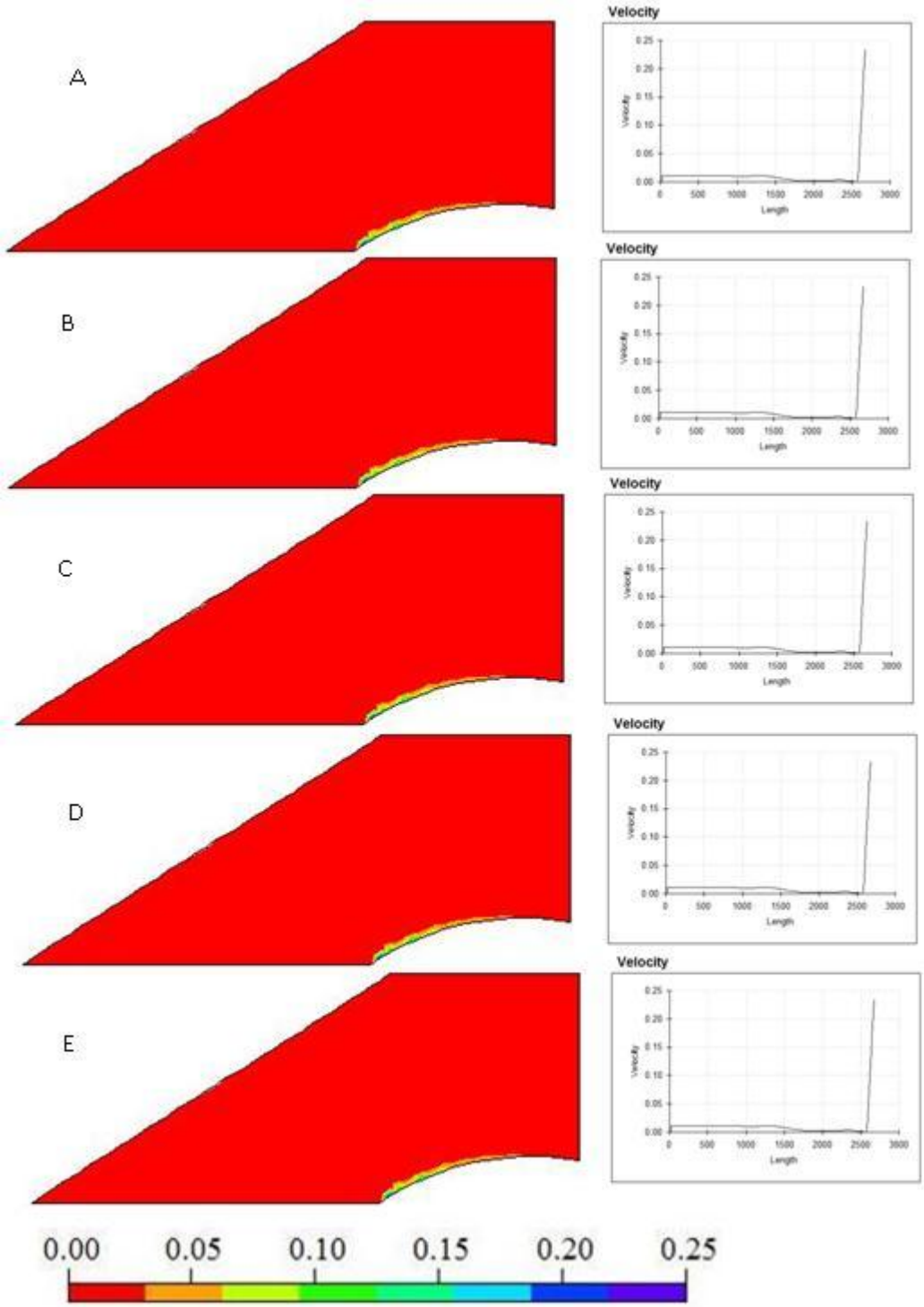

Figure B12: Velocity (cm/hr) contours and profiles (at Line AA) at the end of December of A) 2nd year, B) 4th year, C) 6th year, D) 8th year and E) 10th year for simulation S12 (SBL, small size pile)

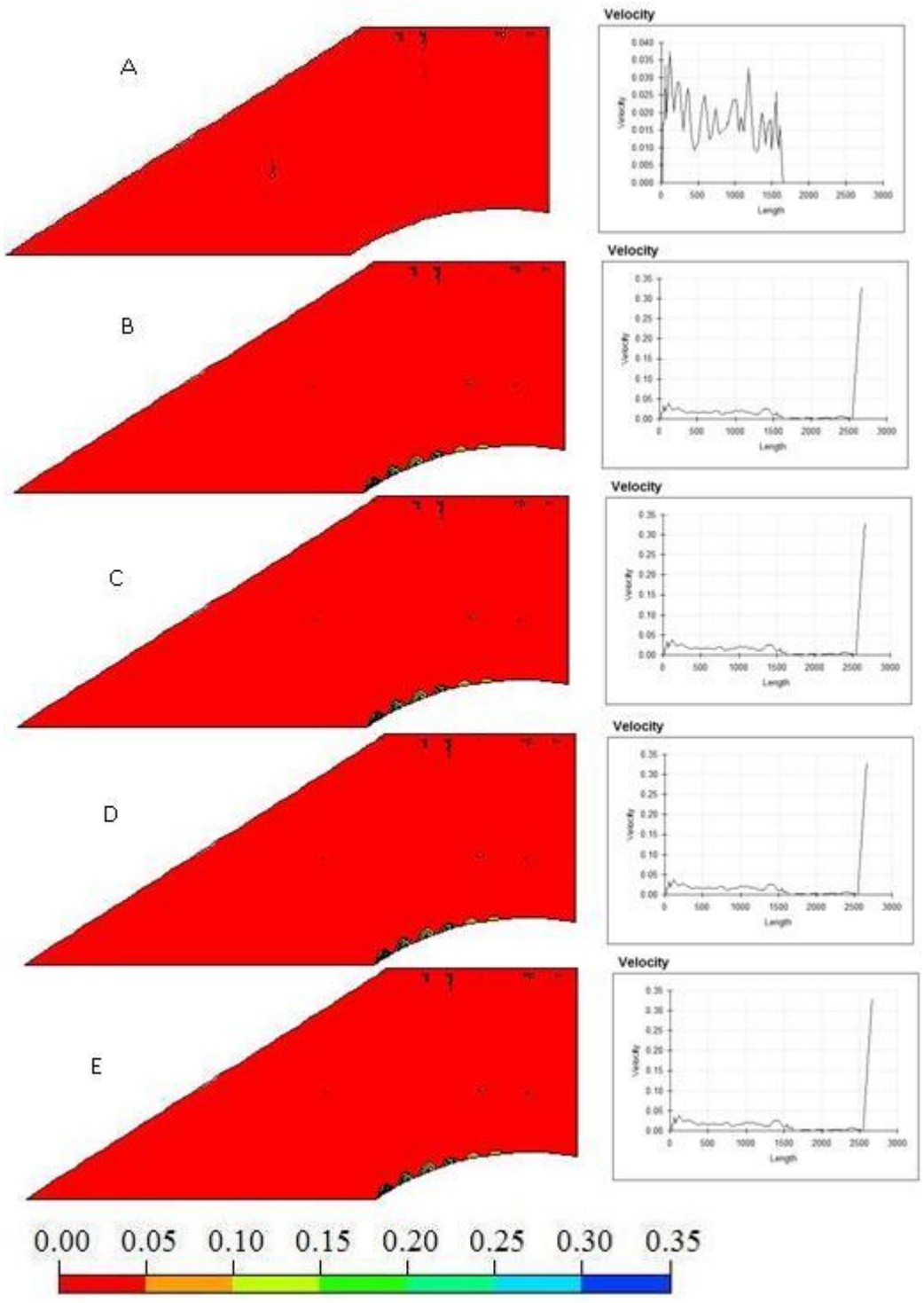

Figure B13: Velocity (cm/hr) contours and profiles (at Line AA) at the end of December of A) 2nd year, B) 4th year, C) 6th year, D) 8th year and E) 10th year for simulation S13 (GRV with two horizontal SBL layers, small size pile)

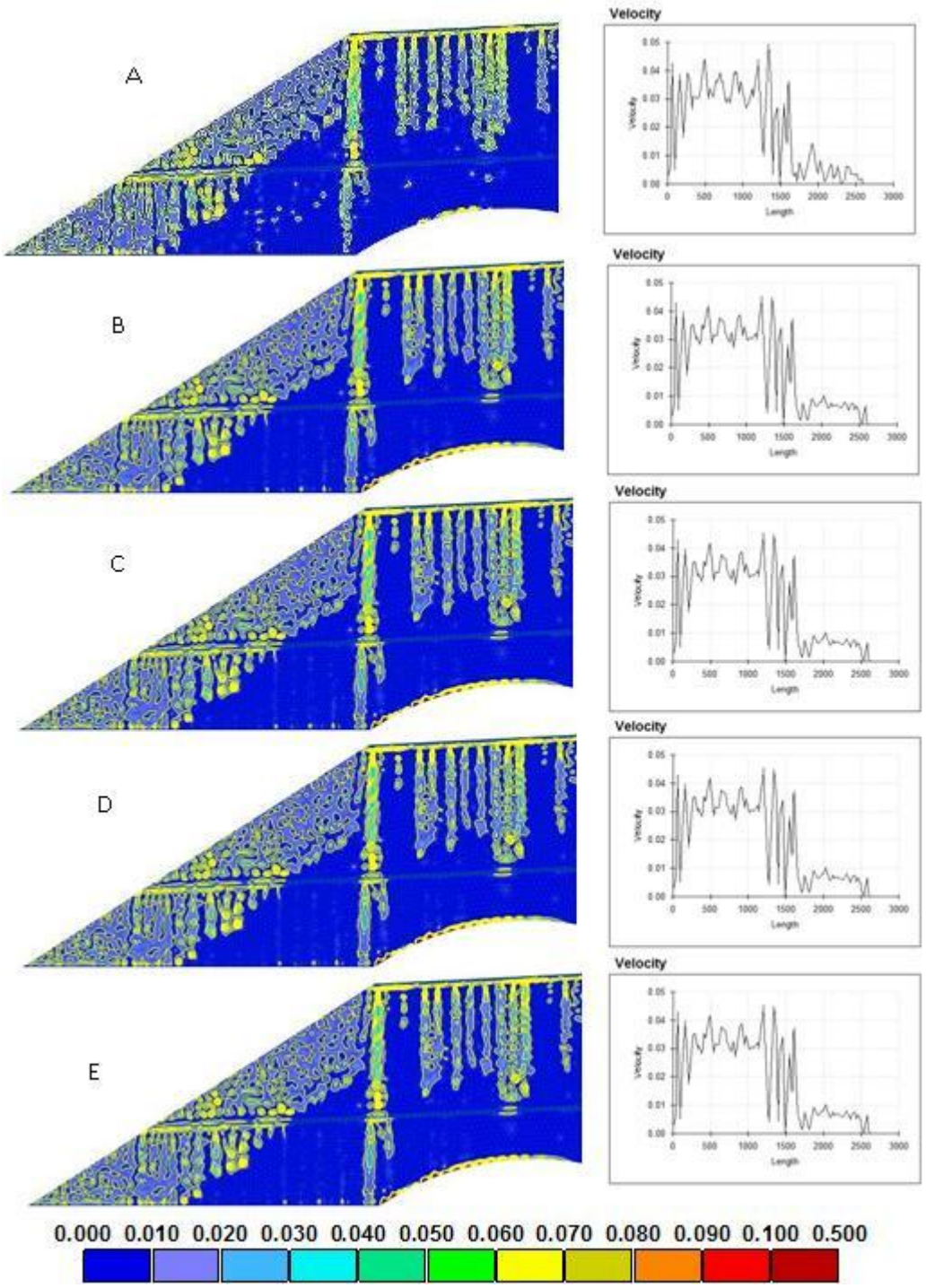

Figure B14: Velocity (cm/hr) contours and profiles (at Line AA) at the end of December of A) 2nd year, B) 4th year, C) 6th year, D) 8th year and E) 10th year for simulation S14 (GRV with two inclined at 5% SBL layers, small size pile)

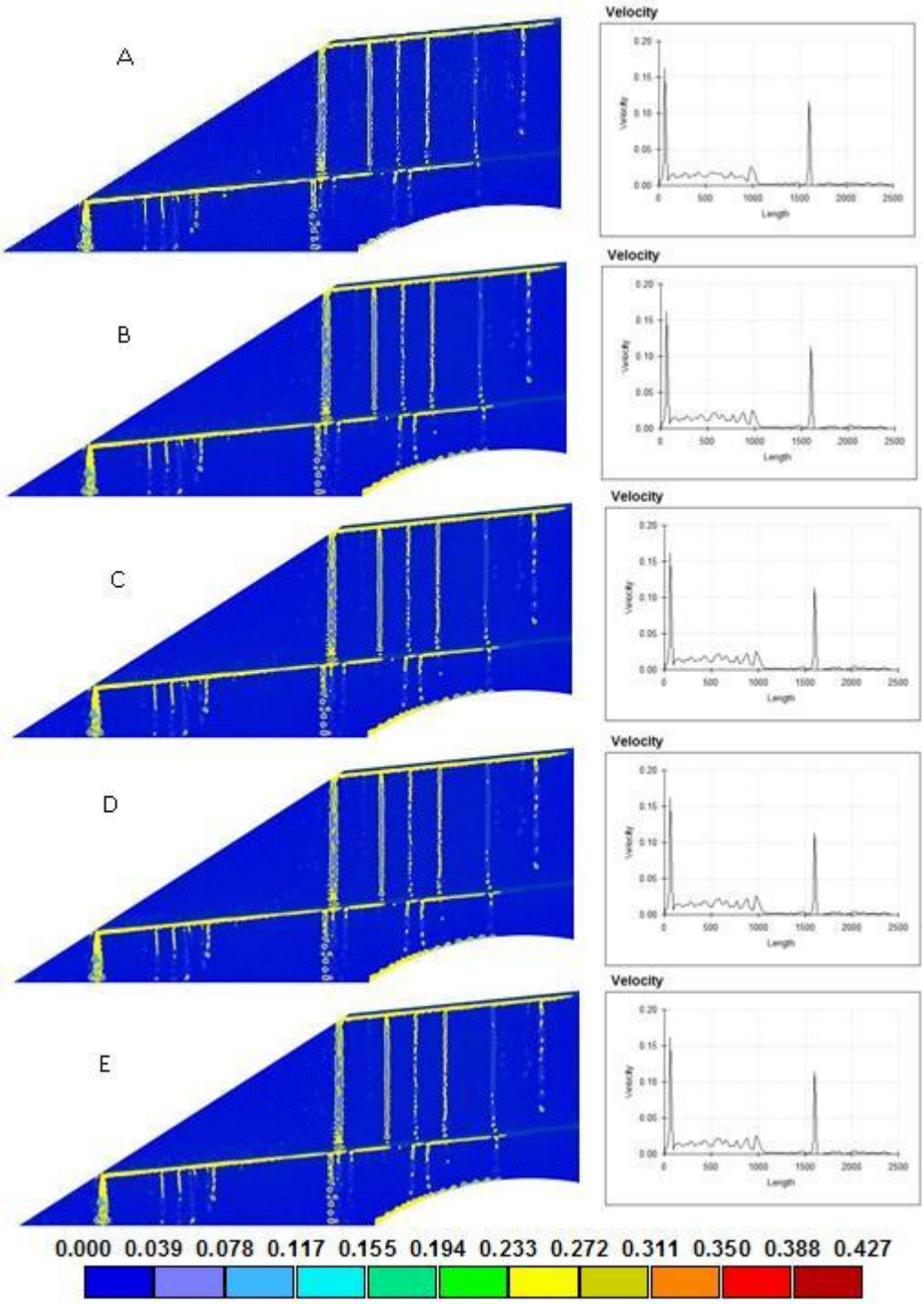

Figure B15: Velocity (cm/hr) contours and profiles (at Line AA) at the end of December of A) 2nd year, B) 4th year, C) 6th year, D) 8th year and E) 10th year for simulation S15 (GRV with two inclined at 10% SBL layers, small size pile).

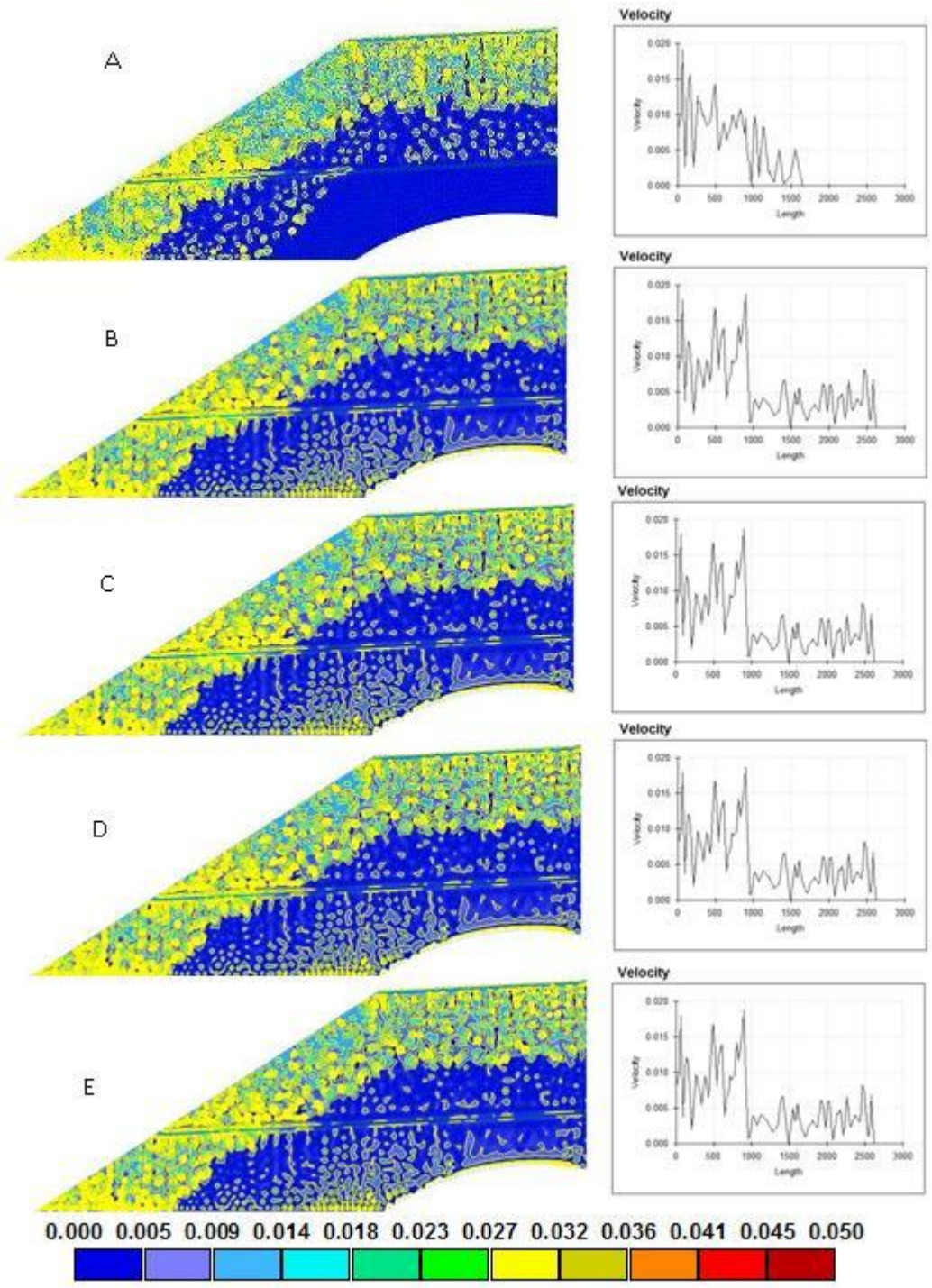

Figure B16: Velocity (cm/hr) contours and profiles (at Line AA) at the end of December of A) 2nd year, B) 4th year, C) 6th year, D) 8th year and E) 10th year for simulation S16 (GRV with two inclined at 5% SLT layers, small size pile)

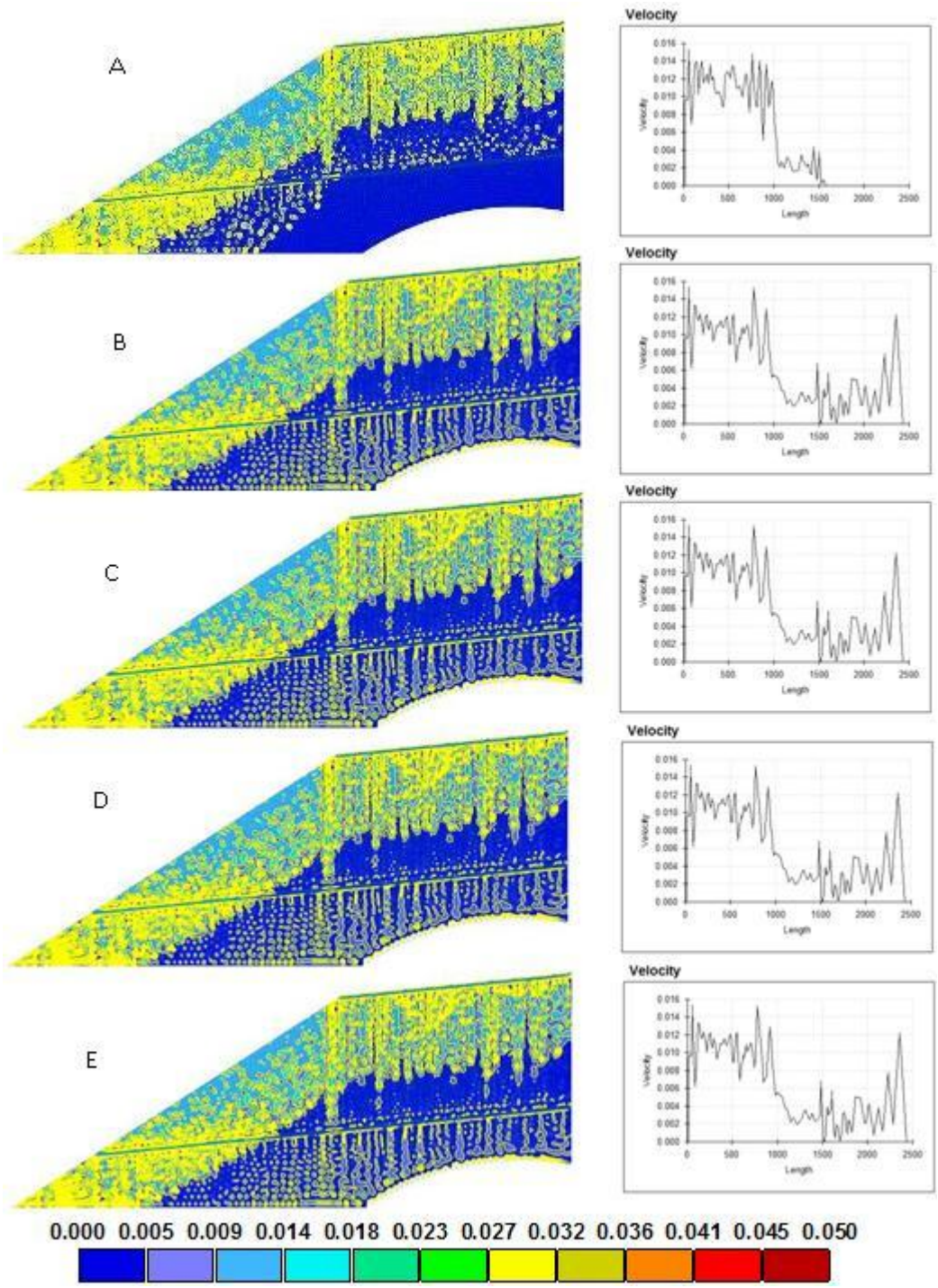

Figure B17: Velocity (cm/hr) contours and profiles (at Line AA) at the end of December of A) 2nd year, B) 4th year, C) 6th year, D) 8th year and E) 10th year for simulation S17 (GRV with two inclined at 10% SLT layers, small size pile).

L'École Polytechnique se spécialise dans la formation d'ingénieurs et la recherche en ingénierie depuis 1873

École Polytechnique de Montréal

École affiliée à l'Université de Montréal

Campus de l'Université de Montréal
C.P. 6079, succ. Centre-ville
Montréal (Québec)
Canada H3C 3A7

www.polymtl.ca

ÉCOLE
POLYTECHNIQUE
MONTRÉAL